

OPEN FILE REPORT O-14-01

**GEOLOGIC MAP OF THE SOUTHERN OREGON COAST
BETWEEN PORT ORFORD AND BANDON,
CURRY AND COOS COUNTIES, OREGON**

by Thomas J. Wiley¹, Jason D. McClaughry², Lina Ma¹, Katherine A. Mickelson¹,
Clark A. Niewendorp¹, Laura L. Stimely³, Heather H. Herinckx⁴, and Jonathan Rivas⁵



2014

¹ Oregon Department of Geology and Mineral Industries, 800 NE Oregon Street, Suite 965 Portland, OR 97232

² Oregon Department of Geology and Mineral Industries, Baker City Field Office, Baker County Courthouse, 1995 3rd Street, Suite 130, Baker City, OR 97814

³ Oregon Department of Geology and Mineral Industries, Newport Field Office, 313 SW 2nd, Suite D, Newport, OR 97365

⁴ Department of Geology, Portland State University, 17 Cramer Hall, 1721 SW Broadway Street, Portland, OR 97201

⁵ Department of Geological Sciences, California State University–Northridge, 18111 Nordhoff Street, Northridge, CA 91330

NOTICE

This manuscript is submitted for publication with the understanding that the United States Government is authorized to reproduce and distribute reprints for governmental use. The views and conclusions contained in this document are those of the authors and should not be interpreted as necessarily representing the official policies, either expressed or implied, of the U.S. government.

This product is for informational purposes and may not have been prepared for or be suitable for legal, engineering, or surveying purposes. Users of this information should review or consult the primary data and information sources to ascertain the usability of the information. This publication cannot substitute for site-specific investigations by qualified practitioners. Site-specific data may give results that differ from the results shown in the publication.

*Cover photograph: View northwest, along the beach, near Bandon on the southern Oregon coast.
Sea stacks in the foreground are composed of sandstone and meta-volcanic rock
(WGS84 geographic coordinates: 383213E., 4773497N.).*

Oregon Department of Geology and Mineral Industries Open-File Report O-14-01
Published in conformance with ORS 516.030

For copies of this publication or other information about Oregon's geology and natural resources, contact:

Nature of the Northwest Information Center
800 NE Oregon Street, Suite 965
Portland, OR 97232
(971) 673-2331
<http://www.naturenw.org>

For additional information:
Administrative Offices
800 NE Oregon Street #28, Suite 965
Portland, OR 97232
Telephone (971) 673-1555
Fax (971) 673-1562
<http://www.oregongeology.org>
<http://egov.oregon.gov/DOGAMI/>

TABLE OF CONTENTS

INTRODUCTION	1
GEOGRAPHIC AND GEOLOGIC SETTING	4
Gold Beach terrane	6
Sixes River terrane	7
Pickett Peak terrane	8
Western Klamath terrane, Elk subterrane	8
Yolla Bolly terrane, Snow Camp subterrane of the Western Klamath terrane, and Siletz terrane	8
Paleogene sedimentary rocks that overlap western Jurassic terranes and eastern terrane of the Sixes River terrane	9
Lower Pleistocene and Miocene rocks	9
PREVIOUS WORK	10
METHODOLOGY	12
EXPLANATION OF MAP UNITS	14
Overview of map units along the southern Oregon coast	16
Upper Cenozoic surficial deposits	19
Lower Pleistocene and Miocene rocks	29
Lower Cenozoic and Mesozoic rocks	34
Other rocks	40
STRUCTURAL GEOLOGY	41
Folding and faulting	42
Linear features crossing the continental margin	47
Elevated marine platforms	48
ACKNOWLEDGMENTS	48
REFERENCES	49
APPENDIX — GEOGRAPHIC INFORMATION SYSTEMS (GIS) DATABASE	56
Geodatabase specifications	56
Geologic maps	59
Geochemical analytical methods	60
Geochronology analytical methods	61
Bedding (strike and dip)	62
Structure (foliations)	63
Water well logs	64

LIST OF FIGURES

Figure 1. Location of the map area in southwestern Oregon 2

Figure 2. Current project area. 3

Figure 3. Tectonic setting of the Pacific Northwest region of the United Sates 4

Figure 4. Tectonostratigraphic terranes in southwestern Oregon 5

Figure 5. Sources of geologic mapping used during the preparation of this report 11

Figure 6. Time-rock chart showing the 73 geologic units identified by this study 15

Figure 7. Large-scale linear features on the continental margin lie along projected trends of offshore fracture zones 41

Figure A1. Southwestern Oregon coast geodatabase feature datasets 57

Figure A2. Relationships between tables and MapUnitPolys feature class in the geodatabase 57

Figure A3. Southwestern Oregon coast geodatabase feature classes 58

Figure A4. Southwestern Oregon coast geodatabase relationships 59

Figure A5. Plates 1,2, and 3 accompanying this report. 59

LIST OF TABLES

Table 1. Partial chronological listing of maps and reports on which this study builds 10

Table 2. Correlation of marine terraces along the southern and central Oregon coast. 26

Table 3. Representative XRF analyses for rocks in the Port Orford, Langlois, and Bandon, Oregon areas 33

MAP PLATES

Plate 1. Geologic map of the Cape Blanco and Sixes 7.5-minute quadrangles, Curry County, Oregon

Plate 2. Geologic map of the Floras Lake and Langlois 7.5-minute quadrangles, Curry and Coos Counties, Oregon

Plate 3. Geologic map of the Bandon 7.5-minute quadrangle, Coos County, Oregon

SPREADSHEETS AND SHAPEFILES (IN DIGITAL APPENDIX)

Geochemistry:	SC2014_GeoChemistry.xls	SC2014_Geochemistry.shp
Geochronology:	SC2014_GeoChronology.xls	SC2014_Geochronology.shp
Bedding:	SC2014_Bedding.xls	SC2014_Bedding.shp
Foliation:	SC2014_Foliation.xls	SC2014_Foliation.shp
Water Wells:	SC2014_WaterWells.xls	SC2014_WaterWells.shp

INTRODUCTION

This report, digital geodatabase, and the accompanying set of geologic maps were prepared to provide an updated and spatially accurate geologic framework for the southern Oregon coast between Port Orford and Bandon in westernmost Curry and Coos counties (Figure 1). Geologic mapping summarized here represents one part of a multi-year project to map the Oregon coast from the California border north to Coos Bay (Figure 2). Three geologic map plates cover the Cape Blanco – Sixes quadrangles (Plate 1), Floras Lake – Langlois quadrangles (Plate 2), and Bandon quadrangle (Plate 3) at a scale of 1:24,000. These maps show the distribution of contrasting lithologies, critical structural relationships, and surficial geology. They refine our understanding of geologic conditions that control the distribution, quantity, and quality of groundwater resources, the distribution of terrain susceptible to landslides, the nature of seismic hazards, and the distribution of potential aggregate sources and other mineral resources. The geodatabase contains spatial information about geologic polygons and structures and basic data about each geologic unit such as age, lithology, mineralogy, and structure. The geodatabase is supported by this report, which describes the geology, and digital appendices with geochemical, geochronological, structural, and subsurface data interpreted from water wells. Digitization at scales of 1:8,000 or better was accomplished using georeferenced lidar base layers. This geodatabase forms a basis for future geologic, geohydrologic, and geohazard studies in the area. The map plates and database were prepared to show the inferred distribution of bedrock beneath surficial units. Both bedrock and surficial geologic relationships can be interpreted from the maps and geodatabase.

In areas where access was not permitted, derivatives of lidar bare-earth topography, such as slopeshade and hillshade images, were used to resolve conflicts between earlier geologic maps. For example, the distribution of sedimentary rock mapped in the extreme southeastern corner of the Bandon quadrangle (Plate 3) is based on topography similar to that mapped as sedimentary rock by Brownfield and others (1982) in adjacent quadrangles to the south and southeast. Similarly, the lithologies of numerous blocks in the mélange and sea stacks offshore were mapped by using lidar bare-earth topography and digital orthophotographs.

The project is a high priority of the Oregon Geologic Map Advisory Committee and was supported in part during 2013 and 2014 by the U.S. Geological Survey (USGS) STATEMAP component of the National Cooperative Geologic Mapping Program under assistance award G13AC00137. Matching funds were provided by the Oregon Department of Geology and Mineral Industries (DOGAMI). The core product of this study is an Esri ArcGIS™ ArcMap™ 10.1 format geodatabase that combines new and existing mapping in a digital format consistent with the digital statewide Oregon Geologic Data Compilation database (OGDC-5 [Ma and others, 2009]).

The geologic map and geodatabase were prepared by creating geologic interpretations of bedrock and surficial geology and then merging them using ArcMap 10.1 software. This mechanical merge results in a map that may appear more detailed than the underlying data support, particularly where contacts in the bedrock and surficial geology are nearly co-located (for example, where landslides head near a bedrock contact). In some areas, numerous tiny polygons were generated along these contacts. Such polygons represent artifacts rather than observations.

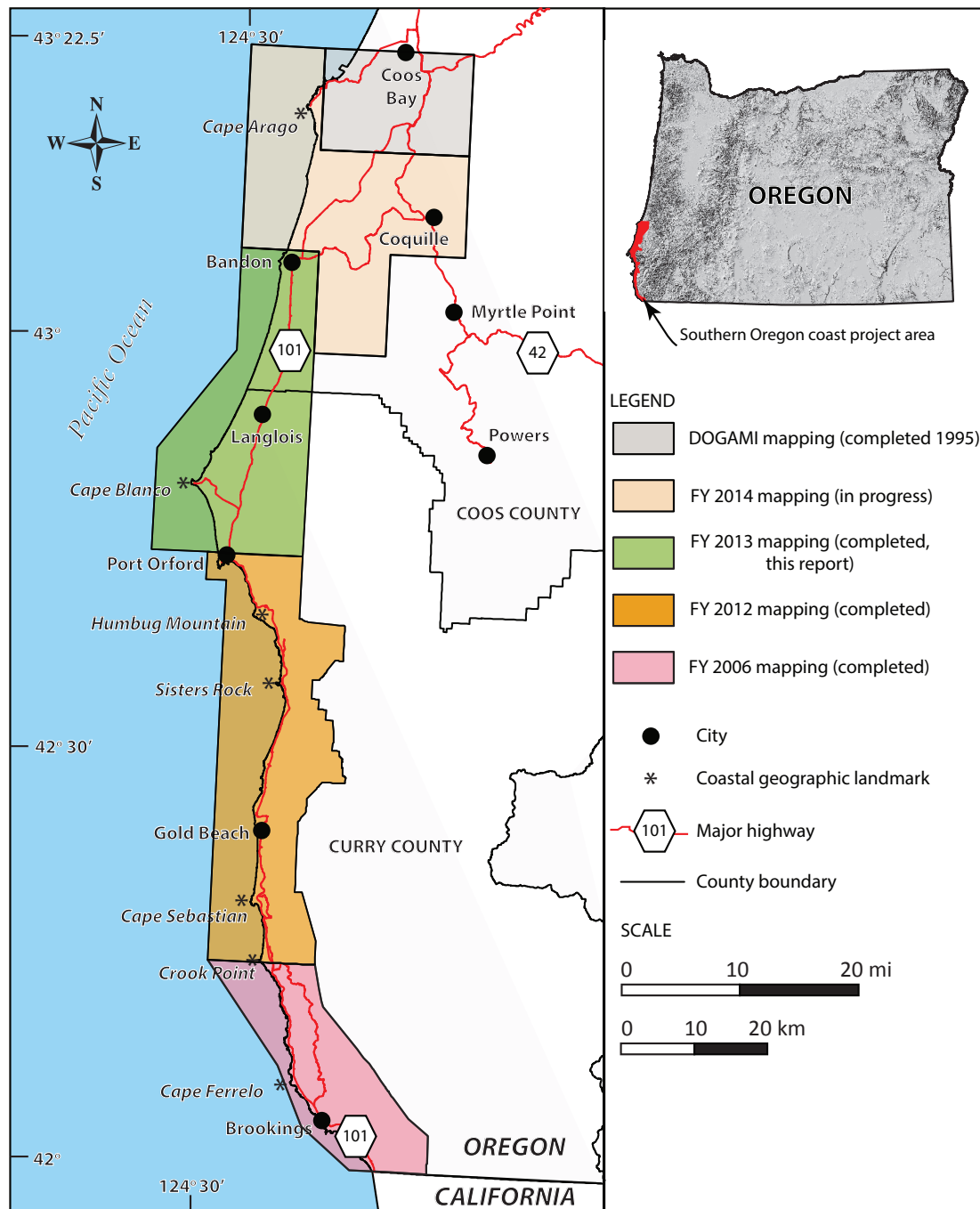


Figure 1. Location of the map area in southwestern Oregon, including major cities, geographic locations, and highways discussed in the text. Light-red shade is the area mapped by the Oregon Department of Geology and Mineral Industries during FY (fiscal year) 2006; orange shade is the area mapped during FY 2012; green shade is the current map area discussed in this report. The tan-shaded area includes quadrangles anticipated for geologic mapping during FY 2014. The gray-shaded area was mapped at the 1:24,000 scale by Madin and others (1995) and Black and Madin (1995).

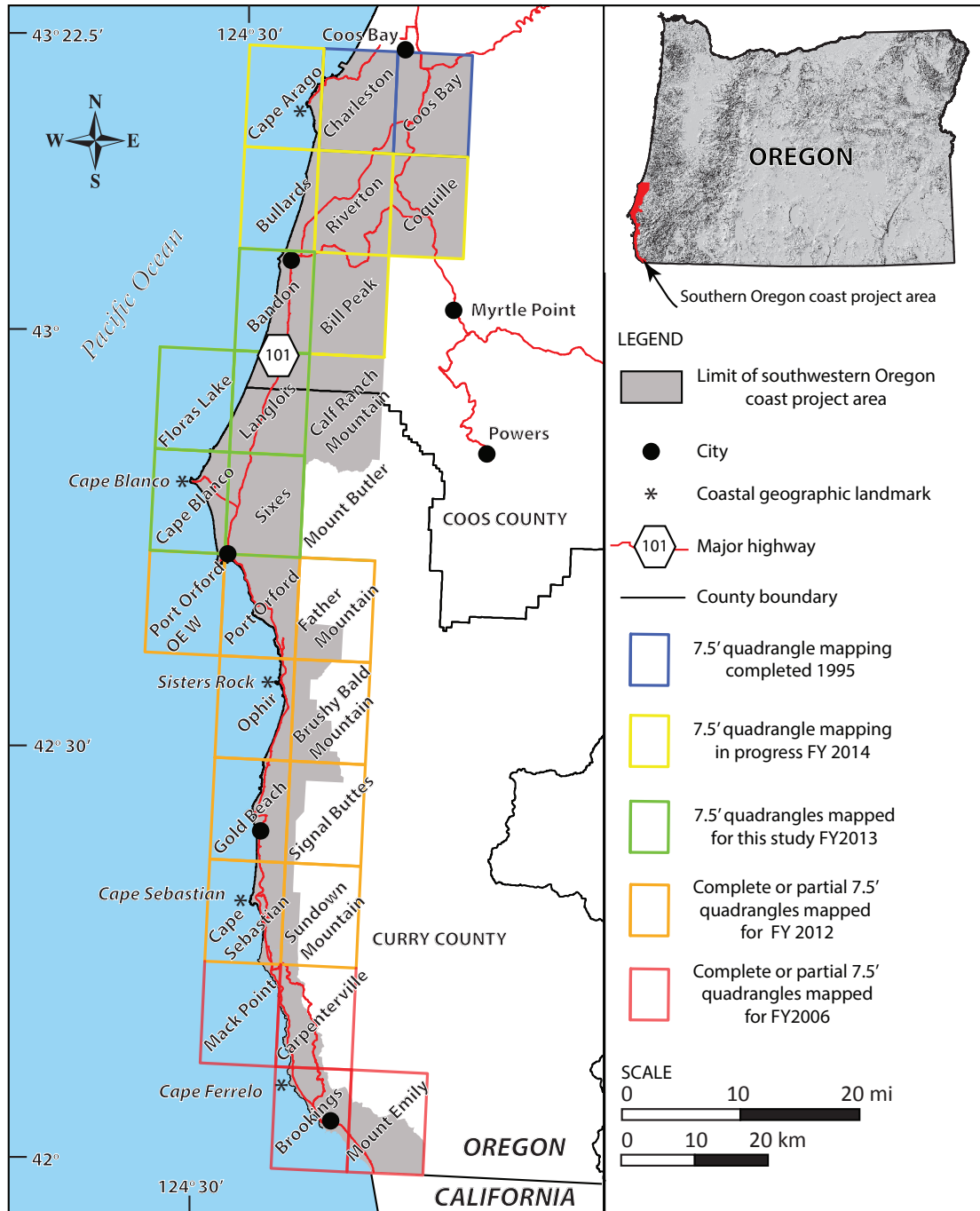


Figure 2. The current project area (gray shade within green-outlined 7.5-minute quadrangles) encompasses approximately 388 km² (150 mi²) along the southern Oregon coast and parts of five 7.5-minute quadrangles. Gray shade is the entire southern Oregon coast mapping area. Red-outlined quadrangles include geologic mapping completed during FY (fiscal year) 2006; green-outlined quadrangles include geologic mapping completed during this study; orange-outlined quadrangles include geologic mapping completed during FY 2012; yellow-outlined quadrangles are areas proposed for geologic mapping in FY 2014; blue-outlined quadrangles were mapped at the 1:24,000 scale by Madin and others (1995) and Black and Madin (1995).

GEOGRAPHIC AND GEOLOGIC SETTING

The coastal region of southwestern Oregon is typically rugged, with a 1- to 7-km-wide (0.6 to 4.3 mi), wave-cut coastal bench that changes abruptly into deeply incised, upland topography of the Coast Range. Topographic relief is moderate, ranging from sea level to numerous ridges and mountains including, from south to north, Grassy Knob (714 m [2,342 ft]), Grouselous Mountain (776 m [2,546 ft]), Summit Mountain (738 m [2,420 ft]), White Mountain (680 m [2,229 ft]), Round Top (410 m [1,344 ft]), Morton Butte (222 m [729 ft]), and Woodens Butte (295 m [968 ft]) (see map plates). The Coast Range is drained in the map area by a number of west-flowing streams. Major stream drainages include the Elk River, Sixes River, Floras Creek, Fourmile Creek, Twomile Creek, and the Coquille River. The rugged coastal relief is accompanied by a wet maritime climate (precipitation is ~188 cm/yr [74 in/yr]) and dense vegetation. Due to steep topography and thick, impenetrable forests, good outcrops of unaltered rock are generally limited to sea stacks, coastal bluffs, stream bottoms, road cuts, and areas of active logging.

Bedrock geology along the southern Oregon coast is composed of complexly folded, faulted, and variably metamorphosed Mesozoic tectonostratigraphic terranes that record a history of oceanic, volcanic arc, and continental margin sedimentation, magmatism, and terrane accretion during the Late Jurassic and Cretaceous (Dott, 1971; Roure and Blanchet, 1983; Blake and others, 1985; Diller, 1896, 1901, 1903). These terranes are situated inboard of the active Cascadia subduction zone, where oceanic crust is presently being obliquely subducted beneath the North American continental plate (Figure 3). To the east, late Mesozoic terranes of the study area are overthrust along regional-scale thrust faults by Mesozoic and older terranes of the Klamath Mountains province. Blake and others (1985) recognized six discrete terranes underlying the coastal area of southwestern Oregon (Figure 4), all of which are separated by major faults or fault zones. Most often these fault zones are low-angle thrusts, so that the terrane assemblage represents stacks of subhorizontal nappes (Blake and others, 1985). The terrane assemblage in the study area includes the Gold Beach, Sixes River, Pickett Peak, and Western Klamath (Elk subterrane) terranes (Blake and others, 1985). The Snow Camp terrane is located east of the study area, the

Siletz terrane is located to the north and northeast, and the Yolla Bolly terrane is located to the south. The various tectonostratigraphic terranes are overlapped by Upper Cretaceous and younger sedimentary sequences that give minimum ages for amalgamation of the terranes.

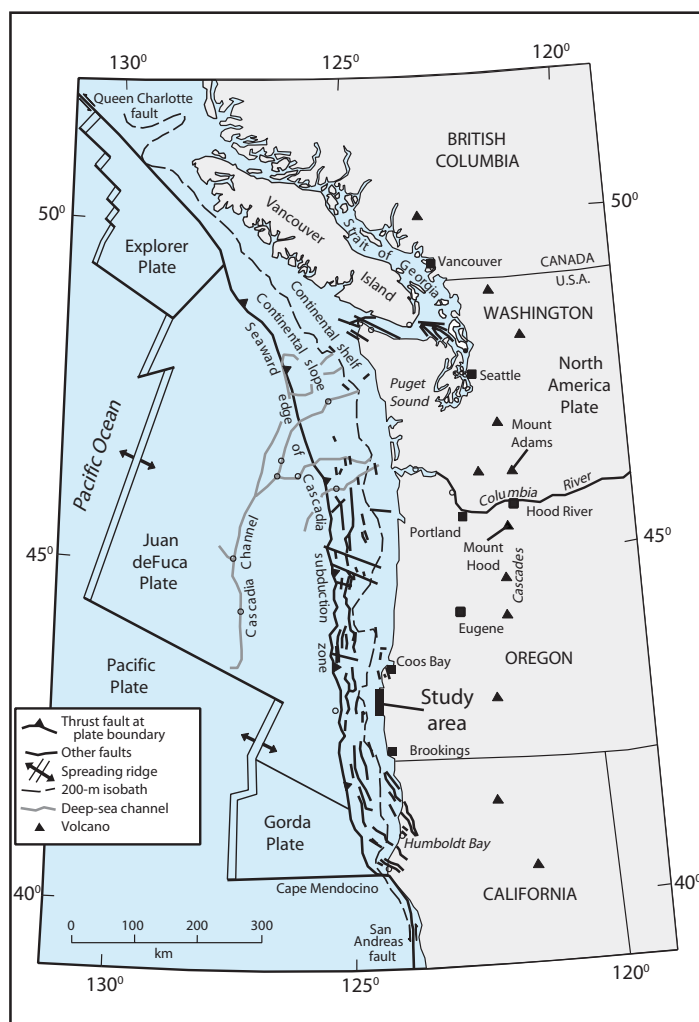


Figure 3. Tectonic setting of the Pacific Northwest region of the United States (modified from Nelson and others, 2004) showing the Cascadia Subduction Zone and regional plate boundaries, selected Quaternary faults in the North American plate, and the location of the study area along the southern Oregon coast. The deformation front (barbed line) is defined by bathymetry where the abyssal plain meets the continental slope and is inferred to represent the surface projection of the Cascadia thrust fault.

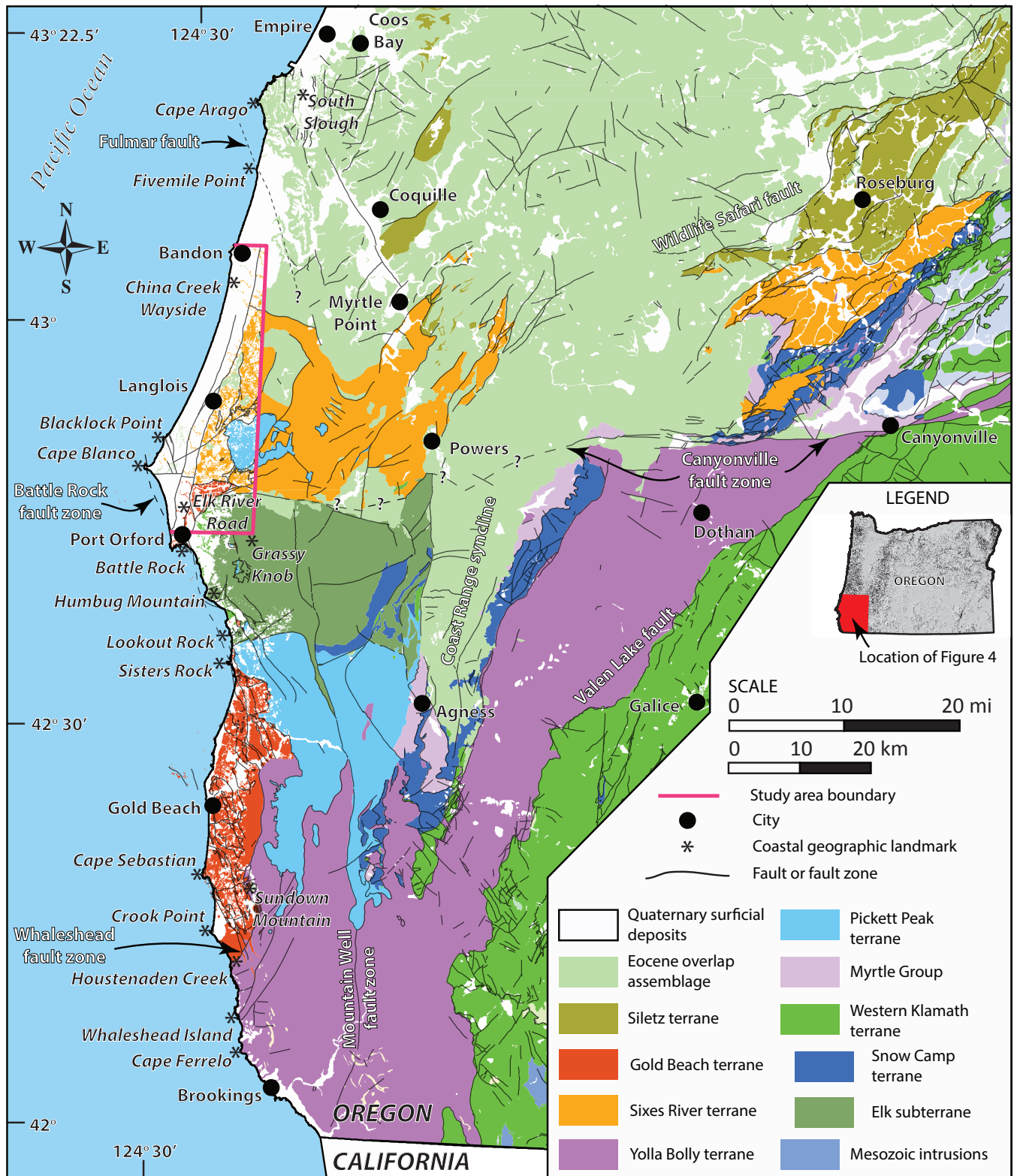


Figure 4. Tectonic sketch map showing tectonostratigraphic terranes of southwestern Oregon. Geology from Ma and others (2009) with terrane boundaries modified from Blake and others (1985).

Gold Beach terrane

The Gold Beach terrane is the westernmost terrane along the southern Oregon coast, extending in a narrow strip from Whaleshead Island on the south to Cape Blanco on the north (Figure 4, Plate 1; Blake and others, 1985; Bourgeois and Dott, 1985). It is separated from the Sixes River, Yolla Bolly, and Western Klamath terranes to the east by the north-trending, high-angle Battle Rock fault zone and its southern extension, the Whaleshead fault zone (Figure 4). Between Port Orford and Cape Blanco the Battle Rock fault zone steps west such that the northernmost exposures of the Otter Point Formation (**KJos**) at Cape Blanco lie west of the Sixes River terrane while the Otter Point Formation at Port Orford lies west of the Elk subterrane of the Western Klamath terrane. Between Port Orford and Cape Blanco, the Gold Beach terrane is separated from the Sixes River terrane by a steeply dipping, east-west-trending fault that we interpret to be the western end of the Canyonville fault.

The Gold Beach terrane includes the Lower Cretaceous and Upper Jurassic (Tithonian to Hauterivian) Otter Point Formation (**KJos**; Koch, 1966; Aalto and Dott, 1970) and an unconformable, overlapping sequence of mid- to Upper Cretaceous sedimentary units that include the Albian(?) to lower Campanian Houstonaden Creek Formation (Bourgeois, 1980a), the middle-late Campanian Cape Sebastian Sandstone, and the Campanian to lower Maastrichtian(?) Hunters Cove Formation (Dott, 1971).

The Otter Point Formation is a structurally complicated succession of volcanoclastic sandstone, and mudstone that forms uplands south of the western extension of the Canyonville Fault and erosionally resistant headlands and sea stacks along the coastline at Cape Blanco (Plate 1; Koch, 1963, 1966; Aalto, 1968; Aalto and Dott, 1970; Dott, 1971; Walker, 1977). In the study area volcanic rocks associated with the Otter Point Formation are represented only by relatively small, probably fault bounded, blocks. However, to the south, between Sundown Mountain and Sisters Rock the otherwise sedimentary-dominated formation includes north-northwest-trending bands of pillow lava and volcanic breccia (McClaghry and others, 2013). Linear zones, defined by concentrations of variously indurated blocks of volcanic rock (**KJov**) and serpentinite (**Spu**) mark the surface traces of major intraformational shear zones and faults. Metamorphism in the Otter Point Formation is limited to numerous veins of laumontite; pillow lavas locally display the effects of ocean-floor metamorphism defined by the presence of prehnite, pumpellyite, and epidote (Blake and others, 1985). Rocks composing the Otter Point Formation are pervasively sheared, folded, and faulted to the

point where original stratigraphic continuity is difficult to determine. The structural character of the Otter Point Formation is consistent with that of a “broken formation” (Hsü, 1968; Festa and others, 2010, 2012), where strata are significantly disrupted, but lack the pervasively deformed matrix, mixing, or “exotic” elements (e.g., lithologies derived from outside the formation, such as blueschist) characteristic of a *mélange* (Berkland and others, 1972; Wood, 1974; Silver and Beutner, 1980; Raymond, 1984; Cowan, 1985). Sedimentary strata in the Otter Point Formation are thought to have been deposited as turbidites, principally in deep water, submarine slope, fan, and fan-channel settings adjacent to an island arc (Aalto and Dott, 1970; Dott, 1971). Pervasive shearing of sedimentary and volcanic units within the Otter Point Formation indicates tectonic emplacement (accretion) along the continental margin over a period of time extending from the Late Jurassic to the Early Cretaceous.

Upper Cretaceous rocks are largely absent in the study area. Their mapped distribution on offshore sea stacks southwest of Cape Blanco is compiled from Hunter and others (1970). Sea stack exposures are mapped together as unit **Kugb**. These rocks are likely similar to those that crop out along the coast south of Gold Beach (Hunter and others, 1970). There, three mid- to Upper Cretaceous formations include conglomerate, sandstone, and mudstone that differ compositionally from the Otter Point Formation (Bourgeois, 1980a,b; Bourgeois and Dott, 1985) which they overlie with angular unconformity. Sandstone in these younger formations is dominantly volcano-lithic, feldspathic arenite. Means of eight grain counts from mid- to Upper Cretaceous formations by Hunter and others (1970) have 28% quartz, 29% rock fragments, and 25% feldspar with minor mica, heavies, cement, and detrital matrix. Clasts in Houstonaden Creek Formation conglomerate consist largely of volcanic lithologies not found in the Otter Point Formation. Conglomerate clasts in the overlying Hunters Cove Formation and Cape Sebastian Sandstone are similar to those in the older Otter Point Formation. Upper Cretaceous rocks exposed north of Blacklock Point may be part of the Gold Beach terrane, but are here mapped as Cretaceous rocks associated with the Sixes River terrane that surrounds the outcrop. East of Gold Beach the Otter Point Formation is unconformably overlain by lithologically distinct Cretaceous chert-pebble conglomerate and mudstone, but these rocks have not been recognized this far north.

The mid- to Upper Cretaceous sequence grades upward from deep water to shallow water and back to deep water facies. The oldest formation, the Houstonaden Creek Formation, may have been faulted into its present position

above the Otter Point Formation. The overlying Cape Sebastian Sandstone and Hunters Cove Formation are inferred to have been deposited in a borderland-type basin that developed concurrently with a seascape of steeply faulted Hostenaden Creek and Otter Point strata (Bourgeois and Dott, 1985). Although the Upper Cretaceous overlap units in the Gold Beach terrane are pervasively faulted, they are not intensely sheared. Upper Cretaceous rocks in the Gold Beach terrane are unmetamorphosed.

Sixes River terrane

The Sixes River terrane (Figure 4) includes intensely sheared broken formation composed of Tertiary, Upper Cretaceous, Lower Cretaceous and Upper Jurassic sedimentary rocks and large areas of mudstone- and fine sandstone-matrix *mélange*. Sedimentary rocks within the Sixes River terrane were previously mapped as Otter Point Formation by Lent (1969), Dott (1971), Beaulieu and Hughes (1976), and Brownfield and others (1982). Unlike the Otter Point Formation in the Gold Beach terrane, the sedimentary sequences in the Sixes River terrane have a quartzofeldspathic composition (Lent, 1969). *Mélange* units within the terrane are defined by numerous exotic tectonic blocks (knockers) including high-grade blueschist, garnet schist, and eclogite (Coleman and Lanphere, 1971). In this report the terrane is divided into three adjacent subterranees that contain blocks of exotic blueschist and garnet schist but have important tectono-stratigraphic features that are not shared. Two of these are present within the map area; the third is exposed east of the study area.

Cape Blanco (western) subterrane—The Cape Blanco (western) subterrane of the Sixes River terrane consists of mudstone- and fine-sandstone-matrix *mélange* that enclose a suite of harder blocks of various lithologies including sandstone, conglomerate, chert, serpentinite, glaucophane schist, and garnet schist (eclogite). These rocks differ from the other two subterranees of the Sixes River terrane in that they contain relatively mica-poor middle Eocene turbidites at Cape Blanco (Bandy, 1944). These thin-bedded turbidites were mapped as a single body by Addicott (1983) and, alternatively, as slivers in the *mélange* unit of the terrane by Dott (1971). In this report these rocks are interpreted as forming some, or all, of the *mélange* matrix. The *mélange* in this area is younger than fossils indicate for the Fulmar and Whitsett subterranees exposed farther to the east. Micaceous middle Eocene sedimentary rocks assigned to the Sacchi Beach beds north of Bandon (outside the study area) have fossil assemblages similar to those collected from dismembered

turbidites (*mélange* matrix) at Cape Blanco (Bandy, 1941, 1944). The Cape Blanco subterrane is separated from the Gold Beach terrane by the northern extension of the Battle Rock – Whaleshead fault zone and from the Fulmar subterrane by the Blacklock Point fault or a similar fault buried beneath Miocene and younger sedimentary rocks farther east.

Fulmar (central) subterrane—The Fulmar (central) subterrane of the Sixes River terrane includes a mudstone and fine-sandstone matrix *mélange* with overlying Cretaceous and lower Eocene sedimentary rock. The lower Eocene section includes turbidites that are part of the sandstone of Fivemile Point, a mica-poor, quartzofeldspathic wacke that is unlike lower Eocene sandstone recognized farther to the east (Snively, 1987) in the Whitsett subterrane. The boundary between the Fulmar subterrane and the Cape Blanco subterrane is tentatively considered to be the Blacklock Point fault, a significant shear zone that juxtaposes *mélange* of the Cape Blanco subterrane (**TJs**), serpentinite (**Spu**), and Upper Cretaceous sedimentary rocks (**Ku**) at Blacklock Point. The actual fault boundary may be buried beneath Miocene rocks (**Tmf**, **Tme**, **Tmc**) farther to the northeast.

Whitsett (eastern) subterrane (not present at the surface in the study area, may be present in the subsurface)—The eastern part of the Sixes River terrane includes a basal mudstone- and fine-sandstone-matrix *mélange* and overlying Cretaceous(?) and lower Eocene sedimentary rocks. This subterrane may be present in the subsurface in the extreme eastern part of the study area, but it is not exposed at the surface. The Whitsett subterrane is distinguished from the Fulmar and Cape Blanco subterranees by the contrasting provenance of lower Eocene sandstone east and west of the Fulmar fault and by the presence of the exotic Whitsett limestone lentils (blocks) of Diller (1898). This group of far-traveled mid-Cretaceous age (Albian and/or Cenomanian, ca. 113 to 93.9 Ma) blocks crop out south of Roseburg, but probably originated in southern latitudes (Sliter, 1984). The Whitsett subterrane of the Sixes River terrane is likely separated from the Fulmar subterrane by the Fulmar fault or a similar north-northwest-trending structure. Snively and others (1985) recognized that the Fulmar fault separates stratigraphically different sequences in offshore areas north of Fivemile Point (north of study area). This fault, or perhaps a similar structure buried beneath the Tertiary overlap sequence somewhere between Bandon and Coquille, separates the Whitsett subterrane from the Fulmar subterrane to the west.

Pickett Peak terrane

The Pickett Peak terrane is exposed over an area extending from Agness on the east to Lookout Rock on the coast (outside present study area); the southernmost exposures are near the Pistol River (outside present study area) and the northernmost near Floras Creek (Plate 2; Figure 4). Unlike structurally lower terranes, the Pickett Peak terrane is present in the study area north and south of the Canyonville fault. The Pickett Peak terrane includes the Colebrooke Schist (**Kcqs**), a metamorphic assemblage of phyllite, psammite, schist, and gneiss that have thin-bedded shale and sandstone and associated minor pillow lava, tuff, and chert protolith (Diller, 1903; Dott, 1971; Coleman, 1972; Blake and others, 1985). Mineral assemblages indicate that metamorphic grade of the schist is intermediate between blueschist and greenschist facies. An underlying serpentinite-matrix mélange contains blocks of volcanic rock, sandstone, and chert (Plate 2, cross section A-A'). The most common lithologies within the Pickett Peak terrane are quartz-mica phyllite, schist, and serpentinite. Possible protoliths for these rocks include fine-grained, pelitic sediments of the Galice Formation and meta-igneous blocks derived from the Josephine and Coast Range ophiolites (Coleman, 1972; Katrib, 2006). K/Ar ages reported by Dott (1971), date the age of metamorphism of the Colebrooke Schist between 142 and 125 Ma. The schist has been correlated to the Redwood Creek and South Fork Mountain schists in Northern California (Cashman and Cashman, 1989). The Colebrooke Schist forms a nappe that structurally overlies serpentinite (serpentinite-matrix mélange) and low-grade metamorphic rocks of the Gold Beach and Yolla Bolly terranes south of the Canyonville fault and the Sixes River terrane north of the fault. Where its contact with the Western Klamath terrane (Elk subterrane) is exposed, the Colebrooke Schist and a subjacent serpentinite-matrix mélange lie structurally beneath Lower Cretaceous sedimentary rocks of the Humbug Mountain Conglomerate (**Khcg**).

Western Klamath terrane, Elk subterrane

The Western Klamath terrane is the youngest part of a generally westward-younging stack of eastward-dipping, imbricate thrust sheets within the Klamath Mountains (Figure 4). Along the southern Oregon coast, an outlier of the Western Klamath terrane, known as the Elk subterrane, is exposed between Humbug Mountain and Port Orford. It consists of unmetamorphosed conglomerate, sandstone, and mudstone assigned to the Lower Cretaceous (Berriasian or Valanginian) Humbug Mountain Conglomerate (**Khcg**) and Rocky Point Formation (**Krp**) of Koch (1963, 1966).

Along the Elk River, south of the study area, the Galice Formation is in complex fault contact with an Upper Jurassic sheeted dike complex, the Colebrooke Schist (**Kcqs**), and a serpentinite matrix mélange containing a diverse assemblage of igneous, meta-sedimentary, and high-grade metamorphic rocks (Giaramita and Harper, 2006; McClaughry and others, 2013).

A few miles to the east the Western Klamath terrane is represented by the Upper Jurassic (Oxfordian to early Kimmeridgian) Galice Formation, a sequence of dark slate and slaty mudstone, meta-graywacke, minor greenstone, thin-bedded sandstone, and chert (Dott, 1971; MacDonald and others, 2006; Giaramita and Harper, 2006). The Galice Formation was deposited conformably upon both the ca. 160 to 157 Ma Rogue-Chetco volcano-plutonic arc complex and the ca. 164 to 162 Ma Josephine ophiolite (Harper and others, 1994), and was regionally metamorphosed to prehnite-pumpellyite to lower greenschist facies during the Late Jurassic (Nevadan orogeny; Blake and others, 1985; Harper and others, 1988; MacDonald and others, 2006).

Within the Elk subterrane but south of the study area, the Galice Formation is intruded by the Late Jurassic or Early Cretaceous Pearse Peak Diorite, an intrusive body consisting of hornblende-biotite-quartz diorite (Beaulieu and Hughes, 1976). Radiometric ages for the pluton range between 148 ± 4 Ma and 144 ± 7 Ma (K/Ar biotite; Giaramita and Harper, 2006, recalculated from Dott, 1965).

Yolla Bolly terrane, Snow Camp subterrane of the Western Klamath terrane, and Siletz terrane

Three other tectonostratigraphic terranes, the Yolla Bolly, the Snow Camp subterrane of the Western Klamath terrane, and Siletz terrane, occur nearby.

The Yolla Bolly terrane consists mainly of volcanogenic to quartzofeldspathic sedimentary rocks (sandstone, mudstone, and conglomerate) distinguished by detrital muscovite or K-feldspar bearing wacke that forms a broken formation of dismembered turbidites assigned to the Lower Cretaceous and Upper Jurassic (Tithonian to Hauterivian) Dothan Formation. Also included are tectonic and submarine landslide (olistostrome) blocks of pillow lava, volcanic and volcanoclastic rock, radiolarian chert, and serpentinite. The terrane extends from the Valen Lake thrust fault on the east to the southernmost coastal community of Brookings on the west (Figure 4; Dott, 1971; Blake and others, 1985). The Yolla Bolly terrane is separated from the Gold Beach terrane to the north and west by the Whaleshead fault zone. East of the present study area the Yolla Bolly terrane crops out north and south of the Canyonville fault, which offsets

rocks of the Dothan Formation in an apparent right-lateral or up-to-the-north sense. The Yolla Bolly terrane in Oregon is equivalent to parts of the adjacent Franciscan Group in California that have similarly been mapped as amalgamated exotic terranes (Blake and others, 1985; Seiders and Blome, 1987), as *mélange* (Walker and MacLeod, 1991), and as a somewhat more intact accretionary complex with exotic components (Roure, 1986).

The Snow Camp subterrane of the Western Klamath terrane contains rocks correlative to the Coast Range ophiolite and a related overlap sequence, the Myrtle Group (Blake and others, 1985). These rocks crop out north and south of the Canyonville fault about 60 miles (100 km) east of the study area. The stratigraphy of this subterrane is very similar in age and lithology to that of the Elk subterrane of the Western Klamath terrane, differing mainly in the relative amounts of fine- and coarse-grained Late Jurassic (Oxfordian-Kimmeridgian) sediment (e. g., Galice Formation in the Elk subterrane, Riddle Conglomerate in the Snow Camp subterrane). The Riddle Conglomerate is similar to but in part older than the Humbug Mountain Conglomerate, and the Days Creek Formation is similar to the Rocky Point Formation.

The Siletz terrane consists of a thick accumulation of Paleocene and early Eocene oceanic basalt and less common diabase and gabbro overlain by early Eocene sedimentary rocks (Wells and others, 2000). North of the Canyonville fault, between Coquille and Roseburg, these rocks are thrust beneath the Sixes River terrane along the Wildlife Safari and related faults.

Paleogene sedimentary rocks that overlap western Jurassic terranes and eastern terrane of the Sixes River terrane

Eocene sedimentary rocks assigned to the Umpqua Group and younger formations such as the Tyee Formation lap across the Western Klamath terrane and adjacent parts of the Sixes River, Siletz, and Yolla Bolly terranes. These rocks record unroofing of the Klamath Mountains composite terrane and the Siletz terrane. Deposition of sedimentary sequences across terrane boundaries indicate minimum ages for juxtaposition of the terranes. Farther west, lower Eocene rocks including the sandstone of Fivemile Point have unique characteristics that distinguish them from coeval rocks in the Umpqua Group (Snively, 1987). Micaceous sandstone formations including the middle Eocene Sacchi Beach beds, Coaledo Formation, and Tyee Formation that crop out in the overlap sequence near Coquille, Oregon, contrast with relatively coeval mica-poor rocks in the Cape Blanco subterrane of the Sixes River terrane.

Lower Pleistocene and Miocene rocks

A Miocene sequence including, from base to top, the sandstone of Floras Lake, the Empire Formation, and the diatomite of China Creek laps across the contact between the Gold Beach and Sixes River terranes between Port Orford and Bandon (Plates 1, 2, and 3). The early Miocene age (>18 Ma) of the sandstone of Floras Lake is a minimum age for the juxtaposition of Gold Beach and Sixes River terranes.

Lower Pleistocene strata of the Port Orford Formation crop out north of the mouth of the Elk River.

PREVIOUS WORK

Table 1 shows a list of previous regional geologic investigations used to inform the current study of the southern Oregon coast. The index map shown in Figure 5 summarizes the sources of mapping used for our geologic depiction and other sources consulted during the preparation of this report. Following Diller (1903), the geology of the coastal area between the California border and Coos Bay has been mapped by a number of workers, each focusing on small parts of the area and at a variety of scales (Howard, 1961; Koch, 1960; Howard and Dott, 1961; Dott, 1962; Kaiser, 1962; Widmier, 1962; Schwab, 1963; Burt, 1963; Koch, 1963, 1966; Lent, 1969; Baldwin, 1969; Lund and Baldwin, 1969; Hunter and others, 1970; Dott, 1971; Coleman, 1972; Baldwin and others, 1973; Baldwin, 1974; Beaulieu and Hughes, 1975, 1976; Ramp and others, 1977; Gullixson, 1981; Brownfield and others, 1982; Walker and MacLeod, 1991; Madin and others, 1995; Black and Madin, 1995). Various other studies have examined more detailed aspects of regional tectonics (Coleman, 1972; Heller, 1983; Blake and others, 1985; Roure and Blanchet, 1983; Roure, 1986; Bourgeois and Dott, 1985), petrography and provenance of the Otter Point Formation (Goodfellow, 1987), invertebrate paleontology of the Cape Blanco area (Bandy, 1941, 1944; Baldwin, 1945; Addicott, 1983), mineral resources (Libbey and others, 1947; Boggs, 1969), and coastal landforms (Lund, 1973, 1975). The tectonics of Pleistocene coastal terraces was discussed by Janda (1969, 1970), Kelsey (1990), Muhs and others (1990), McInelly and Kelsey (1990), and Kelsey and Bockheim (1994). Tsunami hazard maps have been produced by DOGAMI for the length of the coast between the California border and Bandon (Priest and Baptista, 1995a–p; Priest and others, 2000, 2002; DOGAMI, 2012a–g). A hazard inventory map of the Oregon coastal zone was published by Beaulieu and others (1974). Geologic hazards including landslides (Burns and Watzig, 2014), subduction zone earthquakes (Goldfinger and others, 2012), and tsunamis (Witter and others, 2003, 2011) are treated in greater detail in other reports and data releases.

Because good outcrops may be short-lived, widely separated, or quickly overgrown, older geologic maps cited in this report should be consulted for alternative interpretations.

Table 1. Partial chronological listing of maps and reports on which this study builds.

Author	Year	Subject	Scale
Diller	1903	Description of the Port Orford quadrangle	
Bandy	1941	Invertebrate paleontology of Cape Blanco	
Baldwin	1945	Cenozoic stratigraphy, southern Oregon coast	
Dott	1962	Geology of the Cape Blanco area	
Koch	1963	Mesozoic orogenesis and sedimentation, Klamath Province	1:79,200
Addicott	1964	Invertebrate fauna of southwestern Oregon	
Koch	1966	Stratigraphy and tectonic history, Port Orford-Gold Beach area	
Aalto	1968	Sedimentology of the Otter Point Formation	
Boggs	1969	Distribution of heavy minerals in the Sixes River	
Lent	1969	Geology of the southern Langlois quadrangle	1:31,250
Baldwin	1969	Geologic map of the Myrtle Point area	1:250,000
Lund & Baldwin	1969	Diorite intrusions between Sixes and Pistol Rivers	
Janda	1969	Age of marine terraces near Cape Blanco	
Hunter & others	1970	Geology of the stacks and reefs off the southern Oregon coast	
Dott	1971	Geology of the southwestern Oregon coast	1:62,500 1:250,000
Brownfield	1972	Geology of the Floras Creek drainage	1:31,250
Coleman	1972	The Colebrooke Schist of southwestern Oregon	
Baldwin & others	1973	Geology and mineral resources of Coos County	1:62,500
Baldwin	1974	Eocene stratigraphy of southwestern Oregon	
Beaulieu & others	1974	Geologic hazards inventory of the Oregon Coastal Zone	1:250,000
Lund	1975	Landforms along the coast of Curry County	
Beaulieu & Hughes	1975	Environmental geology of western Coos and Douglas counties	1:62,500
Beaulieu & Hughes	1976	Land-use geology of western Curry County	1:62,500
Ramp & others	1977	Geology, mineral resources, and rock material of Curry County	1:125,000
Blake & others	1985	Tectonostratigraphic terranes in southwest Oregon	
Brownfield & others	1982	Geology of the Langlois quadrangle	1:62,500
Garey	1987	Radiolaria from the Otter Point Complex	
Snively	1987	Geologic framework of the OR-WA continental margin	
Seiders & Blome	1987	Upper Cretaceous rocks in coastal southwest Oregon	
Goodfellow	1987	Petrography/provenance of sandstones Otter Point Formation	
Kelsey	1990	Deformation of coastal terraces, Cape Blanco	1:728,952
McInelly & Kelsey	1990	Deformation of coastal terraces near Bandon	1:10,934,280
Muhs and others	1990	Uplift rates for late Pleistocene marine terraces	
Walker & MacLeod	1991	Geologic map of Oregon	1:500,000
Kelsey & Bockheim	1994	Coastal landscape evolution	
Kelsey & others	1998	Coseismic subsidence recorded in Sixes River estuary	
Kelsey & others	2002	Cascadia earthquakes recorded in Sixes River estuary	
Witter & others	2003	Cascadia earthquakes recorded in Coquille River estuary	
Kelsey & others	2005	Tsunami history of Bradley Lake	
Peterson & others	2007	Upland coastal dune sheets in Oregon	1:295,200

Reports used to compile the southwestern Oregon coast geodatabase are shown in boldface. Author(s), date, abbreviated subject(s), and map scale (if appropriate) are shown; more complete references are listed at the end of this report.

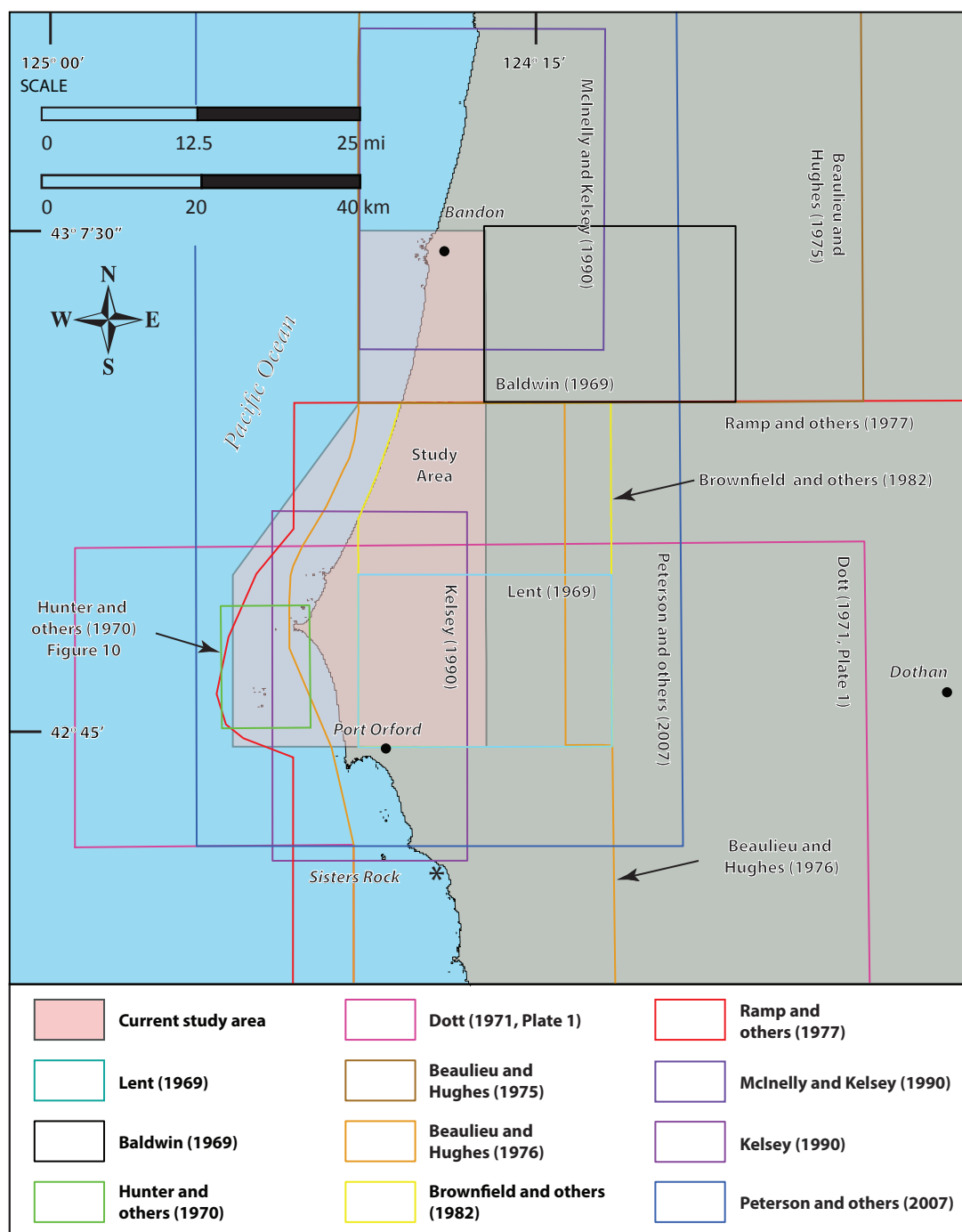


Figure 5. Sources of geologic mapping used during the preparation of this report.

METHODOLOGY

Geologic data were collected digitally using a GPS-enabled Apple™ iPad 2 loaded with iGIS™, a geographic information system software package compatible with Esri ArcGIS™. Digital mapping used tiled, hillshaded raster images, derived from high-resolution (8 pts/m²) lidar digital elevation models (DEMs) as basemaps. Additional basemap information was derived from standard 1:24,000-scale USGS digital raster images (DRGs) and digital orthophoto imagery (2013) obtained from Google Earth™. Fieldwork conducted during 2013 and 2014 consisted largely of data collection along major highways and roads. Where access was available, secondary roads across rangelands and timberlands provided more detailed information between otherwise widely spaced traverses. The geology shown for offshore sea stacks has been compiled from earlier work by Weissenborn and Snively (1968) and Hunter and others (1970). The distribution of approximately 1,350 landslide deposits mapped in the area was determined remotely, using an established protocol for the inventory mapping of landslide deposits from lidar imagery developed by Burns and Madin (2009). A small percentage (~15 percent) of remotely mapped landslide deposits were field checked for accuracy during the course of fieldwork. The shoreline boundary depicted on the geologic maps represents the land-water interface at the mean high water tidal datum as determined from lidar by the National Oceanic and Atmospheric Administration (NOAA). Current shoreline data for North America is available for download from the NOAA shoreline data explorer at <http://www.ngs.noaa.gov/CUSP/>.

New mapping was compiled with published and unpublished data, and converted into digital format using Esri ArcGIS™ ArcMap™ 10.1 GIS software. On-screen digitizing was performed on a Cintiq™ touch monitor using georeferenced 1-m lidar DEMs and 1:24,000-scale USGS digital raster images (DRGs) as base maps. Geologic interpretations were aided by GIS analyses based in part on 1-m lidar DEMs, USGS 10-m DEMs, and 2011 National Agriculture Imagery Program (NAIP) digital orthophotos. The mapped distribution of surficial deposits is derived in part from soils maps and descriptions published by the Natural Resource Conservation Service (NRCS) of the U.S. Department of Agriculture (Haagen, 1989; Fillmore, 2005). Lidar DEMs were used to depict the distribution of both bedrock and surficial geologic units at a maximum scale of 1:8,000. The geologic time scale used is the September, 2010, version of the International Stratigraphic Commission's Inter-

national Stratigraphic Chart (<http://www.stratigraphy.org/ICSchart/StratChart2010.pdf>) revised from that of Gradstein and others (2004) and Ogg and others (2008).

Mapping was supported by new and compiled X-ray fluorescence (XRF) geochemical analyses of whole-rock samples, new and compiled radiometric age determinations, thin-section petrography, strike and dip measurements of inclined bedding, and structural measurements of foliations (Plates 1, 2, and 3; appendix). Whole-rock geochemical samples were prepared and analyzed by X-ray fluorescence (XRF) at the Department of Geosciences, Franklin and Marshall College, Lancaster, Pennsylvania. Analytical procedures for the Franklin and Marshall X-ray laboratory are described by Boyd and Mertzman (1987) and Mertzman (2000), and are available online at <http://www.fandm.edu/x7985>. Major element determinations are normalized to a 100-percent total on a volatile-free basis and recalculated with total iron expressed as FeO*. Descriptive rock unit names for volcanic rocks are based in part on the online British Geological Survey classification schemes (Gillespie and Styles, 1999; Robertson, 1999; Hallsworth and Knox, 1999) and normalized major element analyses plotted on the total alkalis (Na₂O + K₂O) versus silica (SiO₂) diagram (TAS) of Le Bas and others (1986), Le Bas and Streckeisen (1991), and Le Maitre and others (1989, 2004). Four new ²⁰⁶Pb/²³⁸U radiometric age determinations, derived from detrital zircons in sandstones were prepared and analyzed by Jonathan Rivas under the direction of Dr. Joshua Schwartz at California State University–Northridge. Chang and others (2006) described the sample preparation methods and data collection techniques employed for obtaining the zircon ages. Microsoft Excel® spreadsheets tabulating geochemical analyses, isotopic ages, strike and dip measurements, and additional structural measurements are provided as part of this publication and are located in the appendix.

In this report, volcanic rocks with fine-grained (<1 mm [0.04 in]; Mackenzie and others, 1997; Le Maitre and others, 2004) average crystal or particle size in the groundmass are described as having “coarse groundmass” if the average size is <1 mm (0.04 in) and they can be determined using the naked eye (>~0.5 mm [0.02 in]); as having “medium groundmass” if crystals of average size cannot be determined by eye, but can be distinguished using a hand lens (>~0.05 mm [0.02 in]); as having “fine groundmass” if crystals or grains of average size can only be determined using a microscope (or by hand lens recognition of phyl-

lite-like sparkle or sheen in reflected light, indicating the presence of crystalline groundmass); or as having a "glassy groundmass" if the groundmass has (fresh), or originally had (altered), groundmass with the characteristics of glass (conchoidal fracture; sharp, transparent edges; vitreous luster; etc.). Mixtures of crystalline and glassy groundmass are described as intersertal; ratios of glass to crystalline materials may be indicated by textural terms including holocrystalline, hypocrySTALLine, hyalophitic, and hyalopilitic. Microphenocrysts are defined as crystals larger than the overall groundmass and < 1 mm across (0.04 in).

Intrusive igneous rocks are described as being coarse-grained if crystal diameters exceed 5 mm (0.2 in); as being medium-grained if the absolute range of crystal diameters falls between 1 and 5 mm (0.04 in and 0.2 in); and fine-grained if the absolute range of crystal diameters falls below 1 mm (0.04 in) (Mackenzie and others, 1997; Le Maitre and others, 2004).

The grain size of unconsolidated sediments and clastic sedimentary rocks is described following the Wentworth grade scale (Wentworth, 1922). The term "grit" is used to describe pebbly or granule sandstone and pebble or granular conglomerate with abundant angular grains in the 2 to 4 mm (0.08 to 0.16 in) size range. Hand samples of unconsolidated sediments and clastic sedimentary rocks were compared in the field and/or in the laboratory to graphical rep-

resentations (comparator) of the Wentworth grade scale to determine average representative grain size in various parts of a respective sedimentary geologic unit. Colors given for hand-sample descriptions are from the Rock-Color Chart Committee (1991).

Subsurface geology shown in the geologic cross sections incorporates lithologic interpretations from water-well drill records available through the Oregon Water Resources Department (OWRD) GRID system (see map plates; appendix). An attempt was made to locate water wells and other drill holes that have well logs archived by OWRD. Very few wells were actually visited in the field. Approximate locations were estimated using tax lot maps, street addresses, and aerial photographs to plot well-locations. The accuracy of the locations ranges widely, from errors of circa 0.7 mi (1.1 km) possible for wells located only by section and plotted at the section centroid to a few tens of feet for wells located by address or tax lot number on a city lot with bearing and distance from a corner. For each well, the number of the well log is indicated in the database. This number can be combined with the first four letters of the county name (e.g., CURR 5473), to retrieve an image of the well log from the OWRD web site (http://apps.wrd.state.or.us/apps/gw/well_log/). A database of more than 1600 water-well logs with interpreted subsurface geologic units is provided in the appendix.

EXPLANATION OF MAP UNITS

The stack of tectonostratigraphic terranes that underlies the southern Oregon Coast Range is Upper Jurassic to Paleogene in age (Figures 4, 6; see map plates). Widely separated stratigraphic units, which are often characterized by complex, discontinuous geometries, were grouped on the basis of apparent stratigraphic position, lithology, geochemical composition, and fossil assemblages. Unit names follow local stratigraphic nomenclature when available, but lacking formal rock names, informal names are given on the basis of composition or a well-exposed section.

Bedrock geologic units are locally mantled along the coast by Neogene overlap sequences and Quaternary surficial deposits. Quaternary surficial deposits are divided on the basis of apparent age into Anthropocene, Holocene, and Quaternary units. Following the suggestions of Crutzen (2002) and Wiley and others (2011), we use the term

Anthropocene for the time period beginning with the first significant accumulations of American, Canadian, Californian, Russian, and European settlers' and ships' logs, journals, diaries, maps, charts, artifacts, roads, farms, diversions, or artificial fills and extending to the present day. In Oregon this corresponds to a date of 1792 when Robert Gray first crossed the Columbia River bar. Accordingly, any deposit that 1) contains artifacts of industrial origin, or 2) modifies the geology reliably described in any log, journal, or diary, or reliably depicted on any chart, sketch, or map, or 3) modifies, covers, or can be shown to be associated with erosion of any road, fill, or dam, or 4) is known to postdate 1791, or 5) that can otherwise be shown to postdate deposits meeting criteria 1 to 4, is of Anthropocene age. A time-rock chart showing age ranges for Mesozoic and Cenozoic bedrock and surficial units is depicted in Figure 6.

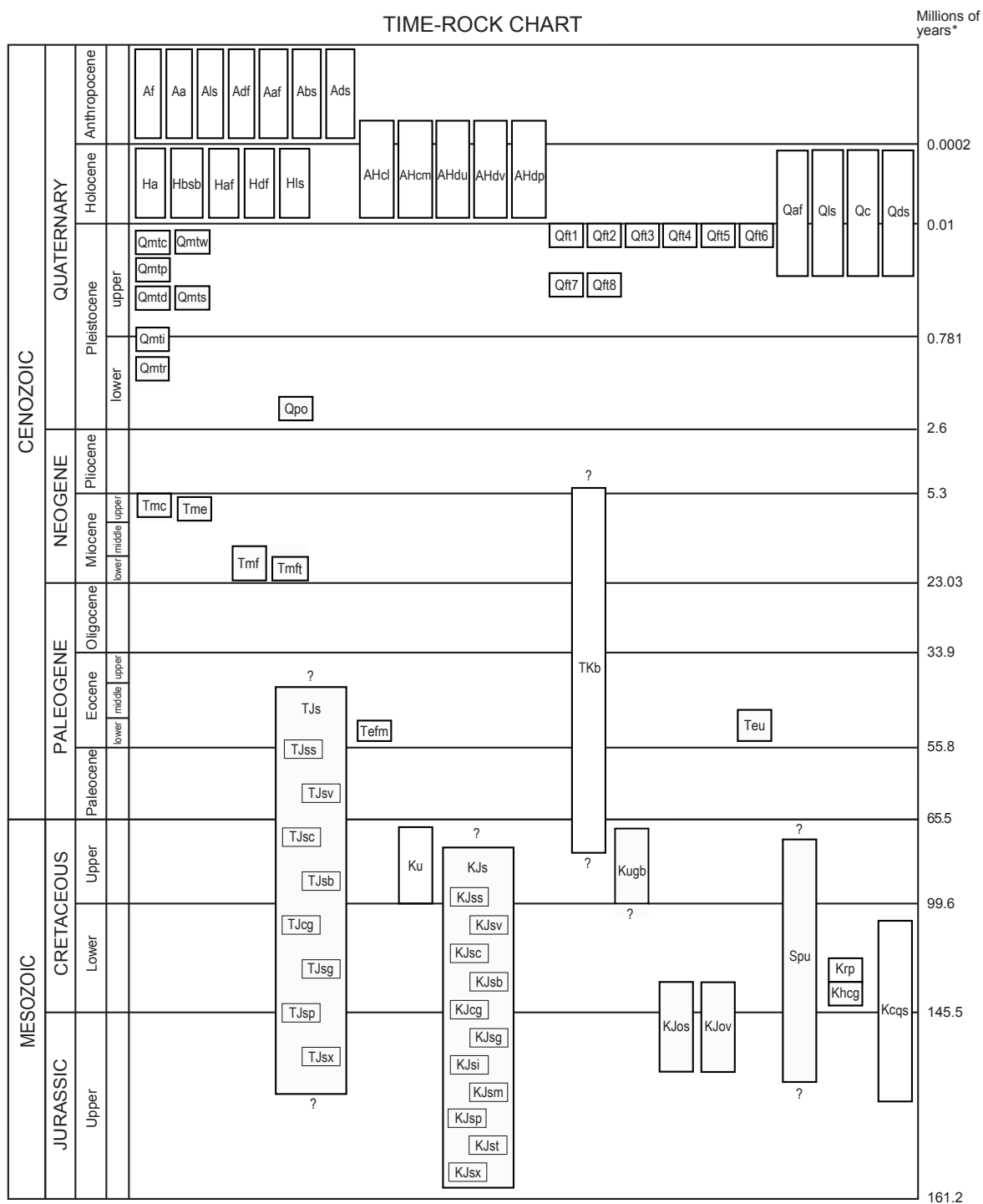


Figure 6. Time-rock chart showing the 73 geologic units in the Bandon, Langlois, and Port Orford areas along the southern Oregon coast identified by this study.

OVERVIEW OF MAP UNITS ALONG THE SOUTHERN OREGON COAST

W Water

UPPER CENOZOIC SURFICIAL DEPOSITS

ANTHROPOCENE SURFICIAL DEPOSITS

Af	modern fill and construction material (Anthropocene)
Aa	alluvium (Anthropocene)
Als	landslide deposits (Anthropocene)
Adf	debris fan deposits (Anthropocene)
Aaf	alluvial fan deposits (Anthropocene)
Abs	beach and berm deposits (Anthropocene)
Ads	foredune deposits (Anthropocene)

ANTHROPOCENE AND HOLOCENE SURFICIAL DEPOSITS

AHcl	coastal lacustrine deposits (Anthropocene and Holocene)
AHcm	coastal marsh deposits (Anthropocene and Holocene)
AHdu	unvegetated dune deposits (Anthropocene and Holocene)
AHdv	vegetated dune deposits (Anthropocene and Holocene)
AHdp	deflation plain sand (Anthropocene and Holocene)

HOLOCENE SURFICIAL DEPOSITS

Ha	alluvium (Holocene)
Hbsb	beach storm berm (Holocene)
Haf	alluvial fan deposits (Holocene)
Hdf	debris fan deposits (Holocene)
Hls	landslide deposits (Holocene)

QUATERNARY SURFICIAL DEPOSITS

Qaf	alluvial fan deposits (Holocene and upper Pleistocene)
Qls	landslide deposits (Holocene and upper Pleistocene)
Qc	colluvium (Holocene and upper Pleistocene)
Qds	upland coastal dune deposits (Holocene and upper Pleistocene)

Fluvial terrace deposits and strath terraces (upper Pleistocene)

Qft1	fluvial terrace sediments 1 (upper Pleistocene)
Qft2	fluvial terrace sediments 2 (upper Pleistocene)
Qft3	fluvial terrace sediments 3 (upper Pleistocene)
Qft4	fluvial terrace sediments 4 (upper Pleistocene)
Qft5	fluvial terrace sediments 5 (upper Pleistocene)
Qft6	fluvial terrace sediments 6 (upper Pleistocene)
Qft7	fluvial terrace sediments 7 (upper Pleistocene)
Qft8	fluvial terrace sediments 8 (upper Pleistocene)

Coastal marine terrace deposits (Pleistocene)

Qmtc	Cape Blanco terrace sediments (south of Floras Creek, upper Pleistocene, ~80 ka).
Qmtw	Whiskey Run terrace sediments (north of Floras Creek, upper Pleistocene, ~80 ka).
Qmtp	Pioneer terrace sediments (upper Pleistocene, ~105 ka).
Qmtd	Seven Devils terrace sediments (north of Floras Creek, upper Pleistocene, ~125 ka).
Qmts	Silver Butte terrace sediments (south of Sixes River, upper Pleistocene, ~125 ka).
Qmti	Indian Creek terrace sediments (upper or lower Pleistocene, >200 ka).
Qmtr	Poverty Ridge terrace sediments (lower Pleistocene).

(continued on next page)

(MAP UNIT AND GEOLOGIC UNIT CORRELATION, continued)

Unconformity

LOWER PLEISTOCENE AND MIOCENE ROCKS

LOWER PLEISTOCENE SEDIMENTARY ROCKS

Qpo Port Orford Formation (lower Pleistocene)

Unconformity

MIOCENE SEDIMENTARY ROCKS

Tmc diatomite of China Creek (upper Miocene, Messinian Stage)

Tme Empire Formation (upper Miocene, Wishkahan Pacific Northwest Molluscan Stage)

Unconformity

Tmf sandstone of Floras Lake (lower and middle Miocene, Wishkahan and
Newportian Pacific Northwest Molluscan Stages)

Tmft tuff (lower Miocene, 18.24 ± 0.86 Ma)

Unconformity

LOWER CENOZOIC AND MESOZOIC ROCKS

PALEOGENE SEDIMENTARY ROCKS

Teu Umpqua Group (lower to middle Eocene)

Unconformity(?)

SIXES RIVER TERRANE

Cape Blanco (western) subterrane

TJs mudstone and sandstone matrix mélange (lower middle Eocene(?) to Upper Jurassic(?))

TJss sandstone

TJsv volcanic and meta-volcanic rocks

TJsc chert

TJsb blueschist

TJcg conglomerate

TJsg garnet schist

TJsp serpentinite and meta-serpentinite

TJsx mélange blocks, undivided

Faulted subterrane boundary

Fulmar (central) subterrane

Tefm sandstone of Fivemile Point (lower Eocene)

Unconformity(?)

Ku sandstone and mudstone turbidites (Upper Cretaceous)

(continued on next page)

(MAP UNIT AND GEOLOGIC UNIT CORRELATION, continued)

Unconformity

KJs	mélange of Sixes River (Upper(?) Cretaceous to Jurassic)
KJss	sandstone
KJsv	volcanic and meta-volcanic rocks
KJsc	chert
KJsb	blueschist
KJcg	conglomerate
KJsg	garnet schist
KJsi	coarse-grained igneous rocks
KJsm	other metamorphic rocks
KJsp	serpentinite and meta-serpentinite
KJst	siltstone
KJsx	mélange blocks, undivided

Volcanic rocks that erupted onto or intruded the Fulmar (central) subterrane

TKb	volcanic rocks (Neogene(?), Paleogene(?), or Cretaceous(?))
------------	---

Faulted terrane boundary

GOLD BEACH TERRANE

Cretaceous sedimentary rocks

Kugb	sedimentary rocks, undivided (Upper(?) Cretaceous)
-------------	--

Unconformity

Lower Cretaceous and Upper Jurassic sedimentary rocks

KJos	Otter Point Formation (Lower Cretaceous and Upper Jurassic, Hauterivian to Tithonian Stages)
KJov	volcanic rocks

Faulted terrane boundary

PICKETT PEAK TERRANE

Kcqs	Colebrooke Schist (Upper Jurassic origin, Lower Cretaceous or later emplacement; 128.3 ± 6 Ma, 128.6 ± 6 Ma, 141.9 ± 10 Ma K/Ar whole rock; metamorphic age)
-------------	---

Faulted terrane boundary

WESTERN KLAMATH TERRANE

Elk subterrane

Krp	Rocky Point Formation (Lower Cretaceous, Valanginian or Berriasian Stage)
Khcg	Humbug Mountain Conglomerate (Lower Cretaceous, Valanginian or Berriasian Stage)

OTHER ROCKS

Spu	Serpentinite, serpentinite-matrix mélange, and serpentinitized ultramafic rock, undivided (Cretaceous(?) and Upper Jurassic(?))
------------	--

UPPER CENOZOIC SURFICIAL DEPOSITS

Mesozoic and Cenozoic rocks exposed along the southern Oregon coast are locally mantled by a veneer of Quaternary surficial deposits (see map plates). Surficial units include alluvial-plain and fluvial terrace deposits, coastal marine terrace deposits, and valley fringing landslide, alluvial fan, and debris fan deposits. Surficial units within the project area are delineated on the basis of geomorphology as interpreted from a combination of field observations, 1-m lidar DEMs, 2011 NAIP orthophotos, and USGS 7.5-minute topographic maps.

W water—Areas covered by ocean. (*Note: Water is included as a unit here because it occurs as a unit in the geodatabase.*)

ANTHROPOCENE SURFICIAL DEPOSITS

Af modern fill and construction material (Anthropocene)—Man-made deposits of poorly sorted and crudely layered mixed gravel, sand, clay, and other engineered fill (see map plates). These deposits usually contain rounded to angular clasts ranging from small pebbles up to the largest size that can be moved with road building equipment. The orientation of clasts is typically less uniform than is found in naturally occurring imbricated or bedding-parallel gravel. Deposits mapped as modern fill and construction material include those that make up jetties, tiered cranberry fields (“bogs”), dams and levies, road embankments, causeways and culvert fills, and mined land (see map plates). The thickness of fill-deposits may exceed 30 m (98 ft). These deposits are assigned an Anthropocene age.

Aa alluvium (Anthropocene)—Unconsolidated gravel, sand, silt, and clay deposited along active stream channels and on adjoining floodplains (see map plates). Gravel deposited as imbricated, massive to cross-stratified accumulations on mid-channel islands and bars is the most common type of near channel alluvium along major tributaries. Thickness of alluvial deposits is generally less than 5 to 7 m (16 to 23 ft); bedrock units may be variably exposed in the base of stream channels within areas mapped as unit **Aa**. Areas mapped as **Aa** are known to have been inundated by record floods during 1861, 1964, 1996

to 1997, and 2006 and include deposits containing man-made debris or artifacts, or deposits filling areas known to have been modified by man such as excavations, roadways, or gravel pits.

Als landslide deposits (Anthropocene)—Unconsolidated, chaotically mixed masses of rock, soil, and colluvium deposited by landslides (i.e., slumps, slides, debris flows, rock avalanches; see map plates). Recent landslide terrain is characterized by sloping hummocky surfaces, locally marked by closed depressions, springs and wet seeps, and scarps. Active or recently active landslides are marked by marginal levees and open ground fissures; tilted trees and bent trunks may be common on the surface. Landslide deposits are traceable uphill to headwall scarps or slip surfaces. Toes to more recent deposits retain convex-up, fan-shaped morphologies. The unit locally includes rock fall, large talus piles, shallow-seated landslides of colluvium, rapidly emplaced debris flow deposits, and more deeply seated bedrock slides. Individual landslide deposits generally cover less than 1.2 hectares (3 acres). Thickness of landslide deposits is highly varied; maximum thickness is several tens of meters. Landslide deposits are assigned an Anthropocene age on the basis of disturbed roads, historic records, and other cultural and physical features. Many old logging roads can be traced on 1-m lidar DEMs to where they are buried by recent landslide lobes. Landslide deposits are typically referred to as clay, boulders, rock, or rock and clay in water well logs.

Adf debris fan deposits (Anthropocene)—Unconsolidated deposits of gravel, sand, silt, and woody debris in fan-shaped accumulations preserved at the outlets of steep, intermittent upland drainages (see map plates). Debris fans typically accumulate through intermittent fluvial deposition and during high-discharge rainfall events when accumulations of soil, colluvium, or landslide deposits are remobilized and transported down slope as fast moving sediment gravity flows (e.g., debris flows). The unit may locally include rapidly deposited talus as a result of rockfall in steep drainages. Debris fans are differentiated from alluvial fans on the basis of steeper gradients over their longitudinal profiles; gradients are greater than 6 percent and, in some cases may exceed 25 percent (Alluvial Fan Process Group: <http://>

www.fs.usda.gov/Internet/FSE_DOCUMENTS/stelprdb5413801.pdf). Individual or coalescing complexes of debris fan deposits generally cover less than 0.8 hectares (2 acres); local thickness of debris fan deposits is variable but is probably <10 m (32 ft). Debris fan deposits are considered to be Anthropocene in age on the basis of stratigraphic position near the mouths of active drainages and relatively youthful-appearing deposit morphology.

Aaf alluvial fan deposits (Anthropocene)—Unconsolidated deposits of gravel, sand, silt, clay, and woody debris preserved in low fan-shaped accumulations that occur at the transition between low-gradient valley floodplains and steeper upland drainages (see map plates). Surfaces of alluvial fans are characterized by anastomosing, intermittent fluvial channels, formed where pools or obstructions, such as log-jams or debris flow levees create flow diversions. Sediment accumulates on the fan surface through normal fluvial deposition, avulsions, and lateral migration as streams emerge from upland settings and the gradient falls below the threshold for further sediment transport. Debris flows occurring during episodic high-discharge precipitation events are also an important mechanism for transport and deposition on the alluvial fan surface. Alluvial fans have gradients ranging from 1 to 6 percent over their longitudinal profile (Alluvial Fan Process Group: http://www.fs.usda.gov/Internet/FSE_DOCUMENTS/stelprdb5413801.pdf). They typically have a steep gradient at the apex, moderate gradient through the middle section, and low gradient near the toe. Individual fans generally cover less than 0.8 hectares (2 acres); local thickness of alluvial fan deposits is variable, but is probably <15 m (50 ft). These deposits are largely considered to be Anthropocene in age on the basis of stratigraphic position near the mouths of active stream-channels and relatively youthful-appearing deposit morphology.

Abs beach and berm deposits (Anthropocene)—Unconsolidated, well-sorted sand, pebbly sand, shelly sand, sandy gravel, and open-framework gravel deposited in active ocean beaches. Locally gravel dominated, particularly on steep, narrow beaches (see map plates). Pebbles and cobbles in open-framework gravel may be imbricated such that most tilt toward oncoming waves. Grain size distribution and thick-

ness of the deposit may change from day to day and year to year as sand and gravel migrate on to, off of, or along the shore. Beach deposits may be limited to the upper or lower parts of the exposed wave cut platform. On some beaches the amount of exposed bedrock can vary greatly from high to low tide and from year to year. Beach deposits may be quickly eroded during major storms. Areas mapped as beach deposits are seasonally ephemeral features that typically contain man-made debris or artifacts. The unit is therefore assigned an Anthropocene age.

Ads foredune deposits (Anthropocene)—Unconsolidated, well-sorted, fine- to medium-grained sand deposited by the wind in near-shore, back-beach settings that parallel the shoreline (see map plates). The unit is typically characterized by unvegetated to moderately grass-covered surfaces on the seaward surface (stoss slopes), with lesser amounts of larger woody shrubs developed on landward slopes (lee slopes). The seaward side of the active foredune is commonly the depositional site of large amounts of driftwood. Thickness of the unit is typically < 8 m (26 ft). The unit is assigned an Anthropocene age on the basis of stratigraphic position directly adjacent (landward) to the active beach (**Abs**) and inclusion of man-made debris or artifacts.

ANTHROPOCENE AND HOLOCENE SURFICIAL DEPOSITS

AHcl coastal lacustrine deposits (Anthropocene and Holocene)—Interbedded laminated mud, massive, organic-rich mud, sandy mud, muddy debris, and sand deposited in coastal lakes (Kelsey and others, 2005). Lakes are widely distributed at the mouths of many coastal drainages in the map area, impounded behind Holocene dune fields between Garrison Lake on the south (Plate 1) and Bradley Lake on the north (Plate 3). Inlets and fringes of lakes are typically covered by marsh deposits (**AHcm**). Lacustrine environments, such as Bradley Lake in the northern part of the map area (Plate 3), contain landward-thinning sand sheets recording periodic marine incursions generated by local tsunamis and seismic shaking on the Cascadia subduction zone (Kelsey and others, 2005). Bradley Lake has been a catchment for tsunami deposits, since its formation after ~7300 yr B.P.,

and since that time has been inundated by at least 16 distinct tsunami disturbance events (Kelsey and others, 2005). The most recent tsunami-generated deposits in Bradley Lake record the A.D. 1700 Cascadia subduction zone earthquake. The unit is assigned an Anthropocene and Holocene age on the basis of impoundment behind Anthropocene and Holocene dune deposits (**Ads**, **AHdu**, **AHdv**; see map plates) and numerous ^{14}C ages obtained from Bradley Lake (Plate 3; appendix).

AHcm coastal marsh deposits (Anthropocene and Holocene)—Interbedded mud, massive, organic-rich mud, and peat deposited in marsh environments along the fringes of coastal lakes and within stream channels emptying into coastal lakes (see map plates). These areas are recognized on the basis of muted topography, saturated ground, abundant vegetation, and sinuous drainage. Areas of marsh are also known to occur within depressions on top of low-lying Quaternary coastal marine terrace deposits and along the margins of stream drainages (**Qmtc**, **Qmtp**, **Qmtw** etc.) but have not been mapped separately here. The unit is assigned an Anthropocene and Holocene age on the basis of association with coastal lakes.

AHdu unvegetated dune deposits (Anthropocene and Holocene)—Unconsolidated, well-sorted, fine- to medium-grained sand deposited by the wind within narrow dunes paralleling the coastal margin between Langlois (Plate 2) and Devils Kitchen, southwest of Bandon (Plate 3). Active dunes lack vegetative cover and include both oblique and parabolic dune forms, with wind-blown sand derived from both beaches (**Abs**) and deflation plains (**AHdp**; Beaulieu and Hughes, 1975; Peterson and others, 2007). Migration rates of dunes range from a few centimeters to several meters per year, depending on the source area (Beaulieu and Hughes, 1975). Dune thickness may locally be up to 20 m (66 ft). The unit is assigned an Anthropocene and Holocene age on the basis of a youthful-appearing morphology, lack of vegetation, stratigraphic association with Holocene lakes (**AHcl**) and marshes (**AHcm**), and ages assigned by Peterson and others (2007). Deposition of these dunes corresponds with the decline in the rate of sea level rise during the middle part of the Holocene, when onshore wave transport delivered inner shelf sand

to beaches. Subsequent eolian transport of surplus beach sand, during peak onshore wind velocities, led to the formation of upland Holocene dune sheets (Peterson and others, 2007).

AHdv vegetated dune deposits (Anthropocene and Holocene)—Unconsolidated, well-sorted, fine- to medium-grained sand deposited by the wind within narrow dunes paralleling the coastal margin between Langlois (Plate 2) and Devils Kitchen, southwest of Bandon (Plate 3). The unit includes well-vegetated dunes associated with low-lying deflation plains (**AHdp**) and unvegetated, active dunes (**AHdu**). The unit is differentiated from older dunes (**Qds**) capping marine terraces, on the basis of topographic setting and differences in the relative degree of soil development (Beaulieu and Hughes, 1975; Peterson and others, 2007). The lower parts of vegetated dunes may be associated with marine sand, clay, lake and marsh deposits, and peat horizons. Dune thickness may locally be up to 20 m (66 ft). The unit is assigned a Holocene age on the basis of a youthful-appearing morphology, stratigraphic association with Holocene active dunes (**AHdu**), lakes (**AHcl**), and marshes (**AHcm**), and ages assigned by Peterson and others (2007). Deposition of these dunes corresponds with the decline in the rate of sea level rise during the middle part of the Holocene, when onshore wave transport delivered inner shelf sand to beaches. Subsequent eolian transport of surplus beach sand, during peak onshore wind velocities, led to the formation of upland Holocene dune sheets (Peterson and others, 2007).

AHdp deflation plain sand (Anthropocene and Holocene)—Unconsolidated, well-sorted, fine- to medium-grained sand deposited by the wind within broad, low-lying areas paralleling the coastal margin between Langlois (Plate 2) and Devils Kitchen, southwest of Bandon (Plate 3). Deflation plains are commonly situated immediately inland from the foredune (**Ads**) environment and lie adjacent to lacustrine and marsh areas (see map plates). Deflation plains are characterized by widespread fields of low transverse dunes or flat areas eroded to the level of the summer water table; water table rise during the winter produces lakes and marshes. Peat and silty clay may therefore underlie many areas mapped as

deflation plain, due to the close association with lakes and marshes. Deflation plains may be sources of windblown sand for larger, nearby dunes (**AHdu**, **AHdv**). Deflation plain sand in the map area is assigned a Holocene age on the basis of stratigraphic association with Holocene dune sand (**AHdv**, **AHdu**; Peterson and others, 2007) and lacustrine (**AHcl**) and marsh (**AHcm**) deposits (Kelsey and others, 2005). Beaulieu and Hughes (1975) indicated a maximum age of 5000 years for deflation plains as they lie at or slightly above modern day sea level.

HOLOCENE SURFICIAL DEPOSITS

Ha alluvium (Holocene)—Unconsolidated, well- to poorly-sorted and stratified gravel, sand, silt, and clay deposited in active stream channels and on adjoining flood plains of major rivers and their tributaries (see map plates). These deposits commonly rest directly on bedrock and may locally include strath terraces. Thickness of the unit probably does not exceed 15 m (50 ft). The unit is considered to be Holocene in age on the basis of stratigraphic position in and near active stream-channels and youthful-appearing deposit morphology. In most places, Holocene (**Ha**) alluvial deposits are incised by modern floodplains (**Aa**) and may have been overtopped during historic flood events.

Hbsb beach storm berm (Holocene)—Unconsolidated sand capped by cobbles, situated within a narrow sea cliff gap 2.5 km (1.6 mi) south of Cape Blanco (Plate 1; Kelsey, 1990). The deposit is ~ 78 m (255 ft) long by 15 m (49 ft) high, parallels the coast, and blocks a narrow valley which was a former drainage outlet for the Sixes River. The deposit lies ~ 19 m (62 ft) above current sea level. Well-rounded cobbles contained in the deposit are clast supported and locally have a landward-dipping imbrication. Cobbles consist of blueschist, diorite, meta-volcanics, and weakly indurated sandstone, derived from the Empire Formation (**Tme**) exposed in nearby sea cliffs. Janda (1969, 1970) and Kelsey (1990) interpreted the deposit to have formed as a beach storm berm formed by one or more great storms. The unit is assigned a Holocene age on the basis wood protruding from the deposit, which has yielded a ^{14}C age of $3,010 \pm 250$ yr B.P. (calibrated age $3,212 \pm 300$ yr B.P.; Janda, 1970;

Plate 1; appendix). Kelsey (1990) reported an initial ^{14}C age of $2,620 \pm 70$ yr B.P. obtained from pholadid shells (*Penitella penita* [Conrad]) contained within the deposit; further reservoir age corrections applied to these data determined a revised age for the death of the pholadid shells around $1,820 \pm 70$ yr B.P. (Plate 1; appendix). The youthful age of the deposit and its occurrence ~ 19 m (62 ft) above current sea level, led Kelsey (1990) to suggest tectonic uplift of the deposit during the latest Holocene.

Haf alluvial fan deposits (Holocene)—Unconsolidated deposits of gravel, sand, silt, clay, and woody debris preserved in low fan-shaped accumulations that occur at the transition between low-gradient valley floodplains and steeper upland drainages (see map plates). Surfaces of alluvial fans are characterized by anastomosing, intermittent fluvial channels, formed where pools or obstructions, such as log-jams or debris-flow levees create flow diversions. Sediment accumulates on the fan surface through normal fluvial deposition, avulsions, and lateral migration as streams emerge from upland settings and the gradient falls below the threshold for further sediment transport. Debris flows occurring during episodic high-discharge precipitation events are also an important mechanism for transport and deposition on the alluvial fan surface. Alluvial fans have gradients ranging from 1 to 6 percent over their longitudinal profile (Alluvial Fan Process Group: http://www.fs.usda.gov/Internet/FSE_DOCUMENTS/stelprdb5413801.pdf). They typically have a steep gradient at the apex, moderate gradient through the middle section, and low gradient near the toe. Individual fans in upland areas generally cover less than 4 hectares (10 acres). Larger, coalescing fans located between the mouths of Floras Creek and Butte Creek, cover an area exceeding 1092.7 hectares (2,700 acres). The local thickness of alluvial fan deposits is variable, but is probably <15 m (50 ft). These deposits are largely considered to be Holocene in age on the basis of stratigraphic position near the mouths of active stream-channels and relatively youthful-appearing deposit morphology.

Hdf debris fan deposits (Holocene)—Unconsolidated deposits of gravel, sand, silt, and woody debris in fan-shaped accumulations preserved at the outlets of steep, intermittent upland drainages (see map plates). Debris fans typically accumulate through intermit-

tent fluvial deposition and during high-discharge rainfall events when accumulations of soil, colluvium, or landslide deposits are remobilized and transported down slope as fast moving sediment gravity flows (e.g., debris flows). The unit may locally include rapidly deposited talus as a result of rockfall in steep drainages. Debris fans are differentiated from alluvial fans on the basis of steeper gradients over their longitudinal profiles; gradients are greater than 6 percent and, in some cases may exceed 25 percent (Alluvial Fan Process Group: http://www.fs.usda.gov/Internet/FSE_DOCUMENTS/stelprdb5413801.pdf). Individual or coalescing complexes of debris fan deposits generally cover less than 7.3 hectares (18 acres); local thickness of debris fan deposits is variable but is probably <10 m (32 ft). These deposits are largely considered to be Holocene in age on the basis of stratigraphic position near the mouths of active drainages and relatively youthful-appearing deposit morphology.

Hls landslide deposits (Holocene)—Unconsolidated, chaotically mixed masses of rock, soil, and colluvium deposited by landslides (i.e., slumps, slides, debris flows, rock avalanches; see map plates). Recent landslide terrain is characterized by sloping hummocky surfaces, locally marked by closed depressions, springs and wet seeps, and scarps. Landslide deposits are traceable uphill to headwall scarps or slip surfaces. Toes to Holocene deposits may retain convex-up, fan-shaped morphologies. The unit locally includes rock fall, large talus piles, shallow-seated landslides of colluvium, rapidly emplaced debris flow deposits, and more deeply-seated bedrock slides. Individual Holocene landslide deposits in the map area range in size from small deposits covering 0.04 hectares (0.1 acres) to larger composite features covering areas up to 115.3 hectares (285 acres) (see map plates). The largest Holocene landslide complexes are associated with the *mélange* of Sixes River (bedrock unit **KJs**); smaller slides are prevalent in many of the upland areas and along lower elevation drainages. Thickness of landslide deposits is highly varied; maximum thickness is several tens of meters. Landslides are assigned a Holocene age where deposits appear relatively fresh, with well-defined hummocks and preservation of relatively small features such as levees and internal scarps; Holocene deposits generally lack the deeply incised streams that typify land-

slide deposits assigned a Quaternary age (**Qls**). Some Anthropocene landslide deposits (**Als**) are probably included in the unit where more precise age indicators are poorly developed or lacking. Landslide deposits are typically referred to as clay, boulders, rock, or rock and clay in water well logs.

QUATERNARY SURFICIAL DEPOSITS

Qaf alluvial fan deposits (Holocene and upper Pleistocene)—Unconsolidated deposits of gravel, sand, silt, clay, and woody debris preserved in fan-shaped accumulations that occur at the transition between low-gradient valley floodplains and steeper upland drainages (Map plates). Surfaces of alluvial fans are characterized by anastomosing, intermittent fluvial channels, formed where pools or obstructions, such as log-jams or debris flow levees create flow diversions. Sediment accumulates on the fan surface through normal fluvial deposition, avulsions, and lateral migration as streams debouch from upland settings and the gradient falls below the threshold for further sediment transport. Debris flows occurring during episodic high-discharge precipitation events are also an important mechanism for transport and deposition on the alluvial fan surface, particularly on the upper fan. Alluvial fans have gradients, ranging from 1 to 6 percent over their longitudinal profile (Alluvial Fan Process Group: http://www.fs.usda.gov/Internet/FSE_DOCUMENTS/stelprdb5413801.pdf). They typically have a steep gradient at the apex, moderate gradient through the middle section, and low gradient near the toe. Individual fans generally cover less than 27 hectares (66 acres); local thickness of alluvial fan deposits is unknown but is probably <10 m (32.8 ft). Alluvial fans are assigned a Quaternary age on the basis of stratigraphic position and surfaces that are more dissected than those characterizing Holocene alluvial fans (**Haf**), and where there is a lack of more precise age indicators.

Qls landslide deposits (Holocene and upper Pleistocene)—Unconsolidated, chaotically mixed masses of rock and soil deposited by landslides (e.g., slumps, slides, debris flows, rock avalanches; see map plates). Deposits may consist of individual slide masses or may form large complexes resulting from multiple generations of landslide activity. Landslide terrain

is characterized by sloping hummocky surfaces, locally marked by closed depressions, springs, and wet seeps, head-scarps and internal scarps, open ground fissures, and tilted trees and bent trunks. Slides are often traceable uphill to headwall scarps or slip surfaces. In more deeply seated landslides, these head scarps commonly expose bedrock. Locally, Quaternary landslide deposits are deeply incised by drainages that contain remobilized rock and debris deposited by sediment-gravity flows. Quaternary landslide complexes in the map area range in size from small deposits covering 0.04 hectares (0.1 acres) to larger composite features covering areas up to 809 hectares (2,000 acres). The largest landslide complexes are associated with the *mélange* of Sixes River (**KJs**) and the contact between *mélange* and the structurally higher Colebrooke Schist (**Kcqs**). Slides occurring within areas of *mélange* often incorporate or flow around large *mélange* blocks which are here mapped as bedrock units; it is unclear in most cases if these are incorporated in the slide mass or if shallow seated slides are creeping around stable or deeply rooted blocks. Thickness of landslide deposits is highly varied, but may be more than several tens of meters in larger deposits. Large areas mapped as Quaternary landslide deposits typically include many discrete deposits of varying age that have not been differentiated here. They probably include inliers of *mélange*. Landslide deposits range in age from Pleistocene, relatively stable features, to those that have been recurrently active in relatively recent time (assigned to units **Als** and **Hls** where recognized). Most landslide deposits are assigned a Quaternary age on the basis of subdued geomorphic expression and incision by streams. Landslide deposits are typically referred to as clay, boulders, rock, or rock and clay in water well logs.

Qc colluvium (Holocene and upper Pleistocene)—Unconsolidated mixtures of rock and soil (see map plates) deposited in rockfall and talus cones beneath steep slopes. Thickness of colluvial deposits is highly varied; maximum thickness is several meters. The unit is assigned a Holocene and Pleistocene age on the basis of stratigraphic position.

Qds upland coastal dune deposits (Holocene and upper Pleistocene)—Unconsolidated, well-sorted, fine- to medium-grained sand deposited by the wind

in upland coastal dune fields (see map plates). Dune fields are situated on top of coastal marine terraces and cover a large portion of the coast between Port Orford and Bandon. Peterson and others (2007) considered these dune fields to collectively form the ~58-km-long (36 mi) by ~7-km-wide (4.3 mi) Bandon dune sheet, which extends north of the map area at least to Cape Arago. The maximum thickness of dune deposits is approximately 15 m (~50 ft). The unit is assigned a late Pleistocene age on the basis of stratigraphic position above late Pleistocene coastal marine terraces. Peterson and others (2007) reported calibrated radiocarbon ages (cal yr BP) and for several sites within the Bandon dune sheet, with dates ranging between 900 and 36,200 cal yr BP. Additional thermoluminescence ages for the Bandon dune sheet range between 38.1 and 111 ka (Peterson and others, 2007). Regional dune dating along the Oregon coast indicates that dune fields were emplaced thousands of years after the youngest (~80 ka) coastal marine terrace was abandoned (Beckstrand 2001; Peterson and others, 2007).

Fluvial terrace deposits and strath terraces (upper Pleistocene)—Unconsolidated deposits of gravel and sand, with subordinate amounts of silt and clay that form fluvial terraces above modern floodplains of major drainages in the map area (see map plates). The terraces are visible on 1-m lidar DEMs as planar to very gently sloping, equal-elevation surfaces (treads). Steeper descending slopes (risers) define the streamside edges of terraces. Individual terrace deposits may be up to 15 m (49 ft) thick, but more typically form thin deposits covering strath terraces formed in discontinuously exposed bedrock.

Subdivided in the map area, on the basis of tread elevation above modern stream level, into the following units:

Qft1 fluvial terrace sediments 1 (upper Pleistocene)—fluvial terrace deposits with tread elevations ranging from 6 to 7.5 m (20 to 25 ft) above modern stream elevation (see map plates). The unit is assigned a late Pleistocene age on the basis of stratigraphic position. Fluvial terrace sediments (**Qft1**) are inset into the ~105 ka Pioneer (**Qmtp**) and ~80 ka Cape

Blanco (**Qmtc**) marine terrace sediments, so are therefore younger than those units (Plate 1).

Qft2 fluvial terrace sediments 2 (upper Pleistocene)— Fluvial terrace deposits with tread elevations ranging from 9 to 10.5 m (30 to 35 ft) above modern stream elevation (see map plates). The unit is assigned a late Pleistocene age on the basis of stratigraphic position. Fluvial terrace sediments (**Qft2**) are inset into the ~105 ka Pioneer (**Qmtp**) and ~80 ka Cape Blanco (**Qmtc**) marine terrace sediments, so are therefore younger than those units (Plate 1).

Qft3 fluvial terrace sediments 3 (upper Pleistocene)— Fluvial terrace deposits with tread elevations ranging from 12 to 13.7 m (40 to 45 ft) above modern stream elevation (see map plates). The unit is assigned a late Pleistocene age on the basis of stratigraphic position. Fluvial terrace sediments (**Qft3**) are inset into the ~105 ka Pioneer (**Qmtp**) and ~80 ka Cape Blanco (**Qmtc**) marine terrace sediments, so are therefore younger than those units (Plate 1).

Qft4 fluvial terrace sediments 4 (upper Pleistocene)— Fluvial terrace deposits with tread elevations ranging from 18 to 21 m (59 to 68 ft) above modern stream elevation (see map plates). The unit is assigned a late Pleistocene age on the basis of stratigraphic position. Fluvial terrace sediments (**Qft4**) are inset into the ~105 ka Pioneer (**Qmtp**) and ~80 ka Cape Blanco (**Qmtc**) marine terrace sediments, so are therefore younger than those units (Plate 1).

Qft5 fluvial terrace sediments 5 (upper Pleistocene)— Fluvial terrace deposits with tread elevations ranging from 24 to 27 m (80 to 88 ft) above modern stream elevation (see map plates). The unit is assigned a late Pleistocene age on the basis of stratigraphic position. Fluvial terrace sediments (**Qft5**) are inset into the ~105 ka Pioneer (**Qmtp**) and ~80 ka Cape

Blanco (**Qmtc**) marine terrace sediments, so are therefore younger than those units (Plate 1).

Qft6 fluvial terrace sediments 6 (upper Pleistocene)— Fluvial terrace deposits with tread elevations ranging from 30.5 to 36.5 m (100 to 120 ft) above modern stream elevation (see map plates). The unit is assigned a late Pleistocene age on the basis of stratigraphic position. Fluvial terrace sediments (**Qft6**) are inset into the ~105 ka Pioneer (**Qmtp**) and ~80 ka Cape Blanco (**Qmtc**) marine terrace sediments, so are therefore younger than those units (Plate 1).

Qft7 fluvial terrace sediments 7 (upper Pleistocene)— Deeply incised fluvial terrace deposits with tread elevations up to 54.9 m (180 ft) above modern stream elevation (see map plates). The unit is assigned a late Pleistocene age on the basis of stratigraphic position. Fluvial terrace sediments (**Qft7**) are inset into the >200 ka Indian Creek (**Qmti**) and Poverty Ridge (**Qmtr**) marine terrace sediments, so are therefore younger than that unit; older fluvial terrace treads (**Qft7**) reside at higher relative elevations above the modern stream level than the backedge of the ~105 ka Pioneer (**Qmtp**) marine terrace sediments, so are older than that unit.

Qft8 fluvial terrace sediments 8 (upper Pleistocene)— Deeply incised fluvial terrace deposits with tread elevations up to 109 m (358 ft) above modern stream elevation (see map plates). The unit is assigned a late Pleistocene age on the basis of stratigraphic position. Fluvial terrace sediments (**Qft8**) are inset into the >200 ka Indian Creek (**Qmti**) and Poverty Ridge (**Qmtr**) marine terrace sediments, so are therefore younger than that unit; older fluvial terrace treads (**Qft8**) reside at higher relative elevations above the modern stream level than the backedge of the ~105 ka Pioneer (**Qmtp**) marine terrace sediments, so are older than that unit.

Coastal marine terrace deposits (Pleistocene)—Gravel and sand interpreted as nearshore, beach, dune, and stream facies deposited on ancient marine platforms. In gravel facies, the transition from onshore to beach processes is often marked by a reversal of imbrication, with clasts in beach and marine environments indicating landward flow and clasts in fluvial and fan environments indicating seaward flow. Sand facies are typically pale yellowish orange (10YR 8/6), well sorted, and medium grained, containing subrounded grains of quartz, feldspar, and lithics.

The distribution of marine terrace deposits has been determined from field observations, morphology interpreted from lidar, elevation, degrees of

erosional dissection, and modification of previous mapping by Brownfield (1972), Beaulieu and Hughes (1975, 1976), Kelsey (1990), McInelly and Kelsey (1990), Muhs and others (1990), and Kelsey and others (1996). Unit names applied to coastal marine terraces follow the local stratigraphic nomenclature established by Griggs (1945), Janda (1969, 1970), Kelsey (1990), McInelly and Kelsey (1990), and Kelsey and others (1996). Table 2 (modified from Kelsey and others, 1996) graphically displays the ages and stratigraphic correlations of locally named coastal terrace units along the southern Oregon coast between the California border and Cape Arago.

Table 2. Correlation of marine terraces along the southern and central Oregon coast after Kelsey and others (1996).

South-Central Oregon				Southern Oregon*			
Cape Arago*		Cape Blanco ^β		Kelsey and Bockheim (1994)		T. J. Wiley (unpublished mapping, 2007)	
Terrace	Assigned Age (ka)	Terrace	Assigned Age (ka)	Terrace	Assigned Age (ka)	Terrace	Assigned Age (ka)
Whiskey Run	80	Cape Blanco	80	Harris Beach	80	Qtc1	80
Pioneer	105	Pioneer	105	Brookings	105	Qtc2	105
Seven Devils	125	Silver Butte	125	Gowman	125	Qtc3, Qtc4, Qtc5	125
Metcalf	≥200	Indian Creek	≥200	Aqua Vista	≥200	Qtc4, Qtc5, Qtc6	≥200
				Cornett		Qtc6, Qtc7	
				Homestead		Qtc8, Qtc9	
		Poverty Ridge		Alder Ridge		Qtc10	

* Age assignments for southern Oregon marine terraces near Brookings reported by Kelsey and Bockheim (1994); ages reported by T. J. Wiley (unpublished mapping, 2007) are from Kelsey and Bockheim (1994).

¥ Age assignments for Cape Arago marine terraces reported by Muhs and others (1990) and McInelly and Kelsey (1990).

β Age assignments for Cape Blanco marine terraces reported by Kelsey (1990) and Muhs and others (1990).

Qmtc Cape Blanco terrace sediments (south of Floras Creek, upper Pleistocene, ~80 ka)—Undissected to slightly dissected terrace sediments forming a locally restricted (~2.3 km² [0.9 mi²]), wave-cut bench extending from Cape Blanco on the south to Floras Lake on the north (Plates 1 and 2). Cape Blanco terrace sediments are juxtaposed against the Pioneer terrace (**Qmtp**), separated by a subvertical to vertical erosional unconformity. The unconformity is recognized by the truncation of both the soil and gravels of the older Pioneer terrace and by a distinctive shell-rich cobble unit that occurs at the base of the Cape

Blanco terrace (Addicott, 1964; Kennedy, 1978; Muhs and others, 1990; Kelsey, 1990). The Cape Blanco terrace overlies a marine platform that is younger than that occupied by the Pioneer terrace, but elevations of the two adjacent marine platforms are approximately the same elevation. Kelsey (1990) interpreted Cape Blanco terrace sediments to represent deposits emplaced within the surf zone grading upward into beach deposits. Thickness of the terrace cover sediment ranges from ~ 6 to 11 m (19.6 to 36 ft). Backedge elevations for the terrace range from ~64 m (210 ft) at Cape Blanco on the south to ~ 22 m (72 ft) on the

north, near Floras Lake (Plates 1 and 2). The width of the preserved terrace at Cape Blanco is ~1.2 km (0.7 mi)

The unit was first recognized and informally named the Cape Blanco terrace by Kelsey (1990), who assigned the sediments a late Pleistocene age. The extent of epimerization of amino acids in *Saxidomus* shells in the Cape Blanco terrace is the same as shells of the same genus recovered from the numerically dated, ~80 ka Whiskey Run terrace (**Qmtw**; oxygen isotope stage 5a; Kelsey, 1990). The Cape Blanco terrace is correlative to terrace 1 (Harris Beach) mapped by Kelsey and Bockheim (1994) and unit Qtc1 mapped by T. J. Wiley (unpublished mapping, 2007) in the Cape Ferrelo-Brookings area, and is coeval with the Whiskey Run terrace (**Qmtw**) mapped in the northern part of the map area (Table 2; Plate 3).

Qmtw Whiskey Run terrace sediments (north of Floras Creek, upper Pleistocene, ~80 ka)—Undissected to slightly dissected terrace sediments forming an extensive (~14.5 km² [5.6 mi²]) platform, extending from Floras Creek on the south to Bandon on the north (Plates 2 and 3). Outside the map area, the terrace extends farther north, at least to Cape Arago (22 km [13.7 mi] north of Bandon). Thickness of the terrace cover sediment ranges from ~3 to 20 m (9.8 to 65.6 ft). The Whiskey Run terrace surface attains a maximum backedge elevation of 35 m (115 ft) at Cape Arago (north of map area) and gradually descends in elevation to the south; north of the Coquille River, the terrace surface lies near sea level. South of the Coquille River, the terrace is again emergent with backedge elevations ranging from ~30 m (99 ft) at Bandon to near sea level at Floras Creek (Plates 2 and 3). The width of the preserved terrace ranges from ~2.4 km (1.5 mi) at Bandon to 0.6 km (0.4 mi) at Floras Creek.

The unit was informally named the Whiskey Run terrace by Griggs (1945) for terrace sediments at the Pioneer mine type section, located between Bandon and Cape Arago. Muhs and others (1990) and Kelsey (1990) assigned

Whiskey Run sediments a late Pleistocene age on the basis of uranium series analysis of fossil corals collected at Coquille Point in Bandon, which yielded an age of 83 ± 5 ka (Plate 3; appendix). The Whiskey Run terrace is correlative to terrace 1 (Harris Beach) mapped by Kelsey and Bockheim (1994) and unit Qtc1 mapped by T. J. Wiley (unpublished mapping, 2007) in the Cape Ferrelo-Brookings area, and is coeval with the Cape Blanco terrace sediments (**Qmtw**) mapped in the southern part of the map area (Table 2; Plates 1 and 2).

Qmtp Pioneer terrace sediments (upper Pleistocene, ~105 ka)—Slightly dissected terrace sediments forming a regionally extensive (~56.5 km² [21.8 mi²]) platform between Port Orford on the south and Bandon on the north (see map plates). The terrace extends farther north at least to Coos Bay and farther south, past Gold Beach (outside map area; McClaghry and others, 2013). Pioneer terrace sediments are juxtaposed against the Silver Butte terrace (**Qmts**), on the south (Plate 1) and the Seven Devils terrace (**Qmtd**) on the north (see map plates), separated by a subvertical to vertical erosional unconformity. The Pioneer terrace overlies a marine platform that is younger than that occupied by the Silver Butte or Seven Devils terraces, but elevations of the adjacent marine platforms are approximately the same. Pioneer terrace sediments were deposited in a broad range of nearshore environments, including below surf settings, grading upward to shallower water surf and beach settings (Kelsey, 1990). The Pioneer terrace is distinguished from the Cape Blanco terrace on the basis of a thicker cover bed sequence. Thickness of the terrace cover sediment ranges from ~16 to 23 m (52.5 to 75.5 ft). Backedge elevations for the terrace range from ~17 m (57 ft) at Port Orford on the south to ~61 m (200 ft) east of Bandon (see map plates). The width of the preserved terrace ranges from ~6.5 km (4 mi) south of the Elk River to ~1 km (0.6 mi), north of Floras Creek.

The unit was informally named the Pioneer terrace by Griggs (1945) for terrace sediments

at the Pioneer mine type section, located between Bandon and Cape Arago. Kelsey (1990) and Muhs and others (1990) assigned the sediments a late Pleistocene age on the basis of the extent of epimerization of amino acids in *Saxidomus* shells and correlation with an interstadial high stand of the sea around 105 ka (Oxygen isotope stage 5c). The Pioneer terrace is correlative to terrace 2 (Harris Beach) mapped by Kelsey and Bockheim (1994) and unit Qtc2 mapped by T. J. Wiley (unpublished mapping, 2007) in the Cape Ferrelo-Brookings area, and to the Pioneer terrace (Qmtp) mapped in the Gold Beach area by McClaghry and others (2013; Table 2).

Qmtd Seven Devils terrace sediments (north of Floras Creek, upper Pleistocene, ~125 ka)—Moderately to deeply dissected terrace sediments forming a narrow, continuous (~8.8 km² [3.4 mi²]) platform between Floras Creek (Plate 2) on the south and Seven Devils on the north (outside map area, ~11 km [6.8 mi] north of Bandon). Thickness of the terrace cover sediment ranges from ~3 to 18 m (9.8 to 59 ft). Backedge elevations for the terrace range from ~57 m (187 ft) at Floras Creek on the south to ~105 m (346 ft) east of Bandon on the north (Plates 2 and 3). The width of the preserved terrace ranges from ~1.3 km (0.8 mi) east of Bandon to ~0.1 km (0.06 mi), south of Floras Creek.

The unit was informally named the Seven Devils terrace by Griggs (1945) for terrace sediments at the Seven Devils mine type section, located between Bandon and Cape Arago. McNelly and Kelsey (1990) suggested a late Pleistocene age of ~125 ka for the Seven Devils terrace, equivalent to the last interglacial period. The Seven Devils terrace is correlative to terrace 3 (Gowman terrace) mapped by Kelsey and Bockheim (1994) and units Qtc3, Qtc4, Qtc5 mapped by T. J. Wiley (unpublished mapping, 2007) in the Pistol River-Cape Ferrelo-Brookings area, and is coeval with the Silver Butte terrace (Qmtd) mapped in the northern part of the map area (Table 2; Plate 1).

Qmts Silver Butte terrace sediments (south of Sixes River, upper Pleistocene, ~125 ka)—Moderately to deeply dissected terrace sediments forming an elevated marine platform of limited aerial extent (~2.3 km² [0.9 mi²]) between Silver Butte on the south and the Sixes River on the north (Plate 1). Silver Butte terrace deposits are poorly exposed, but consist of an intermixed section of marine and alluvial sediments (derived from the Sixes River). Intermixed marine and fluvial deposits grade upward into deposits emplaced within surf zone and beach settings (Kelsey, 1990). Thickness of the terrace cover sediment ranges from ~15 to 34 m (~50 to 110 ft). Backedge elevations for the terrace range from ~50 m (165 ft) on the north to ~64 m (210 ft) on the south, near Silver Butte (Plate 1). The width of the preserved terrace ranges from ~1.2 km (0.7 mi) near the Sixes River to ~0.3 km (0.2 mi), north of Silver Butte (Plate 1).

The unit was informally named the Silver Butte terrace by Janda (1970). The Silver Butte terrace contains no fossils, but Kelsey (1990) suggested a late Pleistocene age of ~125 ka, equivalent to the last interglacial period, on the basis of soil development. The Silver Butte terrace is correlative to terrace 3 (Gowman) mapped by Kelsey and Bockheim (1994) and units Qtc3, Qtc4, Qtc5 mapped by T. J. Wiley (unpublished mapping, 2006) in the Pistol River-Cape Ferrelo-Brookings area, and is coeval with the Seven Devils terrace (Qmtd) mapped in the northern part of the map area (Table 2; Plates 2 and 3; McNelly and Kelsey, 1990).

Qmti Indian Creek terrace sediments (upper or lower Pleistocene, >200 ka)—Deeply dissected terrace sediments forming a broad (~20 km² [7.7 mi²]), structurally warped and faulted platform capping bedrock ridges between Rocky Point, south of Port Orford (outside map area; McClaghry and others, 2013) and the Sixes River on the north (Plate 1). The marine sequence residing atop the Indian Creek wave-cut platform consists on the west (outer edge) of offshore to relatively deep nearshore deposits. Eastern exposures (inner edge) near the terrace backedge consist

of nearshore deposits grading upward into to relatively deep nearshore deposits. Directly adjacent to the backedge, the terrace cover grades upward from nearshore to beach to eolian deposits (Janda, 1970; Kelsey, 1990). Thickness of the terrace cover sediment ranges from ~30 to 40 m (~98 to 131 ft; Kelsey, 1990). Backedge elevations for the terrace reach a maximum elevation of 237 m (778 ft) between the Elk River and the Sixes River. The width of the preserved terrace is ~4 km (0.7 mi) near the Sixes River to ~0.3 km (0.2 mi), north of Silver Butte (Plate 1).

The unit was informally named the Indian Creek terrace by Janda (1970). The Indian Creek terrace contains no fossils, but soil development suggests a Pleistocene age older than 200 ka, predating the last interglacial period (Kelsey, 1990). The Indian Creek terrace is correlative to terrace 4 (Aqua Vista) mapped by Kelsey and Bockheim (1994) and units Qtc4, Qtc5, Qtc6 mapped by T. J. Wiley (unpublished mapping, 2006) in the Cape Ferrelo-Brookings area, and to the Metcalf terrace sediments mapped east and northeast of Bandon (outside map area) by McInelly and Kelsey (1990) (Table 2).

Qmtr Poverty Ridge terrace sediments (lower Pleistocene)—Deeply dissected, and structurally warped terrace sediments forming a broad (~10 km² [3.9 mi²]), structurally warped platform capping bedrock ridges between Humbug Mountain, south of Port Orford (outside map area; McClaughry and others, 2013) and Stone Butte on the north (Plate 1). Inland exposures of the terrace are characterized by a base of interstratified marine sand and pea gravel grading upward to mostly clay-altered, pebble-cobble alluvium. Oceanward exposures are characterized by marine sand and gravel (Kelsey, 1990). Thickness of the terrace cover sediment in the Port Orford area is approximately 55 m (180 ft) (Kelsey, 1990). Backedge elevations for the terrace reach a maximum elevation of 481 m (1,580 ft) near Stone Butte (Plate 1) on the north to 192 m (630 ft) along the southern edge of Humbug Mountain (outside map area; McClaughry

and others, 2013). The width of the preserved terrace is ~4 km (0.7 mi) southeast of Port Orford (outside map area; McClaughry and others, 2013).

The unit was informally named the Poverty Ridge terrace by Janda (1970). Poverty Ridge terrace sediments overlie a deep saprolite layer in the Port Orford area and are assigned an early Pleistocene age on the basis of the inclusion of early Pleistocene *Clinocardium* fossils (Kelsey, 1990). The Poverty Ridge terrace is correlative to terrace 7 (Alder Ridge) mapped by Kelsey and Bockheim (1994) and unit Qtc10 mapped by T. J. Wiley (unpublished mapping, 2007) in the Cape Ferrelo-Brookings area (Table 2); equivalents to the Poverty Ridge terrace have not been identified in the map area north of Floras Creek.

Unconformity

LOWER PLEISTOCENE AND MIOCENE ROCKS

LOWER PLEISTOCENE SEDIMENTARY ROCKS

Qpo Port Orford Formation (lower Pleistocene)—Weakly cemented sandstone, conglomerate, and argillaceous siltstone that crop out along the beach southeast of Cape Blanco from the Cape Blanco State Park beach access road south to the Elk River. The section dips 8° to 1° to the southwest; younging toward the mouth of the Elk River.

The lowest part of the formation includes a maximum of about 10 m (33 ft) of buff (5Y8/4 to 10YR8/2) sandstone and associated pebbly sandstone and conglomerate preserved locally along a channeled basal unconformity (well exposed near the beach access road at Cape Blanco State Park; Plate 1). These rocks are overlain by a prominent brown (5YR6/1) basal cobble and boulder conglomerate, ~10 m (~33 ft) thick, exposed in the sea cliff and along the access road. Clasts in this conglomerate include dark-colored (5YR3/1), fine-grained lithologies and light-colored (~N7) diorite clasts.

Sandstone beds are locally fossiliferous with abundant pelecypods and gastropods. Near the mouth of the Elk River, muddy, medium-gray (N4-N5) fos-

siliferous sandstone contains distinctive hand-sized coalescing concretions. Flat-lying loose sand forms the basal bed of overlying terrace deposits associated with the upper Pleistocene Pioneer terrace (**Qmtp**).

In 1903, Diller mapped these rocks as part of the Neogene Empire Formation. Earlier, in 1902, he had proposed subdividing the Empire Formation and named this section the Elk River Beds (Diller, 1902). Baldwin (1945) revised the nomenclature, raising this section to formation rank, naming it the Port Orford Formation, and assigning it a Pliocene age. Addicott (1983) revised the age based on early Pleistocene fossils from the lower part of the formation.

Unconformity

MIOCENE SEDIMENTARY ROCKS

Tmc diatomite of China Creek (upper Miocene, Messinian Stage)—Diatomite, diatomaceous mudstone, and diatomaceous fine-grained sandstone that crop out on the low sea cliff at the mouth of China Creek and in cliffs overlooking Bradley Lake. Color is light brown (5YR 6/4) to pale brown (5YR 5/2) where fresh, and yellowish gray (5Y 8/1) to white where weathered. Outcrops are jointed with a wide range of spacings, but the sediment itself appears to have been massive to very indistinctly layered. Grain size varies gradually across the exposures and sharp internal contacts were not observed. Some weathered surfaces suggest that locally there may be zones of indistinct coarse-sand-sized pellets with compositions virtually identical to that of the rock as a whole. Thickness of the unit is at least 5 m (16 ft; assuming the unit dips only shallowly). A late late Miocene age (Delmontian Californian Stage – approximately equivalent to late Messinian ICS stage) is assigned for the unit on the basis of diatoms and other microfossils collected on the low sea cliff below the China Creek Wayside (Orr and others, 1971; Orr and Zaitzeff, 1970), as well as correlation of its distinctive lithology and similarities to strata reported from wells offshore (Fowler and others, 1971). Based on 1) Delmontian ages that Orr and others (1971) determined for diatomite from the China Creek Wayside and 2) the absence of common species in that florule and the diatom flora that Addicott (1983) described as upper Mohnian to Delmontian in the Empire For-

mation at Cape Blanco, we assign these rocks a stratigraphic position above Addicott's (1983) "restricted" Empire Formation at Cape Blanco. Structural orientation is not apparent in outcrops in the China Creek and Bradley Lake areas; presumably this unit would have dips intermediate between those in the older Empire Formation and the younger Port Orford Formation, which nowhere dips steeper than about 30°. Dips at China Creek are likely to be much less. Rocks exposed in the low sea cliff below the China Creek Wayside are virtually identical to those in a poorly exposed interval that Madin and others (1995) mapped as Empire Formation on a ridge west of South Slough at Coos Bay (UTM 391371E., 4794931N., WGS 84).

The light colored diatomite and mudstone is generally well jointed but otherwise massive with very rare tubular burrows. Joints are highlighted by tan to brown (5YR4/3) to orange selvage zones that locally have thin parallel bands of liesegang staining. Many of the selvage zones are harder than the surrounding rock and stand proud from the outcrop as much as a centimeter. Indistinct coarse-sand-sized pellets(?) or casts(?) are locally apparent in weathered samples of the rock but do not appear to define discreet layers. The rock is dark yellowish gray (5Y7/2) where wet or fresh and weathers white when dry.

This section crops out between an area underlain by older sandstone- and mudstone-matrix mélange to the north and low relief areas to the south that are underlain by Quaternary marine terrace sediment and Miocene sandstone of Floras Lake. The pattern and direction of younging suggests that geologic units in this area dip gently and are cut off by an unconformity (Fowler and others, 1971) or down-to-the-south fault located north of China Creek.

Tme Empire Formation (upper Miocene, Wishkahan Pacific Northwest Molluscan Stage)—The Empire Formation consists predominantly of medium- to fine-grained sandstone and pebbly sandstone with important intervals of siltstone and conglomerate. Fresh exposures are typically gray or gray-green (5GY8/1) but are locally light gray (N7) to white (carbonate cemented); weathered exposures are typically tan (5YR7/6) but locally oxidize orange (5YR8/4). Where well exposed, the sandstone typically consists of well sorted, micaceous, quartzo-feldspathic medium sand in thick bedded, parallel laminated, or hummocky and swaley cross-bedded sequences. The ma-

trix sand of pebbly sandstone and conglomerate beds is similar. Poor exposures (most inland exposures) generally appear massive. Beds in the Cape Blanco beach section dip 14° to 15° to the southeast and the thickness there is about 100 m (328 ft). A thin basal pebble conglomerate less than a meter (3.3 feet) thick includes scattered pholad-bored sandstone boulders as large as 1 m in diameter. On the south side of Cape Blanco, beds of fossiliferous sandstone and shell-pebble conglomerate higher in the section are locally carbonate cemented, hard, and light gray (N7) to white. The upper part of the formation is a light-colored diatomaceous silty sandstone. In other places the formation is similarly fossiliferous, typically with gastropods and pelecypods (see Addicott, 1983).

The formation crops out at Cape Blanco State Park in the headland beneath the lighthouse, where it rests unconformably on Otter Point Formation, and along the beach northwest of the beach access road. The beach cliff exposures unconformably overlie the sandstone of Floras Lake (**Tmf**) and unconformably underlie the Port Orford Formation (**Qpo**). Dissimilar diatom flora subtly suggest that the mid- to late Miocene Empire Formation predates the late Miocene diatomite of China Creek (**Tmc**). The Empire Formation may form a small channel fill cut into the sandstone of Floras Lake between Blacklock Point and Floras Lake. Poorly exposed soft, brown, fossiliferous sandstone encountered in the Johnson Creek, Ferry Creek, and Geiger Creek drainages east and southeast of Bandon have been mapped as sandstone of Floras Lake but may be Empire Formation.

The type section for these rocks is in the Coos Bay area. The name Empire Beds was originally applied by Diller (1896) and revised to Empire Formation a few years later (Diller, 1899). By 1945 Baldwin had recognized that the upper part of the formation in the Cape Blanco area was unconformable on the lower part and named the upper part the Port Orford Formation. In 1983, Addicott refined the stratigraphic extent of the Empire Formation in this area again, breaking the lower part of the section at Cape Blanco into two units separated by an unconformity and referring to the lower unit as the sandstone of Floras Lake. Addicott's revisions define the Empire Formation in the Cape Blanco area to match the stratigraphic extent of the Empire Formation in the type area near Coos Bay. He assigned older Miocene

strata to the sandstone of Floras Lake. Younger Miocene strata, including the diatomite of China Creek were originally mapped by Diller (1903) as part of the Empire Formation.

The middle to early-late Miocene age (Wishkahan Pacific Northwest Molluscan Stage) of the section along the coast southeast of Cape Blanco is based on fossil ages reported by Addicott (1983). Diatoms and silicoflagellates reported by Addicott (1983) range from late Mohnian to Delmontian. A radiometric age of 18.24 ± 0.86 Ma (Emerson, 2007) from water-laid tuff (**Tmft**) in the upper part of the underlying sandstone of Floras Lake, a few meters beneath the contact with the Empire Formation, suggests a maximum age of about 18 Ma.

Deformation of overlying terrace deposits (Kelsey, 1990) and lidar-based digital elevation models of surface topography show that the Cape Blanco area is higher (uplifted) relative to surrounding terrain.

Along with the sandstone of Floras Lake and the diatomite of China Creek, this formation overlaps the Gold Beach terrane and the Cape Blanco and Fulmar subterrane of the Sixes River Terrane and gives a minimum age for their amalgamation. On the headland beneath the lighthouse at Cape Blanco the unconformity at the base of the Empire Formation shows about 53 m (175 ft) of relief where it dips parallel to a southeastward-tilted surface cut into steeply-dipping beds of the Otter Point Formation

Unconformity

Tmf sandstone of Floras Lake (lower and middle Miocene; Wishkahan and Newportian Pacific Northwest Molluscan Stages)—A light green (5G 7/4) fresh to grayish yellow (5Y 8/4) weathered quartzofeldspathic marine sandstone with pebbly sandstone and conglomeratic layers and lenses.

Sandstone in the Floras Lake – Blacklock Point section is generally medium grained, well sorted, and poorly to well rounded. It contains layers and lenses of well rounded pebbles and conglomerate to 0.75 m (2.5 ft). Sedimentary structures include hummocky and swaley cross stratification and parallel laminations, suggesting that the sandstone was deposited near wave base at a depth of less than a couple hundred meters. A channel of sandstone, pebbly sandstone, and conglomerate cut into the Floras Lake

section, is mapped here as Empire Formation (**Tme**, Plate 1).

Rare sub-meter patches of blueberry-sized blue (5B5/6 to 5PB3/2) concretions (4 to 12 mm [0.16 to 0.50 in.]) were observed at the contact between the Empire Formation and overlying terrace deposits where the contact is well exposed high on the ocean beach west of Floras Lake. Many small faults can be seen to cut the formation in these excellent exposures. Addicott (1983) refined the stratigraphic extent of the Empire Formation, dividing rocks that Diller (1898) mapped as Empire in the Cape Blanco region into two formations, the younger 'restricted' Empire Formation and the older the sandstone of Floras Lake. Addicott's revisions result in an Empire Formation in the Cape Blanco area that matches the stratigraphic extent of the Empire Formation in the type area near Coos Bay. He assigned older Miocene strata to the sandstone of Floras Lake. The sandstone of Floras Lake crops out on the south side of Cape Blanco east of Fin Rock and between Floras Lake and a small headland just north of Blacklock Point.

The lowest exposures of Empire Formation at Cape Blanco include the conglomerate that crops out at the base of Fin Rock, on the southeastern side of the cape. Addicott (1983) considered this to be the base of the unit, but the contact is not exposed at this writing. It is mapped here as an unconformable contact based on terrain that suggests the lower contact roughly parallels bedding. Overall, the conglomerate and pebbly sandstone fines upward to sandstone beneath an 8-m thick (26.2 ft) resedimented or water-laid tuff bed (**Tmft**). Above the tuff bed the formation consists of sandstone. Total thickness of the unit is about 160 m (525 ft). The base of the unit unconformably overlies Upper Cretaceous rocks (**Ku**) north of Blacklock Point and Tertiary-Jurassic mélange of the Cape Blanco subterrane (**TJs**) of the Sixes River terrane at Cape Blanco. The sandstone of Floras Lake is overlain by the Empire Formation (restricted in the sense of Addicott, 1983) southeast of Cape Blanco and possibly by a filled channel of Empire Formation in the section south of Floras Lake.

Addicott (1983) assigned these rocks to the New-Portian and Wishkaham Pacific Northwest Stages of the Miocene based on the fossil assemblages. Emerson (2007) reported a single-crystal plagioclase K/Ar radiometric date for the tuff bed of 18.24 ± 0.86 Ma. Raymond and others (2008) studied magneto-

stratigraphy of the tuff bearing section south of Cape Blanco and report an age range for the formation of Chron C6r to Chron C5en (circa 20.0-18.0 Ma) based on the age of the included tuff reported by Emerson (2007). Raymond and others (2008) reported that the lower 35 m (115 ft) of the Fin Rock section has reverse polarity, the overlying 45 m (148 ft) of the section has normal polarity, the next 35 m (115 ft) has reverse polarity, and the uppermost 40 m (131 ft) of the section, including the tuff, has normal polarity.

Small exposures tentatively mapped as sandstone of Floras Lake occur at the Bandon Fish Hatchery and along Chandler Road near Bandon where the nearest pre-Miocene outcrops suggest that the unit rests unconformably on the Fulmar subterrane of the Sixes River terrane. Elsewhere, the subsurface distribution of sandstone of Floras Lake, Empire Formation, Port Orford Formation, or basal marine terrace is defined by water wells that report shelly material. These localities have all been tentatively included in the sandstone of Floras Lake.

Dunegan (2007) reported that in 1579 Sir Francis Drake, who was sailing up the Pacific Coast in the *Golden Hinde*, named this area New Albion because the white cliffs of the sandstone of Floras Lake and Empire Formation at Cape Blanco reminded him of the white cliffs of Dover.

Locally divided to show:

Tmft tuff (lower Miocene, 18.24 ± 0.86 Ma)— Water-laid ash and fine lapilli dacitic tuff forms a 6 to 7 m (20 to 23 ft) thick section that crops out in the upper part of unit **Tmf** along the sea cliff southeast of Cape Blanco (Plate 1; 373127E., 4743144N., WGS 84). Ash tuff and fine lapilli tuff beds are light gray (N7) to white and locally oxidized pinkish red (5R7/3). The tuff is laminated to low-angle cross bedded and likely resedimented and water-laid. Fine-grained, light gray to white ash about 0.8 m (3 ft) below the top of the unit contains abundant black fossil leaves, stems, and wood of the Cape Blanco flora (Emerson, 2007). Near the top of the sea cliff section southwest of Floras Lake a 1.5 to 2 m (4.9 to 6.6 ft) thick section of gray, thin-bedded, lapilli tuff is exposed, but is too small to show on the maps. There the tuff occurs near the top of unit **Tmf** and is cut by younger channel-filling sandstone and conglomerate (Leithold and Bour-

geois, 1983), that we tentatively map as the base of unit **Tme**. Samples obtained from the tuff by Emerson (2009) have a dacitic chemical composition with 69.28 to 70.97 weight percent SiO₂ and 196 to 250 ppm Zr (Table 3;

appendix). The tuff is assigned an early Miocene age on the basis of stratigraphic position and an ⁴⁰Ar/³⁹Ar age of 18.24 ± 0.86 Ma (plagioclase) obtained by Emerson (2009; Plate 1; appendix).

Table 3. Representative XRF analyses for rocks in the Port Orford, Langlois, and Bandon, Oregon areas.

Sample no.	11058 SCL 13	28 SCJ 13	314-19-1	10163 SCL 13	Emerson-2	Emerson-3	Emerson-4	Emerson-5	100912 SCL 13	314-19-2	100110 SCL 13	73 SCJ 13
Map no.	G-1	na	G-2	G-3	G-4	G-5	G-6	G-7	G-8	G-9	G-10	G-11
Quadrangle	Sixes	Mount Butler	Sixes	Sixes	Cape Blanco	Cape Blanco	Cape Blanco	Cape Blanco	Sixes	Cape Blanco	Bandon	Bandon
Terrane	Gold Beach terrane	Sixes River terrane	Sixes River terrane	Gold Beach terrane	nd	nd	nd	nd	Sixes River terrane	nd	Sixes River terrane	Sixes River terrane
Group	Otter Point Formation	Fulmar subterrane	Fulmar subterrane	Otter Point Formation	nd	nd	nd	nd	Fulmar subterrane	nd	Fulmar subterrane	Fulmar subterrane
Formation	KJov	KJsv	KJsv	KJos	Tmft	Tmft	Tmft	Tmft	TKb	Spu	KJsi	KJsi
Map Unit	KJov	KJsv	KJsv	KJos	Tmft	Tmft	Tmft	Tmft	TKb	Spu	KJsi	KJsi
UTM N (NAD 83)	4736585	4740881	4741470	4741472	4743086	4743086	4743086	4743086	4743198	4747646	4771357	4771367
UTM E (NAD83)	377657	389466	386709	383392	373186	373186	373186	373186	379599	374804	383128	383167
<i>Oxides, weight percent</i>												
SiO ₂	50.00	51.22	50.60	53.23	69.72	70.97	69.28	69.92	47.82	57.43	47.80	47.39
Al ₂ O ₃	16.12	15.69	16.38	16.26	16.28	15.34	15.95	15.83	14.46	16.81	15.47	16.37
TiO ₂	1.58	0.86	1.75	0.82	0.46	0.42	0.46	0.40	1.93	1.36	2.73	2.64
FeO*	11.36	9.70	8.94	9.84	4.47	4.09	4.58	4.20	13.71	9.75	11.96	12.13
MnO	0.20	0.22	0.17	0.19	0.03	0.05	0.03	0.03	0.26	0.13	0.34	0.33
CaO	12.84	9.77	10.85	8.14	1.66	1.71	2.24	1.47	9.24	3.88	11.54	11.45
MgO	6.38	7.53	6.53	6.29	2.74	1.95	2.95	2.57	7.50	3.12	6.72	6.10
K ₂ O	0.12	0.28	0.06	0.38	1.79	2.03	1.58	1.93	0.47	0.68	0.35	0.26
Na ₂ O	1.26	4.64	4.49	4.77	2.76	3.35	2.86	3.58	4.43	6.35	2.83	3.10
P ₂ O ₅	0.15	0.08	0.22	0.08	0.08	0.09	0.08	0.08	0.20	0.50	0.27	0.24
LOI	6.21	4.51	4.78	3.24	12.25	9.99	12.10	10.30	5.66	4.91	2.72	2.45
<i>Trace elements, parts per million</i>												
Ni	105	106	69	65	nd	nd	nd	nd	91	13	90	95
Cr	243	197	180	109	nd	nd	nd	nd	105	22	99	143
Sc	39	33	33	32	nd	nd	nd	nd	35	21	37	33
V	329	261	236	282	nd	nd	nd	nd	342	75	387	393
Ba	93	138	38	115	626	626	537	626	630	1019	103	93
Rb	4.2	6.5	2.1	5.2	nd	nd	nd	nd	12.3	11.7	6.0	5.7
Sr	76	203	149	166	nd	nd	nd	nd	180	289	222	236
Zr	87	45	130	42	169	169	250	169	100	210	158	145
Y	36.7	25.9	42.0	25.0	nd	nd	nd	nd	36.2	131.6	37.7	31.8
Nb	5.7	0.7	9.3	1.3	nd	nd	nd	nd	8.3	4.8	11.7	10.1
Ga	17.2	14.5	21.3	14.9	nd	nd	nd	nd	17.8	21.1	20.9	20.8
Cu	106	80	50	16	nd	nd	nd	nd	160	11	340	275
Zn	96	94	177	35	nd	nd	nd	nd	92	27	93	101
Pb	8	1	<1	<1	nd	nd	nd	nd	12	7	<1	<1
La	11	6	10	12	nd	nd	nd	nd	14	26	7	8
Ce	20	17	20	16	nd	nd	nd	nd	23	53	19	17
Th	<0.5	2.5	4.6	<0.5	nd	nd	nd	nd	2.4	12.5	3.7	4.6
U	<0.5	<0.5	<0.5	<0.5	nd	nd	nd	nd	<0.5	<0.5	<0.5	0.5
Co	47	47	53	42	nd	nd	nd	nd	60	32	59	50

Major element determinations have been normalized to a 100-percent total on a volatile-free basis and recalculated with total iron expressed as FeO*; nd = no data. Samples G-1 to G-3 and G-8 to G-11 collected for this study and analyzed at Franklin and Marshall University; samples G-4 to G-7 from Emerson (2009) and analyzed at ALS Chemex in Vancouver, British Columbia, Canada. Map no. labels correspond to data points shown on geologic map plates 1, 2, and 3.

Unconformity

LOWER CENOZOIC AND MESOZOIC ROCKS

PALEOGENE SEDIMENTARY ROCKS

Teu Umpqua Group (lower to middle Eocene)—Sandstone, pebbly sandstone, conglomerate, and mudstone not mapped separately. Crops out in east-central part of the map area where it overlies the Fulmar and/or Whitsett subterrane of the Sixes River terrane. Mapped distribution in the southeastern part of the Bandon quadrangle (Plate 3) extends mapping by Brownfield and others (1982) based on lidar signatures that indicate the presence of bedded strata. East of the study area the Umpqua Group laps across contacts between Western Klamath, Yolla Bolly, and Sixes River terranes. Formations in the upper part of the group are deposited across Canyonville fault in the vicinity of the Coast Range syncline 48 km (30 mi) east of the study area.

Unconformity(?)

SIXES RIVER TERRANE

Cape Blanco (western) subterrane—Distinguished by the presence of broken formation or *mélange* that includes deformed strata of middle Eocene age. Eocene rocks either form *mélange* matrix in areas south of Blacklock Point or form more restricted broken formation of thin bedded turbidites restricted to the neck at Cape Blanco. Linked to the Whitsett and Fulmar subterrane of the Sixes River terrane based on the common presence of exotic blocks of distinctive glaucophane schist and garnet schist.

TJs mudstone and sandstone matrix *mélange* (lower middle Eocene(?) to Upper Jurassic(?))—Mudstone- and thin-bedded mudstone- and sandstone-matrix *mélange* with infolded sections of thin-bedded mudstone and sandstone turbidites and exotic blocks of various lithologies. These rocks are poorly exposed in an upfaulted section (Empire Formation [Tme] missing) that makes up the neck of the peninsula at Cape Blanco. Similar thin-bedded strata crop

out on a knoll on the north bank of the Sixes River near its mouth. Blocks of various lithologies, believed to be carried in the mudstone- and thin-bedded sandstone-matrix *mélange*, crop out from the draw east of the lighthouse at Cape Blanco to Blacklock Point. Age assigned on the basis of fossil and radiometric ages including lower(?) middle Eocene fossil ages reported by Bandy (1941, 1944), Stewart (1957), and Dott (1971) from Cape Blanco. The composition of the lower(?) middle Eocene sandstone contrasts markedly with that of coeval (Stewart, 1957) micaceous sandstone of the micaceous Sacchi Beach beds (north of the study area). The Sacchi Beach beds form part of the overlap sequence between the Fulmar and Whitsett subterrane of the Sixes River terrane and have provenance similar to, or derived from, the Tyee and Coaledo formations. Locally divided to show individual blocks and groups of blocks including:

TJss sandstone—Medium- to coarse-grained sandstone, grit, and pebbly sandstone. May be calcite cemented with calcite veins and patches. May locally be thick-bedded or massive blocks equivalent to Eocene thin-bedded sandstone that crops out as folded sections of *mélange* matrix at Cape Blanco. Better indurated blocks of sandstone are similar to *Buchia*-bearing rocks described elsewhere in the Sixes River terrane by Blake and others (1985) and are likely Mesozoic.

TJsv volcanic and meta-volcanic rock—Mafic volcanic rocks and possibly related intrusives. Commonly metamorphosed to greenschist facies.

TJsc chert—Green, bluish green, brown, black, gray, and red chert. Some blocks manganese-bearing; some blocks with radiolaria; some blocks banded; some blocks chert-pebble to chert-cobble conglomerate with chert matrix. Fossil ages for chert from the other two subterrane of the Sixes River terrane range from Tithonian to Valanginian (ca. 150 to 134 Ma).

TJsb blueschist—Blue to blue-black colored (5B6/2 to 5PB3/2), glaucophane- and lawsonite-bearing blueschist. Mineral assemblage

es are consistent with either high-pressure (glaucofane bearing) greenschist to blueschist metamorphic facies. Blueschist blocks at Bandon (that are part of unit **KJs**) have radiometric ages of 148.47 ± 8 and 150.28 ± 4 Ma (Plate 3; appendix).

TJcg conglomerate—Pebble and cobble conglomerate. The clast assemblage commonly includes chert, argillite, phyllite, quartz, mudstone, and sandstone and often contains distinctive clasts of limestone, serpentinite, and blueschist. May include rip-up beds or pebbles and/or thin intervals of shale or mudstone. Limestone clasts in the conglomerate may be related to mid-Cretaceous (Albian-Coniacian) Whitsett limestone lentils of Diller (1898; Sliter, 1984) that crop out south of Roseburg. If so, the enclosing conglomerate would be younger.

TJsg garnet schist—Garnet schist.

TJsp serpentinite and meta-serpentinite—serpentinite, meta-serpentinite, and serpentinitized ultramafic rocks.

TJsx mélange blocks, undivided—Mélange blocks recognized and mapped on the basis of topographic expression. Lithologies have not been identified or sampled.

Faulted subterrane boundary

Fulmar (central) subterrane—Distinguished by the presence of lower Eocene arkosic sandstone of Fivemile Point (Snively and others, 1985, as cited by Snively, 1987).

Tefm sandstone of Fivemile Point (lower Eocene)—Sandstone with minor grit, mudstone, pebbly sandstone, conglomerate, and shale in rhythmic bands interpreted as turbidites. Conglomerate and sandstone locally contain distinctive fine-grained cream-colored sedimentary(?) clasts (recycled concretions?) in many outcrops. Distinguished from coeval strata of the Umpqua Group that crop out farther east by its arkosic wacke composition (Snively

and others, 1985). The best exposures are outside the study area at Fivemile Point north of Bandon. The unit was also recognized in offshore wells including the Union Oil Company's Fulmar Well west of Coos Bay (Snively and others, 1985). Sections of steeply dipping beds are broadly warped, suggesting that at least two folding events have occurred.

The sandstone of Fivemile Point is assigned an early Eocene age on the basis of stratigraphic position and microfossils collected at Fivemile Point and in offshore wells (David Bukry, as cited by Miles, 1981; Snively, 1987). One sample (22 SCJ 13; appendix) that might be sandstone of Fivemile Point was collected east of Langlois (Plate 2; Langlois 7.5-minute quadrangle; appendix) for $^{206}\text{Pb}/^{238}\text{U}$ analysis of detrital zircons. One hundred and one detrital zircons yielded peak age populations at 103 Ma, 111 Ma, 118 Ma, 127 Ma, 159 Ma, 166 Ma, 198 Ma, and 209 Ma (appendix). The ten youngest zircons analyzed from 22 SCJ 13 range from 90.4 ± 1.6 to 97.5 ± 2.0 Ma, with the youngest coherent peak population of 10 grains defining a maximum depositional age of ca. 103 Ma (Early Cretaceous [Albian]) for this sample.

Unconformity(?)

Ku sandstone and mudstone turbidites (Upper Cretaceous)—sandstone, grit, and mudstone turbidites that crop out at Blacklock Point. Along the beach north of Blacklock Point the Cretaceous section consists of a fault-bounded sequence, approximately 500 m (1,600 ft) thick, folded into a southeast-plunging syncline. The bottoms of several thick sandstone beds display grooves and related sole markings and internal organization of the beds is consistent with bouma sequences. The Blacklock Point beds are assigned to the Sixes River terrane on the basis of association with mélange units belonging to that terrane. Cretaceous strata north of the Canyonville Fault have all been assigned to the Fulmar (central) subterrane of the Sixes River terrane where they lie west of the projected Fulmar fault that separates Fulmar subterrane from the eastern subterrane. Alternatively, the beds at Blacklock Point may represent a fault sliver or overlap sequence related to Cretaceous strata recognized south of Gold Beach, in the Gold Beach terrane.

Unit **Ku** is assigned a Late Cretaceous age on the basis of 1) non-diagnostic mid- to Late Cretaceous foraminifera reported by Koch (as cited by Dott, 1971), 2) possible correlation with Cretaceous turbidite sequences that overlie the Sixes River terrane or with turbidite sequences in the Hunters Cove or Houstaden Creek Formation described near Cape Sebastian (Dott, 1971; Bourgeois and Dott, 1985; McClaughry and others, 2013; T. J. Wiley, unpublished mapping, 2007) and 3) detrital zircon ages. One sample (42 SCJ 13; appendix) was collected from unit **Ku**, north of Blacklock Point (Plate 2; Floras Lake 7.5-minute quadrangle; appendix) for $^{206}\text{Pb}/^{238}\text{U}$ analysis of detrital zircons. This sample yielded one hundred and six detrital zircons with peak age populations at 92 Ma, 108 Ma, 27 Ma, 158 Ma, 193 Ma, and 1,325 Ma (appendix). The ten youngest zircons analyzed from 42 SCJ 13 range from 76.1 ± 3.0 Ma to 108.2 ± 2.4 Ma. The youngest peak population of ca. 92 Ma (Late Cretaceous [Turonian]) contains only three grains and should be viewed with caution as a maximum depositional age in light of the small number of grains. The second youngest peak is 108 Ma (Early Cretaceous [Albian]) and can also be considered in determining maximum depositional age for this sample.

Unconformity

KJs mélange of Sixes River (Upper(?) Cretaceous to Jurassic)—Mudstone-matrix mélange with infolded sections of thin-bedded mudstone and sandstone (turbidites?) and blocks of various lithologies. Age based on ages of included blocks and on calcareous nannofossils reported by Miles (1981) from the Floras Creek drainage. Locally divided to show the lithologies of blocks including:

KJss sandstone—Medium- to coarse-grained sandstone, grit, and pebbly sandstone. May be calcite cemented with calcite veins and patches.

KJsv volcanic and meta-volcanic rocks—Mafic volcanic rocks. Some blocks probably metamorphosed to greenschist facies. A large exposure of pillowed and columnar lava and entablature between Sixes River and Edson Creek has been mapped with this unit but

may be a faulted sliver of some other terrane. Samples obtained from flow and intrusive blocks in this unit have spilitic (Le Maitre and others, 2004) chemical compositions with 50.6 to 51.22 weight percent SiO_2 , 6.53 to 7.53 weight percent MgO , and 4.49 to 4.64 weight percent Na_2O (Plate 1; Table 3; appendix).

KJsc chert—Green, bluish green, brown, black, gray, and red chert. Some blocks manganeseous; some blocks with radiolaria; some blocks banded; some blocks chert-pebble to chert-cobble conglomerate with chert matrix. Lower Cretaceous and Upper Jurassic ages reported by Blake and others (1985).

KJsb blueschist—Glaucophane and lawsonite bearing blue to blue-black colored schist. Mineral assemblages consistent with either high-pressure greenschist or blueschist metamorphic facies. One of the largest of these, Bandon's Tupper (Grandmother) Rock, was completely quarried to build the Bandon jetties in 1881-1900. Samples from Tupper Rock have K/Ar ages of 148.47 ± 8 Ma and 150.28 ± 4 Ma (Plate 3; appendix). K/Ar ages on blueschist exposed east of the map area in the Sugarloaf and Calf Ranch Mountain areas range from ca. 134 to 153 Ma (134.86 ± 13 Ma; 134.98 ± 8 Ma; 144.25 ± 6 Ma; 145.05 ± 4 Ma; 152.74 ± 4 Ma; Coleman and Lanphere, 1971; Fiebelkorn and others, 1983; Sloan and others, 2003).

KJcg conglomerate—Pebble and cobble conglomerate. May contain distinctive clasts of limestone, serpentine, and blueschist that indicate provenance related to the mélange. Dated blocks of limestone within the mélange range in age from Albian to Cenomanian, suggesting that conglomerate containing limestone is post-Albian and likely post Cenomanian.

KJsg garnet schist—Garnet schist and eclogite.

KJsi coarse-grained igneous rocks—Gabbro and related rocks. Dikes intruding sandstone in sea stacks at Devils Kitchen near Bandon have a gabbroic chemical composition with

47.39 to 47.80 weight percent SiO₂, 2.64 to 2.73 TiO₂, 11.96 to 12.13 weight percent FeO*, and 6.10 to 6.72 weight percent MgO (Plate 3; Table 3; appendix).

KJsm other metamorphic rocks—Green, fine-grained meta-volcanic rocks, fine-grained meta-sandstone, and siltstone, undivided containing actinolite, chlorite, and/or epidote suggesting metamorphism to greenschist facies.

KJsp serpentinite and meta-serpentinite—Serpentinite, meta-serpentinite, and serpentinitized ultramafic rocks.

KJst siltstone—Silicified siltstone.

KJsx mélange blocks, undivided—Mélange blocks recognized on the basis of topographic expression, but lithologies not identified or sampled.

VOLCANIC ROCKS THAT ERUPTED ONTO OR INTRUDED THE FULMAR (CENTRAL) SUBTERRANE OF THE SIXES RIVER TERRANE

TKb volcanic rocks (Neogene(?), Paleogene(?), or Cretaceous(?))—Dikes and/or mafic lava that crop out in the Edson Creek Recreation Area (WGS84 coordinates 385070E., 4741465N.) and along Crystal Creek road (WGS84 coordinates 379650E., 4743205N.)

A small, unmapped, poorly exposed clast, dike, or block of granitic rock was sampled (sample G-9, Plate 1) from the top of the sea cliff along the fault zone southeast of Blacklock Point.

Faulted terrane boundary

GOLD BEACH TERRANE

CRETACEOUS SEDIMENTARY ROCKS

Kugb sedimentary rocks, undivided (Upper(?) Cretaceous)—Sandstone, conglomerate, and mudstone, occurring in offshore sea stacks interpreted by Hunter and others (1970) to be equivalent to the Hunters Cove Formation or Cape Sebastian Sandstone. May

also be equivalent to the Houstonaden Creek Formation of Bourgeois and Dott (1985). The Hunters Cove Formation (Upper Cretaceous, lower Maastichtian[?] and/or Campanian) consists of dark gray (N3), well bedded siltstone and mudstone interbedded with pale orange (10YR) to dark yellowish orange (10YR 6/6) finely laminated and rippled sandstone, and mudstone with minor sandstone-boulder conglomerate. The Cape Sebastian Sandstone is a middle or late Campanian age pale to dark yellowish orange (10YR 8/2 to 10YR 6/6) conglomerate and sandstone. The Houstonaden Creek Formation is an early Campanian and/or Albian(?) sequence of interbedded mudstone, siltstone, and fine sandstone with minor pebble and cobble conglomerate. Outcrops of these rocks lie offshore and were not visited during the present study.

Unconformity

LOWER CRETACEOUS AND UPPER JURASSIC SEDIMENTARY ROCKS

KJos Otter Point Formation, (Lower Cretaceous and Upper Jurassic, Hauterivian to Tithonian Stages)—Dark gray (N3) fresh to dark yellowish orange (10YR 6/6) weathered, well-bedded, volcanoclastic sandstone, mudstone, shale, grit, and conglomerate exposed in the southwestern part of the project area. Well-indurated, fine- to coarse-grained sandstone-dominated sequences consist of angular to subrounded, poorly to very poorly sorted framework grains composed of volcanic lithic fragments, albite, sedimentary lithic fragments, quartz, and detrital chert. The matrix component of sandstone typically contains a mixture of fine dark mud, chlorite, authigenic clay minerals, and carbonate mud (Goodfellow, 1987). Sedimentary structures in sandstone beds include load casts, flute casts, convolute bedding, and small-scale cross bedding, suggesting that these rocks were deposited by turbidity currents on a submarine fan. The abundance of albitic plagioclase grains and the near absence of zircon in these rocks suggests they were deposited in a mid-ocean or ocean island environment isolated from continental sediment sources. Conglomerate is present in places, including a sea stack at UTM NAD83 coordinates 369076E., 4738985N. (Hunter and others, 1970).

This unit forms uplands and erosionally resistant sea stacks along the coastline, including the headland beneath the lighthouse at the tip of Cape Blanco (see map plates; Brownfield and others, 1982; Koch, 1963, 1966; Aalto, 1968; Aalto and Dott, 1970; Dott, 1971; Walker, 1977). The sandstone-dominated formation locally includes blocks of pillow lava and volcanic breccia (**KJov**; see Plate 1). Blocks of other lithologies, including diorite, chert, and serpentinite are included in the Otter Point Formation in areas to the south. Hunter and others (1970) mapped conglomerate on Large Brown Rock offshore (WGS84 coordinates 369076E., 4738985N.). Linear zones that may be surface traces of major shear zones or faults are defined by blocks of volcanic rock. Rocks in the Otter Point Formation are locally pervasively sheared, folded, and faulted to the point where original stratigraphic continuity has been nearly obliterated. Few beds can be traced more than 100 meters. The Otter Point is thus best described as a “broken formation” (in the sense of Hsü, 1968), in regard to the complex structural dismemberment of the formation and absence of truly exotic blocks. Metamorphism of the formation is limited to numerous veins of laumontite; pillow lavas locally display the effects of ocean-floor metamorphism defined by the albitization of plagioclase, and the presence of prehnite, pumpellyite, and epidote (Blake and others, 1985). The Otter Point Formation is assigned an Early Cretaceous and Late Jurassic age on the basis of the wide occurrence of *Buchia piochii* and absence of fossils of other ages (Bourgeois and Dott, 1985). The unit is equivalent to the Otter Point Formation as defined by Koch (1963, 1966), Dott (1971), and Bourgeois and Dott (1985) and is assigned to the Gold Beach terrane following work by Blake and others (1985). In contrast to sandstone collected from other formations in southwest Oregon, sandstone associated with the Otter Point Formation contains relatively few grains of detrital zircon. The formation is divided to show:

KJov volcanic rocks— Blocks of volcanic rock that occur in the study area are grayish black (N2) to medium dark gray (N4) and olive gray (5Y 4/1) basalt that are aphyric to sparsely plagioclase-phyric containing < 1 to 3 percent clear to milky-white, blocky and lath-shaped plagioclase phenocrysts up to 5 mm (0.2 in) across distributed within a fine-grained

groundmass. Some samples have an amygdaloidal texture with former vesicles and/or cavities filled by calcite and chlorite.

These rocks are similar to discontinuous sections of mafic to intermediate composition lava flows, pillow lava, and volcanic breccia that crop out in the Otter Point Formation to the south, between the Pistol River and Ophir (McClaghry and others, 2013). Many outcrops are very poor, and most commonly rubble is all that is visible at the surface. Where well exposed, volcanic units appear to be fault-bounded blocks. Contacts with adjacent sedimentary rocks are presumed to be faults. Flows predominantly consist of aphyric to sparsely plagioclase- and/or clinopyroxene-phyric mafic to intermediate volcanic rock metamorphosed to greenschist facies (greenstone), but more distinctive porphyritic flows and pillow lavas containing large plagioclase megacrysts are locally present.

Petrographic work by McClaghry and others (2013) showed aphyric to sparsely phyric lavas are saussuritized with a microporphyritic texture characterized by relict clinopyroxene and elongated feldspar lathes set in an altered groundmass of clinozoisite, chlorite, and zeolite. Samples obtained from these lavas generally have high-titanium basaltic chemical compositions with 48.16 to 51.05 weight percent SiO₂, 1.46 to 3.15 weight percent TiO₂, and 4.42 to 6.64 weight percent MgO. These flows also contain characteristically elevated amounts of Ni (34 to 255 ppm) and Cr (68 to 605 ppm), with compositions similar to tholeiitic Mid-Ocean Ridge Basalt (MORB). Very high MnO and very low Ba suggest secondary or sea floor alteration affected many samples.

Faulted terrane boundary

PICKETT PEAK TERRANE

Kcqs Colebrooke Schist (Upper Jurassic origin, Lower Cretaceous or later emplacement; 128.3 ± 6 Ma, 128.6 ± 6 Ma, 141.9 ± 10 Ma K/Ar whole-rock, metamorphic age)— Very light gray (N8) to medium bluish gray (5B 5/1), strongly foliated, fine-grained

quartz-mica phyllite (metapelite) and quartz-mica schist exposed in an allochthonous structural nappe along the eastern edge of the map area (see plates). Locally, the unit includes lesser amounts of metasandstone, conglomerate with stretched-pebbles, small bodies of metachert, and pillow lavas. The Colebrooke Schist rests on a subhorizontal, regionally east-dipping thrust contact that truncates underlying structures and geologic units. The maximum thickness of the Colebrooke structural nappe is approximately 915 m (3,000 ft), with an average thickness of 300 to 600 m (1,000 to 2,000 ft) (Coleman, 1972). The Colebrooke Schist is typically crenulated and sheared and contains ubiquitous quartz veins. Metamorphic mineral assemblages (quartz-albite-phengite-chlorite \pm lawsonite \pm calcite) typically are transitional between greenschist and blueschist facies (Coleman, 1972; Blake and others, 1985). Occurrences of serpentinite near the Colebrooke Schist are assigned to a non-terrane-specific unit (**Spu**), but may locally represent the serpentinite matrix *mélange* reported to underlie exposures of Colebrooke Schist elsewhere in the Pickett Peak terrane (McCloughry and others, 2013; Blake and others, 1985). Whole-rock (quartz-mica schist) K/Ar ages ranging between 125 ± 6 Ma and 142 ± 10 Ma and a Rb-Sr isochron date (whole rock) of ~ 130 Ma indicate an Early Cretaceous metamorphic age (Dott, 1971; Coleman, 1972; Lanphere and others, 1978; Brown and Blake, 1987). Equivalent to the Colebrooke Schist as described by Diller (1903) and Coleman (1972). The Colebrooke Schist was assigned to the Pickett Peak Terrane by Blake and others (1985).

Krp Rocky Point Formation (Lower Cretaceous, Valanginian or Berriasian Stage)—Dark gray (N3) to grayish olive green (5GY), well-bedded sandstone and mudstone exposed across the southeastern part of the map area. Good outcrops of the unit are rare and are confined to fresh road cuts and prominent cliffs located between Port Orford and the Sixes River. Where well exposed, the unit consists of medium gray (N5), graded, fine- to medium-grained, subfeldspathic to subfeldspathic-lithic sandstone alternating with beds of dark gray (N3) mudstone. Granule and fine pebble conglomerate is confined to the base of sandstone beds. The unit is separated from the underlying Humbug Mountain Conglomerate (**Khcg**) on the basis of decreasing amounts, and generally thinner, finer-grained intervals of conglomerate. Thickness of the unit may exceed 1,828 m (6,000 ft). The unit is equivalent to the Rocky Point Formation, as defined by Koch (1963, 1966) and Dott (1971) and is assigned to the Elk subterrane of the Western Klamath terrane following the work of Blake and others (1985).

The Rocky Point Formation is assigned an Early Cretaceous age on the basis of the occurrence of *Buchia crassicolis* and other ammonoids (Dott, 1971). One sample (18 SCJ 13; Plate 1; appendix) was collected from the Rocky Point Formation, 0.3 km (0.2 mi) north of Grassy Knob (Father Mountain 7.5-minute quadrangle). Twenty-nine detrital zircons define two peak age populations in this sample at 156 Ma and 171 Ma, neither of which is present in zircon age populations observed in the Early Cretaceous Humbug Mountain Conglomerate (**Khcg**) sample (17 SCJ 13). The ten youngest zircons analyzed from 18 SCJ 13 range from 134.9 ± 4.8 Ma to 154.6 ± 5.5 Ma, with the youngest coherent peak population of 12 grains defining a maximum depositional age of ca. 156 Ma for this sample.

Khcg Humbug Mountain Conglomerate (Lower Cretaceous; Valanginian or Berriasian Stage)—Massive, poorly to moderately sorted, clast-supported, heterolithic pebble and cobble conglomerate and lesser sandstone that is

Faulted terrane boundary

WESTERN KLAMATH TERRANE

Elk subterrane—Partly or wholly equivalent to Myrtle Group (Riddle Conglomerate and Days Creek Formation) that crops out 35 km (22 mi) inland, near Myrtle Creek on Interstate Highway 5. Ophiolite remnants that crop out nearby on the Sixes River are likely equivalent to the Coast Range ophiolite (Snow Camp subterrane of the Western Klamath terrane).

locally exposed along the Elk River Road and near Grassy Knob. The conglomerate typically contains moderately to well-rounded clasts of diorite, andesite, keratophyre, dacite, rhyolite, lapilli tuff, chert, schist, phyllite, slate, vein quartz, amphibolites, propylite, and unmetamorphosed sandstone. Compositions include ~60 percent igneous rocks, 30 percent metamorphic rocks, and 10 percent sedimentary rocks (Koch, 1966; Dott, 1971). In the type area at Humbug Mountain and along the Elk River south of the map area there are zones of boulder conglomerate (McClaghry and others, 2013). The maximum clast size is approximately 0.6 m (2 ft) along Elk River. The matrix is composed of poorly sorted fine- to coarse-grained sandstone largely consisting of angular grains. Stratification is generally poorly defined, but a slight preferential orientation of clasts is locally present. Associated lithic sandstone beds display grading and sedimentary structures consistent with deposition by turbidites. Facing directions in sandstone beds that crop out north of Grassy Knob suggest they are in fault contact with Humbug Mountain Conglomerate to the south and are assigned to the Rocky Point Formation. Thickness of the conglomerate is greater than 762 m (2,500 ft) and it may be up to 1,829 m (6,000 ft) thick along the Elk River. The unit is equivalent to the Humbug Mountain Conglomerate, as defined by Diller (1903), Koch (1963, 1966), and Dott (1971), and is assigned to the Elk subterrane of the Western Klamath Terrane following the work of Blake and others (1985).

The Humbug Mountain Conglomerate is assigned an Early Cretaceous age on the basis of the occurrence of *Buchia crassicolis* and ammonoids (Dott, 1971). One sample (17 SCJ 13; appendix) was collected from the Humbug Mountain Conglomerate on Grassy Knob, 0.3 km (0.2 mi) south of the map area (Father Mountain 7.5-minute quadrangle) for $^{206}\text{Pb}/^{238}\text{U}$ analysis of detrital zircons. This sample yielded eighty-two zircons with peak age populations at 181 Ma, 198 Ma, 226 Ma, 234 Ma, 264 Ma, 444 Ma, 1,094 Ma, and 1,208 Ma (appendix). The ten youngest zircons analyzed from 17 SCJ 13 range from 137.6 ± 6.5

Ma to 162.5 ± 2.4 Ma, with the youngest coherent peak population of 24 grains defining a maximum depositional age of ca. 181 Ma (Early Jurassic [Toarcian]) for this sample.

OTHER ROCKS

Spu serpentinite, serpentinite-matrix mélange, and serpentinitized ultramafic rock, undivided (Cretaceous(?) and Upper Jurassic(?))—Green (hues 10Y to 10G) to black serpentinite that crops out along fault zones. May line fault zones or occur as discrete blocks on fault zones. The rock is typically sheared and locally displays an anastomosing linear and/or planar fabric that largely parallels the associated fault plane(s). Locally, serpentinite encloses blocks of other lithologies, particularly along thrust faults associated with, and geographically near, the basal contact of the Pickett Peak terrane (Colebrooke Schist) where it occurs as serpentinite-matrix mélange. Blocks may retain relict ultramafic textures. This unit is distinguished from mélange blocks designated as units **TJsp** and **KJsp** by association with fault zones and, often, by the absence of enclosing sedimentary mélange matrix.

STRUCTURAL GEOLOGY

Structural geology along this part of the southern Oregon coast is complex, reflecting multiphase development, amalgamation, and accretion of discrete tectonostratigraphic terranes along the Cascadia margin since the Jurassic (Figure 4). No simple regional pattern of structure can easily be portrayed for the southern Oregon coast, but individual domains and phases of deformation can be discerned from careful mapping of bedrock and surficial geology in the area.

Each of the several tectonostratigraphic terranes assembled here displays 1) its own structural history prior to amalgamation, 2) structural regimes related to amalgamation and/or accretion, and 3) post-accretionary structural modifications. As with most terrane models, the one described here (adapted from Blake and others, 1985), assumes separate early histories for regions with distinct stratigraphy even though some of these rock packages may have originated as adjacent provinces in complex tectonic settings.

The general structural pattern recognized in Mesozoic rocks along the Oregon coast to the south—which con-

sists mainly of north- to northwest-trending fault-bounded terranes, lithologic belts, and lesser faults that parallel the coastal margin—is interrupted in the study area by several large northeast- to east-west-trending high-angle faults (map plates). Onshore, the largest of these is mapped here as a western extension of the Canyonville fault (Figure 4; Plate 1). At depth, the poorly located lower plate projection of the Blanco Fracture zone undoubtedly influences structural geology, if only through the isostatic contrast between hotter, younger (closer to the ridge) and colder, older oceanic (farther from the ridge) crust juxtaposed across the zone (Figure 7). Major faults separating Mesozoic terranes also include low-angle thrust faults. Bedrock in the northern two-thirds of the area is pervasively sheared mudstone- and fine-grained sandstone-matrix *mélange* enclosing blocks of many lithologies that originated in diverse environments including deep mantle (blueschist), spreading centers, and volcanic arc(s). Related rocks, including marine limestone, exposed south of Roseburg, formed at low or southern latitudes.

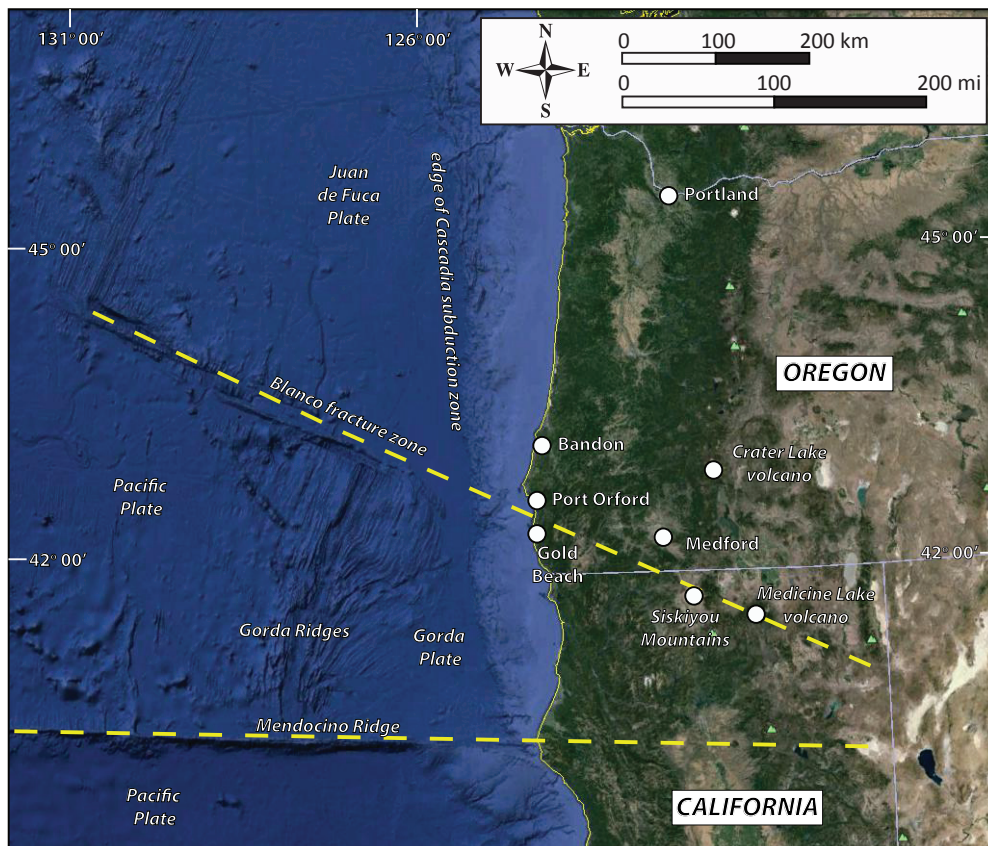


Figure 7. Large-scale linear features on the continental margin lie along projected trends of offshore fracture zones. We speculate that these 1) delineate subcrop of Gorda Plate, 2) reflect accommodation of isostatic contrasts between Pacific, Gorda, and Juan de Fuca blocks, and 3) are zones where other lower plate boundary processes affect the upper plate. Major features that lie along the projected trace of the Blanco fracture zone include the Cape Blanco – Port Orford – Gold Beach segment of the coast, lower Rogue River, Applegate River, Bear Creek (Medford-Ashland), Siskiyou Mountains, Medicine Lake Volcano, and the southern end of the Warner Mountains. The projected trace of the Mendocino Ridge linear is described by Rich and Steele, (1974). Image from Google Earth 2014.

Geologic structure along the southern Oregon coast is defined by the mapped distribution of geologic units, faults, topographic lineaments (as observed in 3-ft lidar DEMs and 10-m DEMs), folds, bedding attitudes, foliations, and lineations (appendix). Many faults or shear zones in the project area are identified by the presence of blocks and irregular bodies of serpentinite along their traces. Primary structural features (e.g., slickensides or fault breccia) are common in mélangé matrix and serpentinite and less common in other lithologies. Fault zones are best exposed along sea cliffs, stream banks, road cuts and in rock pits. The Battle Rock fault zone appears to truncate the western end of the Canyonville fault in a right lateral sense. Along other faults that parallel the coast, the relative amount of offset is not well-constrained, as few stratigraphic piercing points have been recognized and lithologies on opposite sides of fault zones are often indistinguishable. Only locally is the relative amount of offset indicated by offset geologic contacts. The east-trending Canyonville fault zone clearly offsets many of the terrane boundaries in a right-lateral sense.

Structural fabrics apparent in data collected for this report are informative, but are at best reconnaissance in nature. More comprehensive structural, provenance, and sedimentologic studies would undoubtedly allow a better geologic map to be produced, particularly the depiction of otherwise similar clastic sedimentary units.

Folding and faulting

Gold Beach terrane

From Cape Blanco south to Whaleshead Island (near Brookings), rocks belonging to the Gold Beach terrane reflect a complex multiphase structural history that includes Late Jurassic and/or Early Cretaceous, Paleogene, and Neogene deformation. The Otter Point Formation (KJos, KJov), which makes up most of the Gold Beach terrane, is characterized by disharmonic, asymmetric folds, local vertical to overturned bedding, and intense internal shearing. On a large scale, deformation in the formation can be modeled most simply as a system of early north-trending folds and overturned folds that were subsequently refolded about east-west-trending axes, such that axes of the early folds plunge both to the north and to the south. Because the Otter Point Formation is largely broken formation, the folds are dismembered, discontinuous, and difficult to track. South of the study area, this history can explain both the wide range of measured attitudes and the rarity of strikes with east-west trends, strikes that would only occur along fold noses near the intersection of bedding and axial planes. Within the study area, easterly strikes

are more common, particularly in the vicinity of the western extension of the Canyonville Fault. We attribute this to post-Cretaceous deformation associated with faulting. At Cape Blanco deformation is consistent with the regional deformation described above, however the large north-trending faults there could well have influenced the orientation of nearby structures. Thick sandstone beds and thick-bedded sandstone sequences are folded with longer wavelengths than thin-bedded sandstone and mudstone sequences. Locally, the larger structures control the orientations of ridges and valleys and limit the range of strike and dip. Countless small faults dismember the folded beds. These features are truncated by the angular unconformity that predates deposition of the overlying mid- and Upper Cretaceous sequence, the oldest formation of which is the Hostenaden Creek Formation.

McClaghry and others (2013) recognized a number of low-angle thrust faults that cut the Otter Point Formation near Gold Beach. Many of these are associated with variably serpentinitized ultramafic bodies. Medaris (1972) interpreted these ultramafic masses to represent parts of the upper mantle brought from depth beneath an ocean ridge system and then exhumed along major thrust faults during the Late Jurassic and Cretaceous. Previous workers (Dott, 1965; Koch, 1966) have interpreted ultramafic bodies near Gold Beach as narrow, steeply dipping intrusives that were subsequently sheared and serpentinitized during post-intrusive faulting. However, mapped field relationships (see Plate 2, cross section A-A' of this report and Plate 3, cross section A-A', of McClaghry and others, 2013) and earlier work by Coleman (1970 pers. communication cited by Medaris, 1972) demonstrates that some of the ultramafic bodies probably occur as tabular sheets that have been folded and transported along low-angle thrust faults. A tabular sheet-like geometry along major thrust faults is further suggested for the ultramafic masses on the basis of low-angle fault contacts that separate these bodies from the surrounding Sixes River terrane and erosional segmentation of ultramafic bodies into multiple exposure belts (fensters). Metasomatic (roddingite) reaction zones present at contacts between Pickett Peak serpentinite and Sixes River terrane indicate relatively low temperatures of emplacement (Medaris, 1972). Smaller bodies of serpentinite, distributed along other fault zones, may have originated where ultramafic masses rose as diapirs or tectonic intrusions into more dense country rock following major thrusting events (Medaris, 1972). Ultramafic rocks, including serpentinite, occurring within the Gold Beach terrane in the current study area, occur as blocks along fault zones.

Cretaceous rocks (**Kugb**), possibly including the Hunters Cove Formation, Cape Sebastian Sandstone, or Housteneden Creek Formation, are complexly faulted with the older Otter Point Formation in sea stacks southwest of Cape Blanco (Plate 1; Hunter and others, 1970). These rocks record Late Cretaceous and/or Cenozoic deformation, with strata characterized by folding and steeply dipping bedding. Unlike the older Otter Point Formation, these units do not display intense shearing and stratigraphic dismemberment. The largest of these bodies (**Ku?**) crops out at Blacklock Point, north of Cape Blanco, and is problematic in that it is surrounded by a pervasively deformed *mélange* (western or "Cape Blanco" subterrane of the Sixes River terrane) containing blocks or matrix with Eocene fossils. The location of these folded but otherwise little deformed Upper Cretaceous rocks can probably be best explained by coast parallel or oblique faulting.

Upper Cretaceous rocks were deposited in a tectonically active environment, characterized by multiple episodes of syndepositional vertical faulting (Bourgeois and Dott, 1985). Bedding and fold axes measured in Upper Cretaceous rocks also suggest the occurrence of at least two folding episodes, with measured fold axes plunging on average to the east-northeast and west-southwest, and a second, nearly perpendicular set plunging north-northwest and south-southeast (Plate 1; appendix). Howard and Dott (1961) reported the Upper Cretaceous strata near Cape Sebastian are folded into a series of doubly plunging anticlines and synclines, with a general axial trend of N30°W. Post-late Cretaceous compression is indicated south of the study area near Housteneden Creek, where the Housteneden Creek Formation is thrust over the Hunters Cove Formation, and the Otter Point Formation over the Housteneden Creek Formation (Bourgeois and Dott, 1985).

Blocks of intermediate to mafic volcanic rock are mapped within the Otter Point Formation. Although not always well exposed, the larger map patterns associated with these blocks suggests that likely represent dikes, plugs, and lava flows that have been folded and/or structurally "rounded" during deformation and faulting. In places the beads-on-a-string distribution of these blocks suggests that they define fault zones similar to those inferred where blocks of mixed lithologies crop out. South of the study area, McClaughry and others (2013) mapped more extensive sheets of volcanic rock interlayered with sandstone within the Otter Point Formation.

Sixes River terrane

The Sixes River terrane includes an extensive mudstone- and fine-grained sandstone-matrix *mélange* containing distinctive blocks of blue greenschist, blueschist, and garnet schist. It is here tentatively divided into three subterrane that are thought to be juxtaposed along north-northwest-trending bounding faults. The close relationship between these three subterrane is indicated by the presence of blueschist and garnet schist blocks in each. These lithologies are generally uncommon in southwestern Oregon. Much of the Cape Blanco (western) subterrane consists of *mélange* containing blocks or matrix with lower middle Eocene fossils. The Fulmar (central) subterrane includes *mélange* with Cretaceous and Jurassic age blocks overlain by arkosic sandstone of lower Eocene age (Snively and others, 1985; Snively, 1987). The Whitsett (eastern) subterrane includes *mélange* overlain by Cretaceous(?) and lower Eocene volcanic sandstone. The current distribution of radiometric and fossil ages in the *mélange* and overlap sequences, as well as the similarity of the *mélange* lithologies across the terrane, suggests that these rocks represent an episodic westward-younging of *mélange* formation in an otherwise similar setting.

The Fulmar and Whitsett subterrane, as well as the Siletz terrane to the north, are overlapped by micaceous sandstone formations including the Tyee and Coaledo formations and the Sacchi Beach Beds (outside study area). These three formations are as old or older than fossils recovered from *mélange* in the Cape Blanco subterrane. *Mélange* formation continued in the Cape Blanco subterrane while the Whitsett and Fulmar subterrane were being buried by micaceous sandstone. The Miocene sandstone of Floras Lake (**Tmf**), Empire Formation (**Tme**), and diatomite of China Creek (**Tmc**) overlap the Otter Point Formation (**KJos**, **KJov**) of the Gold Beach terrane and *mélange* of the Cape Blanco subterrane of the Sixes River terrane, giving a minimum age for their juxtaposition. To the north and east, the Sixes River terrane is thrust over the Siletz terrane, an oceanic or ocean island basalt sequence of Paleocene and Eocene age, along the Wildlife Safari fault (outside study area). To the south, the Sixes River terrane appears to be truncated along the western extension of the Canyonville fault. Limestone units with histories similar to those of the Whitsett limestone lentils (Diller, 1898) in the Whitsett subterrane of the Sixes River terrane are associated with the Franciscan Complex in Northern California, at Laytonville and near San Jose (Sliter, 1984). Wells and others (2000), mapping the Roseburg 1:100,000 quadrangle, assigned rocks of the eastern subterrane of the Sixes terrane to the

Dothan Formation; however blueschist and garnet schist bearing *mélange* has not been recognized in the Dothan type area south of the Canyonville fault.

Picket Peak terrane

The Picket Peak terrane includes the Colebrooke Schist (**Kcqs**), which forms a regionally extensive structural nappe that overlies *mélange* assigned to two of the Sixes River subterrane (**TJs**, **KJs**) in the east-central part of the map area, and the Otter Point (**KJos**; Gold Beach terrane) and Dothan (Yolla Bolly terrane) formations farther south and east (McClaughry and others, 2013; Ramp and others, 1977), outside the study area. The contacts between the Colebrooke Schist and all other rock units in the map area are faults. The thrust fault contact between the Colebrooke Schist and the structurally lower Otter Point Formation and Sixes River *mélange* has variable orientations that appear to reflect folding of the surface about a northeast-plunging fold axis. The largest and presumably thickest section of the Colebrooke Schist in the study area occurs as a klippe along the divide between Floras Creek and the Sixes River (Plate 1). Faulting that places the Colebrooke Schist over the Sixes River and Otter Point terranes must postdate juxtaposition of those terranes across the western extension of the Canyonville fault zone (described below).

The Colebrooke Schist includes rocks with metamorphic grades transitional between greenschist and blueschist facies (Coleman, 1972). The rock is typically crenulated, with structural trends indicating at least two penetrative deformations. The main foliation (S1) is parallel to relict stratification of the protolith and relates to regional metamorphic recrystallization (Dott, 1971; Coleman, 1972). Superimposed on S1 are S2 planes that exhibit strain-slip cleavages parallel to axial planes of a second set of folds (F2). F2 fold axes generally trend north-south, with shallow, west-dipping axial planes (Coleman, 1972). Statistical analysis of regional foliations and lineations by Coleman (1972) suggest an earlier F1 phase of folding with fold axes that trend northeast-southwest.

After several major episodes of thrust faulting, the Colebrooke Schist was cut by a number of north- and northeast-trending high-angle faults. McClaughry and others (2013) reported that south of Humbug Mountain, near Myrtle Creek, a significant set of northeast-trending faults places the Colebrooke Schist in structural contact with both the Humbug Mountain Conglomerate (**Khcg**) and the Rocky Point Formation (**Krp**). Most previous authors (e.g., Koch, 1963, 1966; Dott, 1971; Beaulieu and Hughes, 1976; Ramp and others, 1977) had interpreted this contact as a thrust

fault placing the Colebrooke Schist structurally above the Humbug Mountain Conglomerate and the Rocky Point Formation. However, such a relationship contradicts that observed along the Elk River, where the Humbug Mountain Conglomerate is thrust over the Colebrooke Schist. More recent work (Roure and Blanchet, 1983; Blake and others, 1985; Giaramita and Harper, 2006) illustrate an opposite sense of displacement on this fault set, showing both the Humbug Mountain Conglomerate and Rocky Point Formation thrust from north to south over the Colebrooke Schist. The discrepancy in the two disparate interpretations may be reconciled by mapped topographic expression of the fault lineaments. Almost exclusively, where these north-east-trending faults separate the Colebrooke Schist from the Humbug Mountain Conglomerate and the Rocky Point Formation, the fault strands run parallel to and bisect ridge noses and crests. This relationship necessitates that the faults are steeply-dipping normal faults, with a down-on-the-north sense of displacement.

Western Klamath terrane, Elk subterrane

Rocks belonging to the Elk subterrane of the Western Klamath terrane display overall structural trends indicative of east-northeast-trending folds in the area east and northeast of Port Orford. Both the Humbug Mountain Conglomerate (**Khcg**) and the Rocky Point Formation (**Krp**) are generally folded about east-northeast-trending fold axes. Bedding attitudes within these units have mean strikes of N60°E (appendix). The relationship between unit contacts and facing directions suggest that some of the folds are faulted. Local variations in strike often indicate the presence of faults or fold noses.

South of the map area, along Elk River and its tributaries, McClaughry and others (2013) recognized a broad erosional window that revealed key structural relationships between units that compose the Elk subterrane. In that area a sequence of structural units including a sheeted dike complex, serpentinite-matrix *mélange*, Colebrooke Schist, Galice Formation, and Humbug Mountain Conglomerate appear to preserve a broad structural dome (Giaramita and Harper, 2006). Evidence for a structural dome in the Elk River area include: 1) Topographically high exposures of the Galice Formation nearly surround the serpentinite-matrix *mélange*, indicating the Galice overlies the *mélange*, separated by a shallow-dipping contact. A lack of contact metamorphism within the *mélange* unit indicates a faulted rather than depositional contact; 2) Mapped field relationships between the Colebrooke Schist and the serpentinite-matrix *mélange*, show a slightly irregular contact whose

geometry indicates a westward dip. Such a relationship places the Colebrooke Schist as a west-dipping structural nappe overlying the serpentinite-matrix *mélange*. Mapped field relationships along Bear Creek to the south indicate that the Galice Formation overlies the Colebrooke Schist along a shallow-dipping fault; 3) The Humbug Mountain conglomerate unconformably overlies the Galice Formation and structurally overrides the Colebrooke Schist between Elk River and the Bear Creek. A low-angle fault rather than an unconformable depositional contact separates the Humbug Mountain Conglomerate from the underlying Colebrooke Schist as is indicated by local bodies of serpentinite that occur along the contact.

Colebrooke Schist and serpentinite-matrix *mélange* on the divide between Sixes River and Floras Creek appear to have low-angle faulted contacts. McClaughry and others (2013) similarly found that the overall map pattern in the upper Elk River area indicates a low-angle fault contact between the Humbug Mountain Conglomerate and the Colebrooke Schist that must have a shallow dip at the surface. South of Floras Creek, at the eastern edge of the study area on the north side of the Canyonville fault, a serpentinite matrix *mélange* and associated Colebrooke Schist are faulted over the mudstone/sandstone matrix *mélange* of the Sixes River terrane.

High-angle faults

Rocks within the map area are offset by a number of Late Cretaceous and younger high-angle, north-northwest- and east-northeast-trending fault zones that crosscut older thrust planes (nappes) along the coastal margin. High-angle faults include those with strike-slip, oblique strike-slip, and normal-displacement; a number of these structures in the study area are mapped as generic faults with an unknown sense of slip as few stratigraphic piercing points are preserved (map plates). Many of the major high-angle faults and shear zones are inferred to have an important strike-slip component on the basis of the intensity of shearing over wide areas, attitudes of many small scale folds and slickensides, relatively straight boundaries, and heterogeneous structural mixing of rock types. A dextral (right-lateral) slip component is indicated on several fault zones south of the map area (Howard and Dott, 1961; Kaiser, 1962; Bourgeois and Dott, 1985; Kelsey, 1990; McClaughry and others, 2013) including the Battle Rock, Whaleshead, Brush Creek, Pistol River, and East Boundary (Howard and Dott, 1961). East- and northeast-trending faults locally trend perpendicular to major north-directed fault zones.

Onshore, many of the high-angle fault zones are located along valleys or marked by linear distributions of serpentinite, while the traces of other faults or fault zones likely correspond, in part, to the mapped distribution of large landslide deposits, debris-flow gullies, or fault-line ridges. Along the coast and farther offshore, high-angle fault zones and shear zones are recognized by linear trains of sea stacks. Good examples of near or offshore fault zones occur near Cape Blanco and Blacklock Point and in the vicinity of Battle Rock at Port Orford, south of the study area. Pervasive high-angle faulting in the Gold Beach terrane has resulted in an often chaotic lensoidal map pattern where fault blocks of geologic units appear to have been “tectonically kneaded” within an environment of wrench faulting (Bourgeois and Dott, 1985).

Major high-angle faults and shear zones in the study area are probably related to the post-Late Cretaceous accretion of the Gold Beach terrane to the continental margin (Blake and others, 1985) and subsequent deformation along the active Cascadia margin. One named example of a north-trending, high-angle fault zone that parallels the coastal margin in the project area is the Battle Rock fault zone exposed at Cape Blanco. The unnamed fault zone that juxtaposes Rocky Point and Otter Point formations is considered an older strand(s) representing major crustal structures bounding tectonostratigraphic terranes along the coast.

Battle Rock fault zone

At Cape Blanco, a fault mapped as the northern extension of the north-northwest-striking Battle Rock fault zone, is a tectonostratigraphic terrane-bounding fault that juxtaposes Otter Point Formation (**KJos**) of the Gold Beach terrane on the west, beneath the lighthouse, against Cape Blanco subterrane of the Sixes River terrane to the east. An older(?) eastern splay of the fault that trends north to northeast between Port Orford and the Canyonville fault juxtaposes Gold Beach terrane on the west against Rocky Point Formation (**Krp**) and Humbug Mountain Conglomerate (**Khcg**) of the Elk subterrane of the Western Klamath terrane on the east (Plate 1; Koch, 1963, 1966; Dott, 1971; Blake and others, 1985; Walker and MacLeod, 1991). The Battle Rock fault zone lies mainly offshore in the study area. To the south it comes ashore near Garrison Lake, runs through the Port Orford area to Battle Rock, and continues offshore to the Humbug Mountain area. The Battle Rock fault zone was first recognized and named the Port Orford shear zone by Koch (1963, 1966), and Dott (1971), and was

later referred to as the Battle Rock fault zone by Kelsey (1990).

Faulting of bedrock strata along the Battle Rock fault zone at Port Orford is accommodated locally by multiple fault strands forming a distributed zone ~2 to 4 km (~1.2 to 2.5 mi) in width. Separate strands along the fault zone are locally identified by the juxtaposition of distinctly different geologic units, the occurrence of serpentinite bodies or other lithologies uncommon to the local stratigraphic section (e.g., anomalous blocks of volcanic rock apparently caught up along fault strands), pervasive shearing in bedrock outcrops, topographic lineaments, and the distribution of bedrock springs (McClaghry and others, 2013). North of Port Orford the fault strands are largely buried under Quaternary terrace deposits. One strand trends offshore, and it or a parallel fault farther offshore intersects Cape Blanco (Plate 1).

The eastern strand of the Battle Rock fault zone exposed southeast of Port Orford represents a major crustal discontinuity, juxtaposing highly deformed and stratigraphically chaotic units of the Otter Point Formation (**KJos**; Gold Beach terrane) on the west against less deformed Rocky Point Formation (**Krp**; Western Klamath terrane) on the east. A dextral strike-slip sense of movement is inferred on this fault strand on the basis of northward translation of the Gold Beach terrane, which is largely exposed between Cape Blanco and Brookings to the south. Paleomagnetic and sedimentologic data presented by Blake and others (1985) and Bourgeois and Dott (1985) argue for a southern source area for the Gold Beach terrane and significant northward translation since the Late Cretaceous. However, the amount of translation accommodated along the Battle Rock fault zone is unknown as no definitive piercing points along the fault zone have been recognized. The eastern strand is truncated by the east-west-trending fault here interpreted to be the western end of the Canyonville fault and so is older than the latest movement on the Canyonville fault.

A western strand of the Battle Rock fault zone continues north, across Cape Blanco, where it juxtaposes Otter Point Formation (**KJos**; Gold Beach terrane) on the west against *mélange* (**TJs**; Cape Blanco subterrane of the Sixes River terrane) on the east. This strand of the fault appears to truncate or offset the extreme western end of the Canyonville fault and so is younger than that part of that fault. It must also post-date complexly deformed Paleogene (middle Eocene) *mélange* or broken formation of the Cape Blanco subterrane. The western strand of the fault offsets the late Miocene Empire Formation (**Tme**; Dott, 1962; Dott, 1971; Beaulieu and Hughes, 1976) and sandstone of Floras Lake (**Tmf**).

Geologic map patterns and bedrock elevations interpreted from well logs (McClaghry and others, 2013) do indicate the possibility that the Indian Creek marine terrace sediments have been, to some extent, folded about an east-west-trending synclinal axis approximately paralleling Hubbard Creek just south of the study area. Kelsey (1990) also indicated that Indian Creek marine terrace sediments on top of the Battle Rock sea stack and adjacent sea cliffs within the Port Orford city limits are pervasively cut by mesoscale faults with less than a few meters offset. Fault strands in the Battle Rock fault zone are not known to offset the Pioneer marine terrace sediments and no lateral displacement of the terrace backedge has been observed. Quaternary reactivation of the Battle Rock fault zone prior to 105 ka is therefore probable, but the true extent of faulting and slip-rates along fault strands remains uncertain.

To the south, the terrane boundary marked by the Battle Rock fault zone lies along the Whaleshead fault zone. That fault zone juxtaposes Otter Point Formation of the Gold Beach terrane to the west against Dothan Formation of the Yolla Bolly terrane to the east (Dott, 1971; Blake and others, 1985; Kelsey and Bockheim, 1994). The Whaleshead fault zone extends from Whaleshead Island on the south, north through the Carpenterville and Bull Gulch areas, to Hunter Creek east of Gold Beach. The precise location of the Whaleshead fault zone farther north (along the eastern edge of the map area) or its relationship with the Battle Rock fault zone extending south from Port Orford is not yet known. Bourgeois and Dott (1985) and Kelsey (1990) suggested that the Battle Rock fault zone marks the northern trace of the Whaleshead fault zone that crops out south of Gold Beach. Segments of this fault zone have been mapped by a number of authors at varying scales including Howard and Dott (1961), Koch (1966), Dott (1971), Beaulieu and Hughes (1976), Ramp and others (1977), Blake and others (1985), Walker and MacLeod (1991), Kelsey and Bockheim (1994), and T. J. Wiley (unpublished mapping, 2007). The entire terrane-bounding fault system was named the Whaleshead fault zone by Blake and others (1985). As it is along the Battle Rock fault zone, faulting of bedrock strata along the Whaleshead fault zone is accommodated locally by multiple fault strands, with most strands mapped as high-angle faults (McClaghry and others, 2013). Separate strands along the fault zone are locally identified by the juxtaposition of distinctly different geologic units, the occurrence of large serpentinite bodies, pervasive shearing in bedrock outcrops, topographic lineaments, and the distribution of bedrock springs. Geometry of the fault zone south of the study area, although poorly defined, suggests that the Otter Point Formation (**KJos**) is on the hanging wall,

with the Whaleshead fault zone dipping northwest. Blake and others (1985) and Bourgeois and Dott (1985) indicated an overall right-lateral slip component on this fault system, although detailed mapping of Quaternary marine terrace platforms by Kelsey and Bockheim (1994) indicated a significant component of vertical and left-lateral strike slip on some southern strands near the coast. The Whaleshead fault zone may have been, in part, active during the Quaternary as several fault strands along Whaleshead Creek (south of study area) are interpreted by Kelsey and Bockheim (1994) to offset 200 ka and older marine terraces. Quaternary vertical slip rates of 0.5 mm/yr and post-200-ka left-lateral slip rates of 2.5 mm/yr were estimated by Kelsey and Bockheim (1994) on at least one strand of the Whaleshead fault zone, but similar young displacement has not been documented on any other strands in the fault zone. An 1,820-year-old cobble beach berm (**Hbsb**) located 2.5 km (1.6 mi) southeast of Cape Blanco lies 19 m (62 ft) above sea level, suggesting uplift rates near the fault may be as high as 6 to 10 mm/yr (0.2 to 0.4 in/yr) (Kelsey, 1990).

Canyonville fault zone

The Sixes River terrane is faulted against the Gold Beach terrane and the Elk subterrane of the Western Klamath terrane along an east-west-trending high-angle right-lateral fault system that is likely the western extension of the Canyonville fault. Tertiary rocks along the Coast Range syncline, 48 km (30 mi) east of Cape Blanco, locally bury this fault, so that no throughgoing strand connects the eastern and western parts of the fault at the surface. However, the geometry of the fault strands is similar and they trend toward one another. Walker and MacLeod (1991) mapped the axis of the Coast Range syncline with a right-lateral bend near the presumed buried position of the fault. The fault has a complex history of motion and reactivation during late Cretaceous and/or Paleogene time. Along its traces it undoubtedly complicates structural relationships and may explain why contrasting structural scenarios have been proposed for different areas.

The early phase of motion on the Canyonville fault produced right lateral offset of the Yolla Bolly – Sixes River terrane contact. This occurred sometime before deposition of lower Eocene strata that lap across the fault and after formation of mid-Cretaceous (Albian to Cenomanian, 123 Ma to 93.9 Ma; Sliter, 1984) limestone lentils in the Whitsett subterrane of the Sixes River terrane. Poorly dated Upper Cretaceous or lower Paleogene sandstone, pebbly sandstone, and conglomerate crop out: 1) north of the Canyonville fault near Winston (Wells and others, 2000) and east of

Tenmile (Wiley and Black, 1994), 2) on or in Fulmar subterrane *mélange* east of Langlois (detrital zircons as young as 90.4 ± 1.6 Ma; Plate 2; appendix) and possibly as conglomerate blocks in *mélange* at Bandon Ocean Wayside south of Coquille Point, and 3) along the fault contact between the Cape Blanco and Fulmar subterrane at Blacklock Point. Presence of these strata north of the fault contrasts with the absence of Upper Cretaceous strata on the south side of the fault. Late phases of motion on this fault cut the Cape Blanco subterrane of the Sixes River terrane which contains lower middle Eocene fossils.

The northern extension of the Whaleshead – Battle Rock fault zone is inferred to cut off the extreme western end of the Canyonville fault somewhere between Garrison Lake and Cape Blanco. The presence of Otter Point Formation and Upper Cretaceous sandstone of the Gold Beach terrane at and just offshore from Cape Blanco suggests that the Sixes River terrane has been offset farther to the north along this steeply dipping fault.

The Colebrooke Schist (Pickett Peak terrane) structurally overlies the Sixes River terrane north of the fault and overlies the Gold Beach and Yolla Bolly terranes south of the fault. In contrast to the underlying terranes, the Colebrooke Schist does not appear to be appreciably offset across the fault. Although this may be due to the low-angle orientation of the fault contact beneath the schist, it seems apparent that emplacement of the schist postdates much of the movement along the fault.

Broad folds

Miocene sedimentary rocks and younger terrace deposits have been folded about a shallowly east-plunging anticlinal axis at Cape Blanco (Cape Blanco anticline; Dott, 1962, 1971; Kelsey, 1990). A broad fold is suggested by opposite dips on Pleistocene terrace deposits as shown on the cross section on Plate 1.

Linear features crossing the continental margin

Satellite imagery shows an east-southeast-trending linear feature that extends from the southern part of the map area inland to Nevada (Figure 7). Rich and Steele (1974) recognized a similar linear features trending inland from Cape Mendocino toward Mount Lassen. On more recent imagery these two linear features can be seen to persist hundreds of miles inland, paralleling and lying more or less along, landward projections of the Blanco and Mendocino fracture zones. The southern linear passes near Mount Lassen, California, and continues to the northern end of Pyramid Lake, Nevada. The northern linear passes through

the Cape-Blanco – Gold Beach area and runs south of Bear Creek Valley (Medford-Ashland area) to a point 80 km (50 mi) north of Pyramid Lake, Nevada. The correspondence of the satellite linears to projections of the two marine fracture zones suggests a relationship to the geology in the Cascadia subduction zone's lower plate. Perhaps the wedge of young, hot, high, and rugged oceanic crust bounded by the two fracture zones, subducted beneath western North America, creates an isostatic dynamic that affects corresponding parts of the upper plate. The observed linears may reflect edge effects related to the limits of this section of crust. Edge effects could include faulting, folding, volcanism, igneous intrusion, alteration, and mineralization. These are, in turn, reflected in drainage patterns. It may be problematic that these linears extend east of the Cascade Range volcanic arc into an area where the subducted slab presumably lies at great depth.

Elevated marine platforms

Elevated marine platforms and terrace deposits preserved along the southern Oregon coast record non-uniform and spatially variable Quaternary uplift of the coastal mountains. South of the study area, near Brookings, rates of uplift on elevated terraces approach 1 mm/yr (0.9 m/ky; Kelsey and Bockheim, 1994). North of the study area, near Cape Blanco, uplift rates on the Pioneer Terrace (**Qmtp**) over the past 80 ky were estimated by Kelsey (1990) to range between 0.7 and 1.5 mm/yr (0.7 and 1.5 m/ky). Uplift rates along the Cape Blanco anticline are estimated to be higher for the last 2 ky, with rates approaching 6 to 10 mm/yr (6 to 10 m/ky; Kelsey, 1990). Kelsey (1990) suggested that, in contrast to the Cape Blanco area, subsidence is occurring within 10 km (6 mi) both to the north and to the south of Cape Blanco.

Pliocene and early Pleistocene deformation rates along the southern Oregon coast were probably similar to the late Pleistocene rates described above. Approximately 10 km (6 mi) south of the Oregon-California border, near California's High Divide, the upper Miocene and lower Pliocene Wimer Formation crops out at an elevation of about 720 m (2,360 ft), while its western equivalent, the St. George Formation, crops out near sea level along the coast near Crescent City.

ACKNOWLEDGMENTS

This report is a product of geologic mapping along the southern Oregon coast that was partially funded by the STATEMAP component of the U.S. Geological Survey (USGS) National Cooperative Geologic Mapping program under assistance award G13AC00137 during 2013 and 2014. Funding for geologic mapping was also provided by the State of Oregon. XRF geochemical analyses were prepared and analyzed by Dr. Stanley Mertzman, Franklin and Marshall College, Pennsylvania. New $^{206}\text{Pb}/^{238}\text{U}$ radio-metric age determinations were prepared and analyzed by

Jonathan Rivas under the direction of Dr. Joshua Schwartz at California State University–Northridge. The authors acknowledge a number of area landowners who provided local knowledge and graciously allowed access to private holdings within the study area. The Oregon Civil Air Patrol provided an airplane that allowed DOGAMI to photograph the study area as an exercise designed to simulate a post-disaster aerial survey. Technical review was provided by Ian P. Madin. Cartography for the map plates was provided by Daniel E. Coe.

REFERENCES

- Aalto, K. R., 1968, The sedimentology of the Late Jurassic (Portlandian) Otter Point Formation of southwestern Oregon: Madison, Wisc., University of Wisconsin, M.S. thesis, 60 p.
- Aalto, K. R., and Dott, R. H., Jr., 1970, Late Mesozoic conglomeratic flysch in southwestern Oregon, and the problem of transport of coarse gravel in deep water: Geological Association of Canada Special Paper 7, p. 53–65.
- Addicott, W. O., 1964, A late Pleistocene invertebrate fauna from southwestern Oregon: *Journal of Paleontology*, v. 38, p. 650–661.
- Addicott, W. O., 1983, Biostratigraphy of the marine Neogene sequence at Cape Blanco, southwestern Oregon: U.S. Geological Survey Professional Paper 774-G, 19 p.
- Baldwin, E. M., 1945, Some revisions of the late Cenozoic stratigraphy of the southern Oregon coast: *Journal of Geology*, v. 53, no. 1, p. 35–46.
- Baldwin, E. M., 1969, Geologic map of the Myrtle Point area, Coos County, Oregon: U.S. Geological Survey Mineral Investigations Map MF-302, scale 1:48,000.
- Baldwin, E. M., 1974, Eocene stratigraphy of southwestern Oregon: Oregon Department of Geology and Mineral Industries Bulletin 83, 40 p., 1 pl., scale 1:250,000.
- Baldwin, E. M., Beaulieu, J.D., Ramp, L., Gray, J., Newton, V. C., Jr., and Mason, R. S., 1973, Geology and mineral resources of Coos County, Oregon: Oregon Department of Geology and Mineral Industries Bulletin 80, 82 p., 4 pl., scale 1:62,500.
- Bandy, O. L., 1941, Invertebrate paleontology of Cape Blanco: Corvallis, Oreg., Oregon State University, M.S. thesis, 138 p.
- Bandy, O. L., 1944, Eocene foraminifera from Cape Blanco, Oregon: *Journal of Paleontology*, v. 18, p. 366–377.
- Beaulieu, J. D., and Hughes, P. W., 1975, Environmental geology of western Coos and Douglas counties, Oregon: Oregon Department of Geology and Mineral Industries Bulletin 87, 148 p., 16 pl., scale 1:62,500.
- Beaulieu, J. D., and Hughes, P. W., 1976, Land-use geology of western Curry County, Oregon: Oregon Department of Geology and Mineral Industries Bulletin 90, 148 p., 16 pl., scale 1:62,500.
- Beaulieu, J. D., Hughes, P. W., and Mathiot, R. K., 1974, Geologic hazards inventory of the Oregon Coastal Zone: Oregon Department of Geology and Mineral Industries Miscellaneous Paper 17, 94 p., 2 pl., scale 1:250,000.
- Beckstrand, D. L., 2001, Origin of the Coos Bay and Florence dune sheets, south central coast, Oregon: Portland, Oreg., Portland State University, M.S. thesis, 192 p.
- Berkland, J. O., Raymond, L. A., Kramer, J. C., Moores, E. M., and O'Day, M., 1972, What is Franciscan?: *American Association of Petroleum Geologists Bulletin*, v. 56, p. 2295–2302.
- Black, G. L., and Madin, I. P., 1995, Geologic map of the Coos Bay quadrangle, Coos County, Oregon: Oregon Department of Geology and Mineral Industries Geological Map Series GMS-97, scale 1:24,000.
- Blake, M. C., Jr., Engebretson, D. C., Jayko, A. S., and Jones, D. L., 1985, Tectonostratigraphic terranes in southwest Oregon, *in* Howell, D.G., ed., *Tectonostratigraphic terranes of the circum-Pacific region: Circum-Pacific Council for Energy and Mineral Resources, Earth Science Series*, no. 1, p. 147–157.
- Boggs, S., Jr., 1969, Distribution of heavy minerals in the Sixes River, Curry County, Oregon: *Ore Bin*, v. 31, no. 7, 133–150.
- Bourgeois, J., 1980a, Sedimentology and tectonics of Upper Cretaceous rocks, southwest Oregon: University of Wisconsin, Ph.D. dissertation, 298 p.
- Bourgeois, J., 1980b, A transgressive shelf sequence exhibiting hummocky stratification: the Cape Sebastian Sandstone (Upper Cretaceous), southwestern Oregon: *Journal of Sedimentary Petrology*, v. 50, no. 3, p. 681–702.
- Bourgeois, J., and Dott, R. H., Jr., 1985, Stratigraphy and sedimentology of Upper Cretaceous rocks in coastal southwest Oregon: Evidence for wrench-fault tectonics in a postulated accretionary terrane: *Geological Society of America Bulletin*, v. 96, p. 1007–1019.
- Boyd, F. R., and Mertzman, S. A., 1987, Composition of structure of the Kaapvaal lithosphere, southern Africa: *in* Mysen, B. O., ed., *Magmatic processes—physicochemical principles: The Geochemical Society, Special Publication 1*, p. 13–24.
- Brown, E. H., and Blake, M. C., Jr., 1987, Correlation of Early Cretaceous blueschists in Washington, Oregon, and northern California: *Tectonics*, v. 6, p. 795–806.
- Brownfield, M. E., 1972, Geology of the Floras Creek drainage, Langlois quadrangle, Oregon: Eugene, Oreg., University of Oregon, M.S. thesis, 92 p.
- Brownfield, M. E., Phillips, R. L., and Lent, R. L., 1982, Geologic map of the Langlois quadrangle, Oregon: Oregon Department of Geology and Mineral Industries Open-File Report O-82-3, scale 1:62,500.

- Burns, W. J., and Madin, I. P., 2009, Protocol for inventory mapping of landslide deposits from light detection and ranging (lidar) imagery: Oregon Department of Geology and Mineral Industries Special Paper 42, 30 p.
- Burns, W. J., and Watzig, R. J., 2014, Statewide Landslide Information Database for Oregon (SLIDO), release 3.0 (SLIDO-3.0): Oregon Department of Geology and Mineral Industries, geodatabase. Web: <http://www.oregon-geology.org/sub/slido/index.htm>
- Burt, W. D., 1963, The geology of the Collier Butte area, southwest Oregon: Madison, Wisc., University of Wisconsin, M.S. thesis, 93 p.
- Cashman, S. M., and Cashman, P. H., 1989, The Redwood Creek Schist—a key to the deformational history of the Northern California Coast Ranges, *in* Aalto, K. R., Harper, G. D., Carver, G. A., Cashman, S. M., Miller, W. C., III, and Kelsey, H. M., Geologic evolution of the northernmost Coast Ranges and western Klamath Mountains, California: Galice, Oregon, to Eureka, California, July 20–28, 1989: American Geophysical Union, Washington, D.C., 53 p. doi: 10.1029/FT308p0053
- Chang, Z., Vervoort, J. D., McClelland, W. C., and Knaack, C., 2006, U-Pb dating of zircon by LA-ICP-MS: Geochemistry, Geophysics, Geosystems, v. 7, no. 5, p. 1–14.
- Coleman, R. G., 1972, The Colebrooke Schist of southwestern Oregon and its relation to the tectonic evolution of the region: U.S. Geological Survey Bulletin 1339, 61 p.
- Coleman, R. G., and Lanphere, M. A., 1971, Distribution and age of high-grade blueschists, associated eclogites, and amphibolites from Oregon and California: Geological Society of America Bulletin, v. 82, p. 2397–2412.
- Cowan, D. S., 1985, Structural styles in Mesozoic and Cenozoic mélanges in the western Cordillera of North America: Geological Society of America Bulletin, v. 96, p. 451–462.
- Crutzen, P. J., 2002, The “Anthropocene”: Journal of Physics IV, France, v. 12, p. 1–5.
- Diller, J. S., 1896, A geological reconnaissance in northwestern Oregon: U.S. Geological Survey 17th annual report, part 1, p. 458–462 and p. 475.
- Diller, J. S., 1898, Roseburg folio, Oregon: U.S. Geological Survey Geologic Atlas of the United States Folio 49, 4 pl., 4 p.
- Diller, J. S., 1899, The Coos Bay coal field, Oregon: U.S. Geological Survey Annual Report 19, pt. 3, p. 309–370.
- Diller, J. S., 1901, Coos Bay folio, Oregon: U.S. Geological Survey Geologic Atlas of the United States Folio 73, 4 pl., 5 p.
- Diller, J. S., 1902, Topographic development of the Klamath Mountains: U.S. Geological Survey Bulletin 196, 69 p.
- Diller, J. S., 1903, Port Orford folio, Oregon: U.S. Geological Survey Geologic Atlas of the United States Folio 89, 4 pl., 6 p.
- DOGAMI, 2012a, Tsunami inundation maps for Bandon, Coos County, Oregon: Oregon Department of Geology and Mineral Industries, Tsunami Inundation Map TIM-Coos-16, 2 pl., scale 1:10,000.
- DOGAMI, 2012b, Tsunami inundation maps for New River, Coos County, Oregon: Oregon Department of Geology and Mineral Industries, Tsunami Inundation Map TIM-Coos-17, 2 pl., scale 1:10,000.
- DOGAMI, 2012c, Tsunami inundation maps for Langlois, Coos County, Oregon: Oregon Department of Geology and Mineral Industries, Tsunami Inundation Map TIM-Coos-18, 2 pl., scale 1:10,000.
- DOGAMI, 2012d, Tsunami inundation maps for Cape Blanco, Curry County, Oregon: Oregon Department of Geology and Mineral Industries, Tsunami Inundation Map TIM-Curr-02, 2 pl., scale 1:10,000.
- DOGAMI, 2012e, Tsunami inundation maps for Denmark, Curry County, Oregon: Oregon Department of Geology and Mineral Industries, Tsunami Inundation Map TIM-Curr-03, 2 pl., scale 1:10,000.
- DOGAMI, 2012f, Tsunami inundation maps for Port Orford, Curry County, Oregon: Oregon Department of Geology and Mineral Industries, Tsunami Inundation Map TIM-Curr-04, 2 pl., scale 1:10,000.
- DOGAMI, 2012g, Tsunami inundation maps for Humbug Mountain, Curry County, Oregon: Tsunami Inundation Map TIM-Curr-05, 2 pl., scale 1:10,000.
- Dott, R. H., Jr., 1962, Geology of the Cape Blanco area, southwest Oregon: Ore Bin, v. 24, no. 8, p. 121–133.
- Dott, R. H., Jr., 1965, Mesozoic-Cenozoic tectonic history of the southwestern Oregon coast in relation to Cordilleran orogenesis: Journal of Geophysical Research, v. 70, no. 18, p. 4687–4706.
- Dott, R. H., Jr., 1971, Geology of the southwestern Oregon coast west of the 124th meridian: Oregon Department of Geology and Mineral Industries Bulletin 69, 63 p., 2 pl., scale 1:250,000 and 1:62,500.
- Dunegan, L., 2007, Insiders’ guide to the Oregon coast: Kearney, Neb., Morris Book Publishing, 275 p.
- Emerson, L. F., 2007, Miocene coastal vegetation preserved by volcanic eruption at Cape Blanco, Oregon: Geological Society of America Abstracts with Programs, v. 39, no. 6, p. 401.

- Emerson, L. F., 2009, The early Miocene Cape Blanco flora of coastal Oregon: Eugene, Ore., University of Oregon, Ph.D. dissertation, 105 p.
- Festa, A., Pini, G. A., Dilek, Y., and Codegone, G., 2010, Mélanges and mélange-forming processes: a historical overview and new concepts: *International Geology Review*, v. 52, nos. 10–12, p. 1010–1105.
- Festa, A., Dilek, Y., Pini, G. A., Codegone, G., and Ogata, K., 2012, Mechanisms and processes of stratal disruption and mixing in the development of mélanges and broken formations: redefining and classifying mélanges: *Tectonophysics*, v. 568–569, p. 7–24.
- Fiebelkorn, R. B., Walker, G. W., MacLeod, N. S., McKee, E. H., and Smith, J. G., 1983, Index to K/Ar age determinations for the state of Oregon: *Isochron/West*, no. 37, p. 3–60.
- Fillmore, M. H., 2005, Soil survey of Curry County, Oregon: Natural Resources Conservation Service Soil Conservation Survey 015, 1043 p. <http://soildatamart.nrcs.usda.gov/Manuscripts/OR015/0/Curry.pdf>
- Fowler, G. A., Orr, W. N., and Kulm, L. D., 1971, An upper Miocene diatomaceous rock unit on the Oregon continental shelf: *Journal of Geology*, v. 79, no. 5, p. 603–608.
- Garey, C. L., 1987, Radiolaria from the Otter Point Complex (Oregon) and the volcano-pelagic strata above the Coast Range Ophiolite (California): Dallas, Tex., University of Texas, M.S. thesis, 157 p.
- Giaramita, M. J., and Harper, G. D., 2006, Geochemistry of ophiolitic rocks associated with the western part of the Elk outlier of the Western Klamath terrane, southwestern Oregon, *in* Snoke, A. W., and Barnes, C. G., eds., *Geological studies in the Klamath Mountains Province, California and Oregon: a volume in honor of William P. Irwin*: Geological Society of America Special Paper 410, p. 152–176.
- Gillespie, M. R., and Styles, M. T., 1999, BGS rock classification scheme, v. 1, Classification of igneous rocks: British Geological Survey Research Report (2nd ed.) RR99-06, 52 p.
- Goldfinger, C., Nelson, C. H., Morey, A. E., Johnson, J. E., Patton, J. R., Karabanov, E., Gutiérrez-Pastor, J., Eriksson, A. T., Gràcia, E., Dunhill, G., Enkin, R. J., Dallimore, A., and Vallier, T., 2012, Turbidite event history—methods and implications for Holocene paleoseismicity of the Cascadia subduction zone: U.S. Geological Survey Professional Paper 1661–F, 170 p.
- Goodfellow, R. W., 1987, Petrography and provenance of sandstones from the Otter Point Formation, southwestern Oregon: Eugene, Ore., University of Oregon, M.S. thesis, 158 p.
- Gradstein, F. M., Ogg, J. G., and Smith, A. G., eds., 2004, *A geologic time scale 2004*: Cambridge, U.K., Cambridge University Press, 589 p.
- Griggs, A.B., 1945, Chromite-bearing sands of the southern part of the coast of Oregon: U.S. Geological Survey Bulletin 945-E, 150 p.
- Gullixson, C. F., 1981, The structure, geologic evolution, and regional significance of the Bethel Creek – North Fork area, Coos and Curry counties, Oregon: Portland, Ore., Portland State University, M.S. thesis, 86 p.
- Haagen, J. T., 1989, Soil Survey of Coos County, Oregon: Natural Resources Conservation Service Soil Conservation Survey 011, 175 p. http://www.nrcs.usda.gov/Internet/FSE_MANUSCRIPTS/oregon/OR011/0/or011_text.pdf
- Hallsworth, C. R., and Knox, R. W. O'B., 1999, BGS rock classification scheme, v. 3, Classification of sediments and sedimentary rocks: British Geological Survey Research Report 99-03, 44 p.
- Harper, G. D., Bowman, J. R., and Kuhns, R., 1988, Field, chemical, and isotopic aspects of submarine hydrothermal metamorphism of the Josephine ophiolite, Klamath Mountains, California-Oregon: *Journal of Geophysical Research*, v. 93, p. 4625–4657.
- Harper, G. D., Saleeby, J. B., and Heizler, M., 1994, Formation and emplacement of the Josephine ophiolite and the age of the Nevadan Orogeny in the Klamath Mountains, California-Oregon: U/Pb zircon and $^{40}\text{Ar}/^{39}\text{Ar}$ geochronology: *Journal of Geophysical Research*, v. 99, p. 4293–4321.
- Heller, P. L., 1983, Sedimentary response to Eocene tectonic rotation in western Oregon: Tuscon, Ariz., University of Arizona, Ph.D. dissertation, 321 p.
- Howard, J. K., 1961, Stratigraphy and structure of the Cape Sebastian-Crook Point area, southwest Oregon: Madison, Wisc., University of Wisconsin, M.S. thesis, 52 p.
- Howard, J. K., and Dott, R.H., Jr., 1961, Geology of Cape Sebastian State Park and its regional relationships: *Ore Bin*, v. 23, no. 8, p. 75–81.
- Hsü, K. J., 1968, Principles of mélanges and their bearing on the Franciscan-Knoxville paradox: *Geological Society of America Bulletin*, 79, p. 1063–1074.
- Hunter, R. E., Clifton, H. E., and Phillips, L., 1970, Geology of the stacks and reefs off the southern Oregon coast: *Ore Bin*, v. 32, no. 10, p. 185–201.

- Janda, R. J., 1969, Age and correlation of marine terraces near Cape Blanco, Oregon: Geological Society of America, Abstracts with Programs, v. 3, p. 29–30.
- Janda, R. J., 1970, Field guide to Pleistocene sediments and landforms and soil development in the Cape Arago-Cape Blanco area of Coos and Curry counties, southern coastal Oregon: Friends of the Pleistocene, October 9–11, 1970, unpublished.
- Kaiser, W. R., 1962, The late Mesozoic geology of the Pearse Peak Diorite—southwest Oregon: Madison, Wisc., University of Wisconsin, M.S. thesis, 75 p.
- Katrib, J., 2006, Source of meta-igneous blocks and structure of the Colebrooke Schist in the Snowcamp Peak area, Pickett Peak terrane, southwestern Oregon: Albany, N.Y., State University of New York at Albany, M.S. thesis, 111 p.
- Kelsey, H. M., 1990, Late Quaternary deformation of marine terraces on the Cascadia Subduction Zone near Cape Blanco, Oregon: Tectonics, v. 9, no. 5, p. 983–1014.
- Kelsey, H. M., and Bockheim, J. G., 1994, Coastal landscape evolution as a function of eustacy and surface uplift rate, Cascadia margin, southern Oregon: Geological Society of America Bulletin, v. 106, p. 824–839.
- Kelsey, H. M., Ticknor, R. L., Bockheim, J. G., and Mitchell, E., 1996, Quaternary upper plate deformation in coastal Oregon: Geological Society of America Bulletin, v. 108, p. 843–860.
- Kelsey, H. M., Witter, R. C., and Hemphill-Haley, E., 1998, Response of a small Oregon estuary to coseismic subsidence and post-seismic uplift in the past 300 years: Geology, v. 26, p. 231–234.
- Kelsey, H. M., Witter, R. C., and Hemphill-Haley, E., 2002, Plate-boundary earthquakes and tsunamis of the past 5500 yr, Sixes River estuary, southern Oregon: Geological Society of America Bulletin, v. 114, p. 298–314.
- Kelsey, H. M., Nelson, A.R., Hemphill-Haley, E., and Witter, R. C., 2005, Tsunami history of an Oregon coastal lake reveals a 4600 yr record of great earthquakes on the Cascadia subduction zone: Geological Society of America Bulletin, v. 117, p. 1009–1032.
- Kennedy, G. L., 1978, Pleistocene paleoecology, zoogeography and geochronology of marine invertebrate faunas of the Pacific Northwest coast (San Francisco Bay to Puget Sound),: Davis, Calif., University of California, Ph.D. dissertation, 824 p.
- Koch, J. G., 1960, Geology of the Humbug Mountain area, southwest Oregon: Madison, Wisc., University of Wisconsin, M.S. thesis, 77 p.
- Koch, J. G., 1963, Late Mesozoic orogenesis and sedimentation, Klamath Province, southwest Oregon coast: Madison, Wisc., University of Wisconsin, Ph.D. dissertation, 282 p., scale 1:79,200.
- Koch, J. G., 1966, Late Mesozoic stratigraphy and tectonic history, Port Orford-Gold Beach area, southwestern Oregon coast: American Association of Petroleum Geologists Bulletin, v. 50, no. 1, p. 25–71.
- Lanphere, M. A., Blake, M. C., Jr., and Irwin, W. P., 1978, Early Cretaceous metamorphic age of the South Fork Mountain Schist in the northern Coast Ranges of California: American Journal of Science, v. 278, p. 798–815.
- Le Bas, M. J., and Streckeisen, A. L., 1991, The IUGS systematics of igneous rocks: Journal of the Geological Society, v. 148, p. 825–833.
- Le Bas, M. J., Le Maitre, R. W., Streckeisen, A., and Zanettin, B., 1986, A chemical classification of volcanic rocks based on the total alkali-silica diagram: Journal of Petrology, v. 27, part 3, p. 745–750.
- Leithold, E. L., and Bourgeois, J., 1983, Sedimentology of the sandstone of Floras Lake (Miocene) transgressive, high-energy shelf deposition, SW Oregon, *in* Larue, D. K., and Steel, R. J., eds., Cenozoic marine sedimentation, Pacific margin, U.S.A.: Los Angeles, Calif., Pacific Section, Society of Economic Paleontologists and Mineralogists, p. 17–28.
- Le Maitre, R. W., Bateman, P., Dudek, A., Keller, J., Lemeyre, J., Le Bas, M. J., Sabine, P. A., Schmid, R., Sorenson, H., Streckeisen, A., Wooley, A. R., and Zanettin, B., 1989, A classification of igneous rocks and glossary of terms: Oxford, Blackwell, 193 p.
- Le Maitre, R. W. (ed.), Streckeisen, A., Zanettin, B., Le Bas, M. J., Bonin, B., Bateman, P., Bellieni, G., Dudek, A., Efremova, S., Keller, J., Lameyre, J., Sabine, P. A., Schmid, R., Sørensen, H., and Woolley, A. R., 2004, Igneous rocks: a classification and glossary of terms—recommendations of the International Union of Geological Sciences: Subcommittee on the Systematics of Igneous Rocks: Cambridge University Press, 236 p.
- Lent, R. L., 1969, Geology of the southern half of the Langlois quadrangle, Oregon: Eugene, Ore., University of Oregon, Ph.D. dissertation, 189 p.
- Libbey, F. W., Lowry, W. D., and Mason, R. S., 1947, Nickel-bearing laterite, Red Flat, Curry County, Oregon: Ore Bin, v. 9, no. 3, p. 19–28.
- Lund, E. H., 1973, Landforms along the coast of southern Coos County, Oregon: Ore Bin, v. 35, no. 12, p. 189–210.
- Lund, E. H., 1975, Landforms along the coast of Curry County, Oregon: Ore Bin, v. 37, no. 4, p. 57–76.

- Lund, E. H., and Baldwin, E. M., 1969, Diorite intrusions between Sixes and Pistol rivers, southwestern Oregon: *Ore Bin*, v. 31, no. 10, p. 193–206.
- Ma, L., Madin, I. P., Olson, K. V., Watzig, R. J., Wells, R. E., and Priest, G. R., compilers, 2009, Oregon geologic data compilation [OGDC], release 5 (statewide): Oregon Department of Geology and Mineral Industries Digital Data Series OGDC-5, CD-ROM.
- MacDonald, J. H., Jr., Harper, G. D., and Zhu, B., 2006, Petrology, geochemistry, and provenance of the Galice Formation, Klamath Mountains, Oregon and California, *in* Snoke, A. W., and Barnes, C. G., eds., *Geological studies in the Klamath Mountains Province, California and Oregon: a volume in honor of William P. Irwin*: Geological Society of America Special Paper 410, p. 77–101.
- Mackenzie, W. S., Donaldson, C. H., and Guilford, C., 1997, *Atlas of igneous rocks and their textures* (7th ed.): Addison Wesley Longman, 148 p.
- Madin, I. P., McNelly, G. W., and Kelsey, H. M., 1995, Geologic map of the Charleston quadrangle, Coos County, Oregon: Oregon Department of Geology and Mineral Industries Geological Map Series GMS-94, scale 1:24,000.
- McCloughry, J. D., Ma, L., Jones, C. D., Mickelson, K. A., and Wiley, T. J., 2013, Geologic map of the southwestern Oregon coast between Crook Point and Port Orford, Curry County, Oregon: Oregon Department of Geology and Mineral Industries Open-File Report O-13-21, 3 pl., scale 1:24,000, database files, 55 p.
- McNelly, G. M., and Kelsey, H. M., 1990, Late Quaternary tectonic deformation in the Cape Arago-Bandon region of coastal Oregon as deduced from wave-cut platforms: *Journal of Geophysical Research*, v. 95, p. 6699–6713.
- Medaris, L. G., 1972, High-pressure peridotites in southwestern Oregon: *Geological Society of America Bulletin*, v. 83, p. 41–58.
- Mertzman, S. A., 2000, K-Ar results from the southern Oregon – northern California Cascade Range: *Oregon Geology*, v. 62, p. 99–122.
- Miles, G. A., 1981, Planktonic foraminifers of the lower Tertiary Roseburg, Lookingglass, and Flournoy formations (Umpqua Group), southwest Oregon, *in* Armentrout, J. M., ed., *Pacific Northwest Cenozoic biostratigraphy*: Geological Society of America Special Paper 184, p. 85–104.
- Muhs, D. R., Kelsey, H. M., Miller, G. H., Kennedy, G. L., Whelan, J. F., and McNelly, G. W., 1990, Age estimates and uplift rates for late Pleistocene marine terraces: southern Oregon portion of the Cascadia Forearc: *Journal of Geophysical Research*, v. 95, p. 6685–6698.
- Nelson, A. R., Aspuith, A. C., and Grant, W. C., 2004, Great earthquakes and tsunamis of the past 2000 years at the Salmon River Estuary, central Oregon coast, USA: *Bulletin of the Seismological Society of America*, v. 94, no. 4, p. 1276–1292.
- Ogg, J. G., Ogg, G., and Gradstein, F. M., 2008, *The concise geologic time scale*: Cambridge University Press, 177 p.
- Orr, W. N., and Zaitzeff, J. B., 1970, Miocene silicoflagellates from southeast Oregon: *Northwest Science*, v. 44, no. 1, p. 12–15.
- Orr, W. N., Ehlen, J., and Zaitzeff, J. B., 1971, A late Tertiary diatom flora from Oregon: *Proceedings of the California Academy of Sciences, Fourth Series*, v. 37, no. 16, p. 489–500.
- Pearson, G. W., Pilcher, J. R., Baillie, M. G. L., Corbett, D. M., and Qua, F., 1986, High-precision ¹⁴C measurement of Irish oaks to show the natural ¹⁴C variation from AD 1840 to 5210 BC: *Radiocarbon*, v. 28, no. 2B, p. 911–934.
- Peterson, C. D., Stock, E., Price, D. M., Hart, R., Reckendorf, F., Erlandson, J. M., and Hostetler, S. W., 2007, Ages, distributions, and origins of upland coastal dune sheets in Oregon, USA: *Geomorphology*, v. 91, p. 80–102.
- Priest, G. R., and Baptista, A. M., 1995a, Tsunami hazard map of Bandon quadrangle, Coos County, Oregon: Oregon Department of Geology and Mineral Industries Open-File Report O-1995-51, scale 1:24,000.
- Priest, G. R., and Baptista, A. M., 1995b, Tsunami hazard map of Bill Peak quadrangle, Curry County, Oregon: Oregon Department of Geology and Mineral Industries Open-File Report O-1995-52, scale 1:24,000.
- Priest, G. R., and Baptista, A. M., 1995c, Tsunami hazard map of Floras Lake quadrangle, Curry County, Oregon: Oregon Department of Geology and Mineral Industries Open-File Report O-1995-53, scale 1:24,000.
- Priest, G. R., and Baptista, A. M., 1995d, Tsunami hazard map of Langlois quadrangle, Curry County, Oregon: Oregon Department of Geology and Mineral Industries Open-File Report O-1995-54, scale 1:24,000.
- Priest, G. R., and Baptista, A. M., 1995e, Tsunami hazard map of Cape Blanco quadrangle, Curry County, Oregon: Oregon Department of Geology and Mineral Industries Open-File Report O-1995-55, scale 1:24,000.

- Priest, G. R., and Baptista, A. M., 1995f, Tsunami hazard map of Sixes quadrangle, Curry County, Oregon: Oregon Department of Geology and Mineral Industries Open-File Report O-1995-56, scale 1:24,000.
- Priest, G. R., and Baptista, A. M., 1995g, Tsunami hazard map of Port Orford quadrangle, Curry County, Oregon: Oregon Department of Geology and Mineral Industries Open-File Report O-1995-57, scale 1:24,000.
- Priest, G. R., and Baptista, A. M., 1995h, Tsunami hazard map of Ophir quadrangle, Curry County, Oregon: Oregon Department of Geology and Mineral Industries Open-File Report O-1995-58, scale 1:24,000.
- Priest, G. R., and Baptista, A. M., 1995i, Tsunami hazard map of Gold Beach quadrangle, Curry County, Oregon: Oregon Department of Geology and Mineral Industries Open-File Report O-1995-59, scale 1:24,000.
- Priest, G. R., and Baptista, A. M., 1995j, Tsunami hazard map of Signal Buttes quadrangle, Curry County, Oregon: Oregon Department of Geology and Mineral Industries Open-File Report O-1995-60, scale 1:24,000.
- Priest, G. R., and Baptista, A. M., 1995k, Tsunami hazard map of Cape Sebastian quadrangle, Curry County, Oregon: Oregon Department of Geology and Mineral Industries Open-File Report O-1995-61, scale 1:24,000.
- Priest, G. R., and Baptista, A. M., 1995l, Tsunami hazard map of Sundown Mountain quadrangle, Curry County, Oregon: Oregon Department of Geology and Mineral Industries Open-File Report O-1995-62, scale 1:24,000.
- Priest, G. R., and Baptista, A. M., 1995m, Tsunami hazard map of Mack Point Mountain quadrangle, Curry County, Oregon: Oregon Department of Geology and Mineral Industries Open-File Report O-1995-63, scale 1:24,000.
- Priest, G. R., and Baptista, A. M., 1995n, Tsunami hazard map of Carpenterville quadrangle, Curry County, Oregon: Oregon Department of Geology and Mineral Industries Open-File Report O-1995-64, scale 1:24,000.
- Priest, G. R., and Baptista, A. M., 1995o, Tsunami hazard map of Brookings quadrangle, Curry County, Oregon: Oregon Department of Geology and Mineral Industries Open-File Report O-1995-65, scale 1:24,000.
- Priest, G. R., and Baptista, A. M., 1995p, Tsunami hazard map of Mount Emily quadrangle, Curry County, Oregon: Oregon Department of Geology and Mineral Industries Open-File Report O-1995-66 scale 1:24,000.
- Priest, G. R., Meyers III., E. P., Baptista, A.M., and Kamphaus, R. A., 2000, Tsunami hazard map of the Gold Beach area, Curry County, Oregon: Oregon Department of Geology and Mineral Industries Interpretive Map IMS-13, 3 p., scale 1:12,000.
- Priest, G. R., Allen, J. C., Meyers III., E. P., and Baptista, A.M., 2002, Tsunami hazard map of the Coos Bay area, Coos County, Oregon: Oregon Department of Geology and Mineral Industries Interpretive Map IMS-21, 20 p., scale 1:24,000.
- Ramp, L., Schlicker, H. G., and Gray, J. J., 1977, Geology, mineral resources, and rock material of Curry County, Oregon: Oregon Department of Geology and Mineral Industries Bulletin 93, 79 p.
- Raymond, K. R., Prothero, D., Emerson, L., and Retallack, G. 2008, Magnetogstratigraphy of the lower Miocene sandstone of Floras Lake and the Cape Blanco flora, Oregon: Geologic Society of America Abstracts with Programs, v. 40, no. 6, p. 477.
- Raymond, L. A., 1984, Classification of mélanges, *in* Raymond, L. A., ed., Mélanges: their nature, origin, and significance: Geological Society of America Special Paper 198, p. 7–20.
- Rich, E. I., and Steele, W. C., 1974, Geologic structures in Northern California as detected from ERTS-1 satellite imagery: *Geology*, v. 2, p. 165–169.
- Ricker, T. R., and Niewendorp, C. A., 2013, Radiometric Age Information Layer for Oregon, release 1: Oregon Department of Geology and Mineral Industries RAILO-1, GIS files.
- Robertson, S., 1999, BGS rock classification scheme, v. 2, Classification of metamorphic rocks: British Geological Survey Research Report 99-02, 24 p.
- Rock Color Chart Committee, 1991, Rock-color chart: Boulder, Colo., Geological Society of America, 7th printing.
- Roure, F., 1986, Une coupe géologique de Golconda au Pacifique (Oregon, nord-ouest du Nevada, nord de la Californie): Evolution Mésozoïque et Cénozoïque de la marge ouest-Américaine: *Institute Français du Pétrole*, ref. 33 755, 295 p.
- Roure, F., and Blanchet, R., 1983, A geological transect between the Klamath Mountains and the Pacific Ocean (southwestern Oregon): a model for paleosubductions: *Tectonophysics*, v. 91, p. 53–72.
- Schwab, F. L., 1963, Geology of the Quosatana Butte area, central Curry County, southwest Oregon: University of Wisconsin, M.S. thesis, 114 p.

- Seiders, V. M., and Blome, C. D., 1987, Stratigraphy and sedimentology of Upper Cretaceous rocks in coastal southwest Oregon: Evidence for wrench-fault tectonics in a postulated accretionary terrane: alternative interpretation and reply: *Geological Society of America Bulletin*, v. 98, p. 739–744.
- Silver, E. A., and Beutner, E. C., 1980, *Mélanges*: *Geology*, v. 8, p. 32–34.
- Sliter, W. V., 1984, Cretaceous low-latitude pelagic limestone from the Franciscan complex, California, and the Sixes River terrane, Oregon: *Geological Society of America Abstracts with Programs*, v. 16, no. 5, p. 333.
- Sloan, J., Henry, C. D., Hopkins, M., Ludington, S. D., (eds.), and Zartman, R. E., Bush, C. A., and Abston, C. C., (compilers), 2003, National Geochronological Database (<http://mrdata.usgs.gov/geochron/>): U.S. Geological Survey Open-File Report 03-236.
- Snively, P. D., Jr., 1987, Tertiary geologic framework, neotectonics, and petroleum potential of the Oregon-Washington continental margin, *in* Scholl, D. S., Grantz, A., and Vedder, J. G., eds., *Geology and resource potential of the continental margin of western North American and adjacent ocean basins; Beaufort Sea to Baja California*: Houston, Tex., Circum-Pacific Council for Energy and Mineral Resources Earth Science Series, v. 6, p. 305–335.
- Snively, P. D., Jr., Wagner, H. C., and Lander, D. L., 1985, Land-sea geologic cross section of the southern Oregon continental margin: U.S. Geological Survey Miscellaneous Investigations Series Map I-1463, scale 1:125,000.
- Stewart, R. E., 1957, Stratigraphic implications of some Cenozoic foraminifera from western Oregon: *Ore Bin*, v. 19, no. 2, p. 11–15.
- Walker, R. G., 1977, Deposition of late Mesozoic resedimented conglomerates and associated turbidites in southwestern Oregon: *Geological Society of America Bulletin*, v. 88, p. 273–285.
- Walker, G. W., and MacLeod, N. S., 1991, Geologic map of Oregon: U.S. Geological Survey, Washington, D.C., scale 1:500,000.
- Weissenborn, A. E., and Snively, P. D., Jr., 1968, Summary report on the geology and mineral resources of the Oregon Islands National Wildlife Refuge, Oregon: U.S. Geological Survey Bulletin 1260-G p. G1–G4.
- Wells, R. E., Jayko, A. S., Niem, A. R., Black G., Wiley, T., Baldwin, E., Molenaar, K. M., Wheeler, K. L., DuRoss, C. B., and Givler, R. W., 2000, Geologic map and database of the Roseburg 30' × 60' quadrangle, Douglas and Coos counties, Oregon: U.S. Geological Survey Open-File Report 00-376, 1:100,000, 55 p.
- Wentworth, C. K., 1922, A scale of grade and class terms of clastic sediments: *Journal of Geology*, v. 30, p. 377–392.
- Widmier, J. M., 1962, Mesozoic stratigraphy of the west-central Klamath Province—a study of eugeosynclinal sedimentation: Madison, Wisc., University of Wisconsin, Ph.D. dissertation, 122 p.
- Wiley, T. J., and Black, G. L., 1994, Geologic map of the Tenmile quadrangle, Douglas County, Oregon: Oregon Department of Geology and Mineral Industries Geologic Map GMS-86, 1:24,000, 5 p.
- Wiley, T. J., McClaughry, J. D., and D' Allura, J., 2011, Geologic database and generalized geologic map of Bear Creek Valley, Jackson County, Oregon: Oregon Department of Geology and Mineral Industries Open-File Report O-11-11, 75 p., scale 1:63,360.
- Witter, R. C., Kelsey, H. M., and Hempill-Haley, E., 2003, Great Cascadia earthquakes and tsunamis of the past 6700 years, Coquille River estuary, southern coastal Oregon: *Geological Society of America Bulletin*, v. 115, p. 1289–1306.
- Witter, R. C., Zhang, Y., Wang, K., Priest, G. R., Goldfinger, C., Stimely, L. L., English, J. T., and Ferro, P. A., 2011, Simulating tsunami inundation at Bandon, Coos County, Oregon, using hypothetical Cascadia and Alaska earthquake scenarios: Oregon Department of Geology and Mineral Industries Special Paper 43, 57 p., scales 1:63,360 and 1:10,000.
- Wood, D. S., 1974, Ophiolites, *mélanges*, blue schists, and ignimbrites: early Caledonian subduction in Wales?, *in* Dott, R. H., and Shaver, R. H., eds., *Modern and ancient geosynclinal sedimentation*: Society of Economic Paleontologists and Mineralogists Special Publication 19, p. 334–343.

APPENDIX — GEOGRAPHIC INFORMATION SYSTEMS (GIS) DATABASE

This appendix describes the digital databases included with this publication.

Geodatabase specifications

Digital data compiled for the southern Oregon coast are stored in an Esri format geodatabase. The following information describes the overall database structure, the feature classes, and supplemental tables.

The data are stored in a file geodatabase and were created using ArcGIS version 10.0 (SP 1). It contains two feature datasets: Geology_FC and Relationships (Figure A1). Geology_FC contains all of the spatially oriented data (feature classes) created for this project. The Relationships feature dataset is used to hold all of the relationships created to connect or relate the supplemental tables to each other, or to the MapUnitPolys feature class.

Figure A2 shows the relationships between the tables and the MapUnitPolys feature class. All supplemental tables eventually relate to the *tblMapUnit*, either through a direct or indirect relationship. The *tblMapUnit* table is the only table with a relationship to the MapUnitPolys feature class.

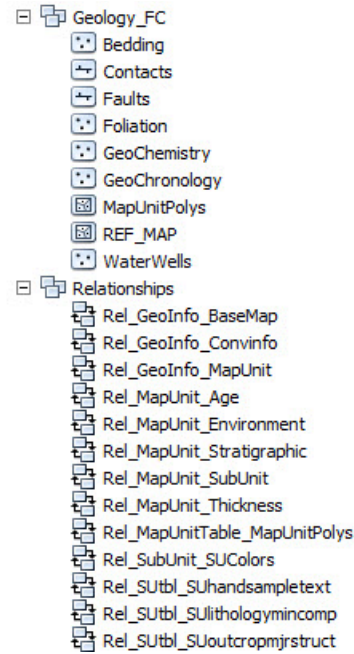


Figure A1. Southwestern Oregon coast geodatabase feature datasets.

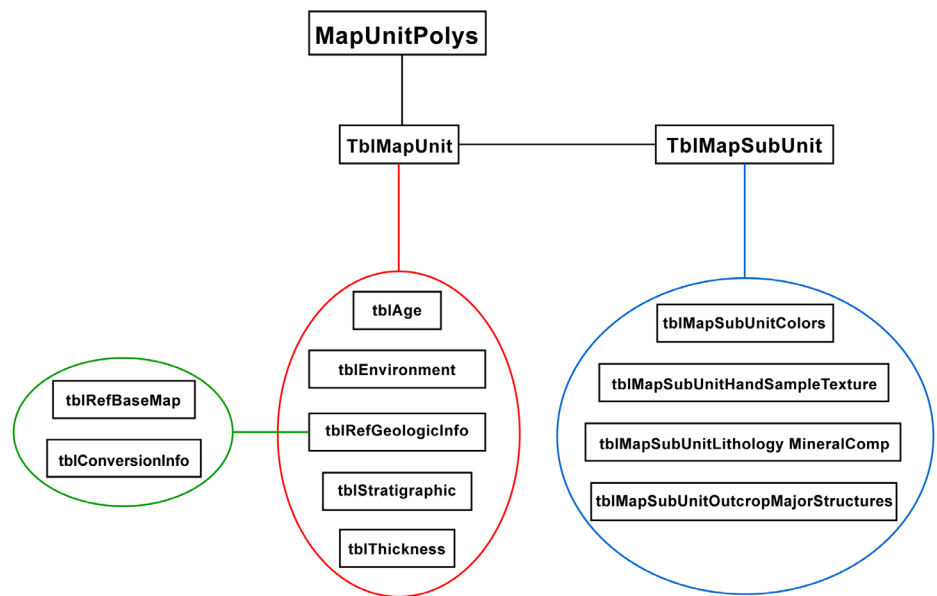


Figure A2. Relationships between tables and MapUnitPolys feature class in the geodatabase.

Geodatabase feature class specifications

Each feature class within the geodatabase has detailed metadata to accompany the data. Please see the metadata for detailed information such as process descriptions, accuracy specifications, and entity attribute descriptions. Figure A3 is provided as a summary description for each feature class.

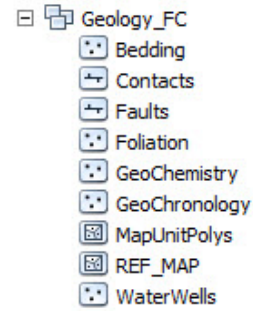


Figure A3. Southwestern Oregon coast geodatabase feature classes.

Feature Class Name	Description
Bedding	This feature class represents point locations where bedding measurements were made, or were compiled from previous studies, along the southern Oregon coast during the course of this study. These data are also contained in the bedding (strike and dip) database described in more detail below.
Contacts	The vector lines in this feature class were drawn to create the map unit polygon boundaries.
Faults	These vector lines represent known fault locations along the southern Oregon coast. The existence and location confidence for the faults are provided in the feature class attribute table.
Foliations	This feature class represents point locations where foliations were measured by the authors during the course of this study or were compiled from previous studies along the southern Oregon coast.
GeoChemistry	This feature class represents point locations where whole-rock samples have been analyzed by X-ray fluorescence (XRF) techniques. Includes data collected by the authors during the course of this study or compiled from previous studies along the southern Oregon coast. These data are also contained in the geochemistry database described in more detail below.
GeoChronology	This feature class represents point locations where $^{206}\text{Pb}/^{238}\text{U}$ (zircon) or other $^{40}\text{Ar}/^{39}\text{Ar}$, K/Ar, ^{14}C , Uranium series, and Thermoluminescence (TL) isotopic ages have been obtained for rock samples along the southern Oregon coast. Includes data collected by the authors during the course of this study or compiled from previous studies. These data are also contained in the geochronology database described in more detail below.
MapUnitPolys	A polygon feature class representing the geologic map units as defined by the authors. A layer file, SC_MapUnitColors.lyr, that can be used to color the polygons with the same colors as the map plates is included.
Ref_Map	This feature class depicts the southern Oregon coast study area.
WaterWells	This feature class represents point locations where water wells were located along the southern Oregon coast. Includes data obtained by the authors from the Oregon Department of Water Resources (OWRD). These data are also contained in the water well database described in more detail below.

Geodatabase table specifications

Figure A4 is provided as a summary description for each table.

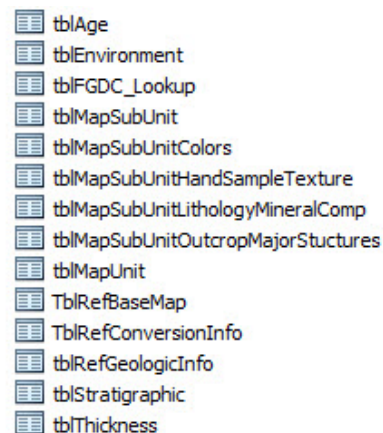


Figure A4. Southwestern Oregon coast geodatabase relationships.

Table Name	Description
<i>tblAge</i>	Contains information about the stratigraphic and radiometric age of the map unit; relates to the <i>tblMapUnit</i> table.
<i>tblEnvironment</i>	Contains information about the genetic environment and landform and whether or not information exists for geochemistry, paleontology, or petrology; relates to the <i>tblMapUnit</i> table.
<i>tblFGDC_Lookup</i>	Contains descriptions for the reference codes used to attribute the line and point features. Codes are defined in the FGDC Digital Cartographic Standard for Geologic Map Symbolization (http://www.fgdc.gov/standards/projects/FGDC-standards-projects/geo-symbol).
<i>tblMapSubUnit</i>	Contains information about the components, or subunits, of the reference map unit; relates to the <i>tblMapUnit</i> table.
<i>tblMapSubUnitColors</i>	Lists colors of the fresh and weathered rock surfaces for a subunit; relates to the <i>tblMapSubUnit</i> table.
<i>tblMapSubUnitHandSampleTexture</i>	Contains information about the texture or appearance of a subunit at a hand sample level; relates to the <i>tblMapSubUnit</i> table.
<i>tblMapSubUnitLithologyMineralComp</i>	Contains information of mineral or composition descriptors for a subunit; relates to the <i>tblMapSubUnit</i> table.
<i>tblMapSubUnitOutcropMajorStructures</i>	Contains information about the structure of a subunit when viewed at the outcrop level; relates to the <i>tblMapSubUnit</i> table.
<i>tblMapUnit</i>	Contains all of the map units defined for the southern Oregon coast; includes the map unit geologic symbol and unit name; relates to the <i>MapUnitPolys</i> feature class.
<i>tblRefBaseMap</i>	Contains information about the base map; relates to the <i>tblGeologicInfo</i> table.
<i>tblRefConversionInfo</i>	Contains information about the conversion process to digital data; relates to the <i>tblRefGeologicInfo</i> table.
<i>tblRefGeologicInfo</i>	Contains the general bibliographic information about the map or database; relates to the <i>tblMapUnit</i> table.
<i>tblStratigraphic</i>	Contains formal or informal stratigraphic classification and names of the map units; relates to the <i>tblMapUnit</i> table.
<i>tblThickness</i>	Contains information about the total thickness of the mapped unit; relates to the <i>tblMapUnit</i> table.

Geodatabase Projection Specifications

All spatial data are stored in the Oregon Statewide Lambert Conformal Conic projection. The datum is NAD83 HARN. The linear unit is international feet. See detailed projection parameters below:

Projection: Lambert_Conformal_Conic
 False_Easting: 1312335.958005
 False_Northing: 0.000000
 Central_Meridian: -120.500000
 Standard_Parallel_1: 43.000000
 Standard_Parallel_2: 45.500000
 Latitude_Of_Origin: 41.750000
 Linear Unit: Foot (0.304800)

Geographic Coordinate System:
 GCS_North_American_1983_HARN
 Angular Unit: Degree (0.017453292519943299)
 Prime Meridian: Greenwich (0.000000000000000000)
 Datum: D_North_American_1983_HARN
 Spheroid: GRS_1980
 Semimajor Axis: 6378137.000000000000000000
 Semiminor Axis: 6356752.314140356100000000
 Inverse Flattening: 298.257222101000020000

Geologic maps

Plates 1, 2, and 3 are geologic maps at a scale of 1:24,000 displaying the geology of the map area. Note that these data were mapped at 1:8,000 scale; 1:24,000-scale plates cannot show all the detail of 1:8,000-scale mapping. Please use the geodatabase to explore in full detail.

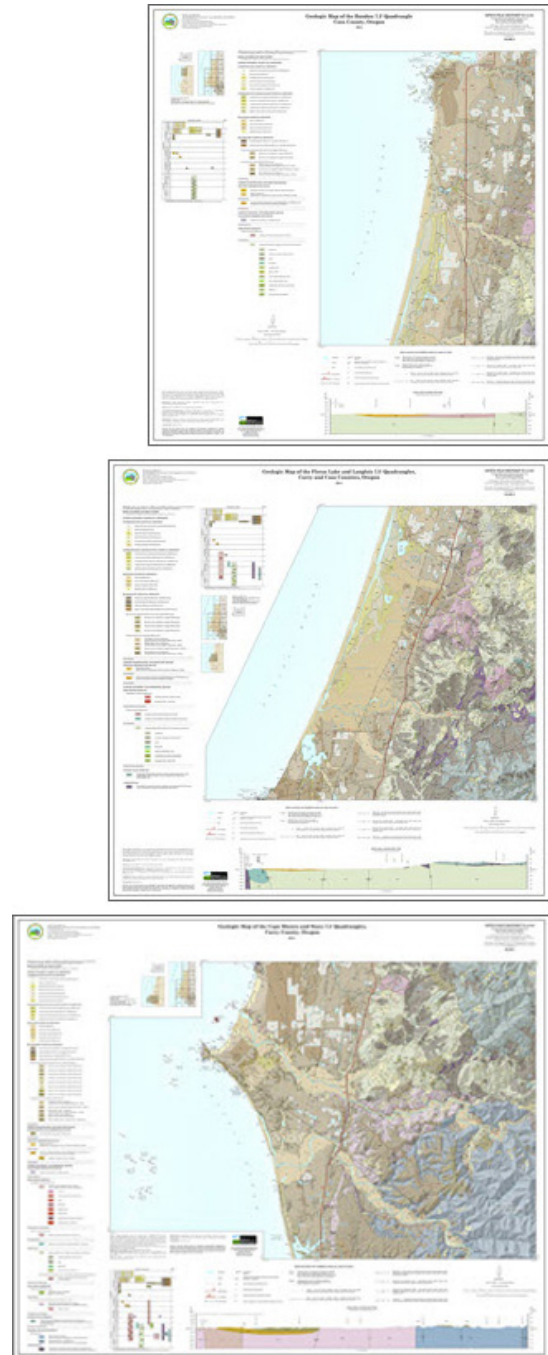


Figure A5. Plates 1, 2, and 3 (south to north) accompanying this report.

Geochemical analytical methods

Geologic mapping along the southern Oregon coast was supported by a number of new X-ray fluorescence (XRF) geochemical analyses of whole-rock samples of igneous rocks. Descriptive rock unit names for igneous rocks are based on normalized major element analyses plotted on the total alkalis ($\text{Na}_2\text{O} + \text{K}_2\text{O}$) versus silica (SiO_2) diagram (TAS) of Le Bas and others (1986), Le Bas and Streckeisen (1991), and Le Maitre and others (1989). New and compiled XRF-geochemical analyses are included in the main geodatabase, and are also provided in a Microsoft Excel® spreadsheet named SC2014_GeoChemistry.xls. A readme file explaining fields listed in the spreadsheet can be found below. The locations of all geochemical samples are given in five coordinate systems: UTM Zone 10 (datum = NAD 27, NAD 83, units = meters), Geographic (datum = NAD 27, NAD 83, units = decimal degrees), and Oregon Lambert (datum = NAD 83, HARN, units = international feet).

Samples denoted by lab abbreviation F & M were analyzed by XRF at the Department of Geosciences, Franklin and Marshall College, Lancaster, Pennsylvania under the direction of S. A. Mertzman. Detailed analytical procedures for the Franklin and Marshall X-ray laboratory were described by Boyd and Mertzman (1987) and Mertzman (2000), and are available online at <http://www.fandm.edu/x7985>. Analytical procedures for the Franklin and Marshall X-ray laboratory were described by Boyd and Mertzman (1987) and Mertzman (2000) and are available online at <http://www.fandm.edu/x7985>. Notes for spreadsheet: nd, no data.

Readme file for southwestern Oregon coast geochemical database spreadsheet columns

SAMPLE_NO	A unique number identifying the sample.
MAP_NO	A unique number identifying the sample on the map plates.
QUADRANGLE	The USGS 7.5-minute quadrangle in which the sample is located.
ELEV_FT	Elevation of sample location in feet.
UTMN_NAD27	Meters north in NAD 27 UTM projection, zone 10
UTME_NAD27	Meters east in NAD 27 UTM projection, zone 10
LAT_NAD27	Latitude in NAD 27 geographic coordinates
LONG_NAD27	Longitude in NAD 27 geographic coordinates
UTMN_NAD83	Meters north in NAD 83 UTM projection, zone 10

UTME_NAD83	Meters east in NAD 83 UTM projection, zone 10
LAT_NAD83	Latitude in NAD 83 geographic coordinates
LONG_NAD83	Longitude in NAD 83 geographic coordinates
N_83HARN	Feet north in Oregon Lambert NAD 83, HARN, international feet
E_83HARN	Feet east in Oregon Lambert NAD 83, HARN, international feet
GROUP	Geologic group that the sample is assigned to. See Geology_FC, MapUnitPolys in the geodatabase.
FORMATION	Geologic formation that the sample is assigned to. See Geology_FC, MapUnitPolys in the geodatabase.
MEMBER	Geologic member that the sample is assigned to. See Geology_FC, MapUnitPolys in the geodatabase.
UNIT	Geologic unit that the sample is assigned to. See Geology_FC, MapUnitPolys in the geodatabase.
MAP_LABEL	Unique label identifying the geologic unit that the sample is assigned to. See Geology_FC, MapUnitPolys in the geodatabase.
TAS_LITH	Rock name assigned based on the total alkalis ($\text{Na}_2\text{O} + \text{K}_2\text{O}$) versus silica (SiO_2) diagram (TAS) of Le Bas and others (1986), Le Bas and Streckeisen (1991), and Le Maitre and others (1989).
NOTES	Special information (e.g., alteration) about certain samples.
MAJOR ELEMENTS, Wt.%	SiO_2 , Al_2O_3 , TiO_2 , FeO^* , MnO, CaO, MgO, K_2O , Na_2O , P_2O_5
TRACE ELEMENTS, ppm	Ni, Cr, Sc, V, Ba, Rb, Sr, Zr, Y, Nb, Ga, Cu, Zn, Pb, La, Ce, Th, U, Co
LOI	Value for loss on ignition as reported by lab.
FE2O3	Iron (III) oxide or ferric oxide reported in original analysis.
FeO	Iron (II) oxide or ferrous oxide reported in original analysis.
REFERENCE	Publication reference, keyed to the reference list in this report.
METHOD	Analytical method used by laboratory that analyzed the sample.
LAB	Analytical laboratory that analyzed the sample.

Geochronology analytical methods

Several new $^{206}\text{Pb}/^{238}\text{U}$ radiometric age-date determinations, derived from detrital zircons in sandstones, were prepared and analyzed by Jonathan Rivas under the direction of Dr. Joshua Schwartz at California State University–Northridge. Zircon dating was performed by laser ablation inductively coupled plasma mass spectrometry (LA-ICP-MS), following the sample preparation and data analysis techniques outlined by Chang and others (2006). Original data for new $^{206}\text{Pb}/^{238}\text{U}$ isotopic ages are located in the digital appendix. Numerous other $^{40}\text{Ar}/^{39}\text{Ar}$, K/Ar, ^{14}C , uranium series, and thermoluminescence (TL) isotopic ages for igneous and metamorphic rocks, as well as Quaternary surficial units, have also been compiled for the area (Janda, 1970; Coleman and Lanphere, 1971; Fiebelkorn and others, 1983; Pearson and others, 1986; Muhs and others, 1990; Kelsey, 1990; Sloan and others, 2003; Kelsey and others, 2005; Peterson and others, 2007; Emerson, 2009; Ricker and Niewendorp, 2013). Please note that K-Ar ages, determined with decay constants prior to 1977, have not been recalculated for this report. The geochronological data points are included in the geodatabase and are also provided as a Microsoft Excel® spreadsheet named SC2014_GeoChronology.xls. A readme file explaining fields listed in the spreadsheet can be found below. The locations of radiometric ages are given in five coordinate systems: UTM Zone 10 (datum = NAD 27, NAD 83, units = meters), Geographic (datum = NAD 27, NAD 83, units = decimal degrees), and Oregon Lambert (datum = NAD 83, HARN, units = international feet). Notes for spreadsheet: na, not applicable; nd, no data.

Readme file for southwestern Oregon coast geochronology database spreadsheet columns

SAMPLE_NO	A unique number identifying the sample.
CORE_ID	A unique label identifying the core from which sample was obtained.
QUADRANGLE	The USGS 7.5-minute quadrangle in which the sample is located.
ELEV_FT	Elevation of sample location in feet.
UTMN_NAD27	Meters north in NAD 27 UTM projection, zone 10
UTME_NAD27	Meters east in NAD 27 UTM projection, zone 10
LAT_NAD27	Latitude in NAD 27 geographic coordinates
LONG_NAD27	Longitude in NAD 27 geographic coordinates
UTMN_NAD83	Meters north in NAD 83 UTM projection, zone 10
UTME_NAD83	Meters east in NAD 83 UTM projection, zone 10
LAT_NAD83	Latitude in NAD 83 geographic coordinates
LONG_NAD83	Longitude in NAD 83 geographic coordinates

N_83HARN	Feet north in Oregon Lambert NAD 83, HARN, international feet
E_83HARN	Feet east in Oregon Lambert NAD 83, HARN, international feet
GROUP	Geologic group that the sample is assigned to. See Geology_FC, MapUnitPolys in the geodatabase.
FORMATION	Geologic formation that the sample is assigned to. See Geology_FC, MapUnitPolys in the geodatabase.
MEMBER	Geologic member that the sample is assigned to. See Geology_FC, MapUnitPolys in the geodatabase.
UNIT	Geologic unit that the sample is assigned to. See Geology_FC, MapUnitPolys in the geodatabase.
MAP_LABEL	Unique label identifying the geologic unit that the sample is assigned to. See Geology_FC, MapUnitPolys in the geodatabase.
LITHOLOGY	Rock type analyzed.
POLARITY	Natural remanent magnetization of the sample analyzed.
AGE_MA	Age determined for the sample in millions of years.
ERROR_MA	Error in age determination in millions of years.
C14 CALAGE (KA)	Calendar age for sample, where age is determined by the radiocarbon dating method. Reported age in thousands of years.
ERROR_yrBP	Error in age determination in years before present.
METHOD	Analytical method used by laboratory that analyzed the sample.
MATERIAL_DATED	Type of material analyzed.
REFERENCE	Publication reference, keyed to the reference list in this report.
NOTES	Special information regarding the sample.

Bedding (strike and dip)

Strike and dip measurements of inclined bedding were taken along the southern Oregon coast during the course of this study by traditional compass and clinometer methods. Additional measurements have been compiled from previous workers. Strikes and dips are reported in both quadrant format (e.g., N30W, 15NE) and azimuthal format using the righthand rule (e.g., 330, 15NE, American convention). Field measured bedding is coded by its appropriate Federal Geographic Data Committee (FGDC) reference number for geologic map symbolization. The measured point data are included in the geodatabase and are also provided as a Microsoft Excel® spreadsheet named SC2014_Bedding.xls. A readme file explaining fields listed in the spreadsheet can be found below. The locations of these point data are given in five coordinate systems: UTM Zone 10 (datum = NAD 27, NAD 83, units = meters), Geographic (datum = NAD 27, NAD 83, units = decimal degrees), and Oregon Lambert (datum = NAD 83, HARN, units = international feet). Strike and dip symbols can be properly drawn by the Esri ArcMap product by opening the layer properties, categorizing by type, choosing the appropriate symbol, and rotating the symbol based on the "Strike_Azi" field. (The advanced button allows you to select the rotation field). The rotation style should be set to geographic in order to maintain the right-hand rule property. Azimuths are given in true north; an additional clockwise correction of about 1.6 degrees is needed to plot strikes and dips properly on the Oregon Lambert conformal conic projection in this area. Notes for spreadsheet: nd, no data.

Readme file for southwestern Oregon coast strike and dip database spreadsheet columns

MAP_UNIT	Geologic unit that the sample is assigned to. See Geology_FC, MapUnitPolys in the geodatabase.
STRUCTURE	Type of geologic structure from which feature was determined.
FGDC_REF	An attribute code assigned to each feature, derived from the Federal Geographic Data Committee (FGDC) digital standard for geologic map symbolization.
STRIKE_QUAD	Strike direction of the inclined plane, stated in a north-directed quadrant format.
DIP	Amount of dip, degrees from horizontal.
QUADRANGLE	The USGS 7.5-minute quadrangle in which the sample is located.
REFERENCE	Publication reference, keyed to the reference list in this report.
STRIKE_AZI	Strike direction of the inclined plane, as determined by employing the right-hand-rule (American convention).
DIP_AZI	Azimuthal direction of dip.
DIP_AMOUNT	Amount of dip, degrees from horizontal.
UTMN_NAD27	Meters north in NAD 27 UTM projection, zone 10
UTME_NAD27	Meters east in NAD 27 UTM projection, zone 10
LAT_NAD27	Latitude in NAD 27 geographic coordinates
LONG_NAD27	Longitude in NAD 27 geographic coordinates
UTMN_NAD83	Meters north in NAD 83 UTM projection, zone 10
UTME_NAD83	Meters east in NAD 83 UTM projection, zone 10
LAT_NAD83	Latitude in NAD 83 geographic coordinates
LONG_NAD83	Longitude in NAD 83 geographic coordinates
N_83HARN	Feet north in Oregon Lambert NAD 83, HARN, international feet
E_83HARN	Feet east in Oregon Lambert NAD 83, HARN, international feet

Structure (foliations)

Measurements of inclined metamorphic foliations were taken along the southern Oregon coast from the Colebrook Schist (**Kcqs**) during the course of this study by traditional compass and clinometer methods. Additional measurements have been compiled from previous workers. Foliations are reported in both quadrant format (e.g., N30W, 15NE) and azimuthal format using the right-hand rule (e.g., 330, 15NE, American convention). Field measured foliations are coded by their appropriate Federal Geographic Data Committee (FGDC) reference number for geologic map symbolization. The measured point data are included in the geodatabase and are also provided as a Microsoft Excel® spreadsheet named SC2014_Foliation.xls. A readme file explaining fields listed in the spreadsheet can be found below. The locations of these point data are given in five coordinate systems: UTM Zone 10 (datum = NAD 27, NAD 83, units = meters), Geographic (datum = NAD 27, NAD 83, units = decimal degrees), and Oregon Lambert (datum = NAD 83, HARN, units = international feet). Inclined foliation symbols can be properly drawn by the Esri ArcMap product by opening the layer properties, categorizing by type, choosing the appropriate symbol, and rotating the symbol based on the “Strike_Azi” field. (The advanced button allows you to select the rotation field). The rotation style should be set to geographic in order to maintain the right-hand rule property. Azimuths are given in true north; an additional clockwise correction of about 1.6 degrees is needed to plot strikes and dips properly on the Oregon Lambert conformal conic projection in this area. Notes for spreadsheet: nd, no data.

Readme file for southwestern Oregon coast foliation database spreadsheet columns

MAP_UNIT	Geologic unit that the sample is assigned to. See Geology_FC, MapUnitPolys in the geodatabase.
STRUCTURE	Type of geologic structure from which feature was determined.
FGDC_REF	An attribute code assigned to each feature, derived from the Federal Geographic Data Committee (FGDC) digital standard for geologic map symbolization.
STRIKE_QUAD	Strike direction of the inclined plane, stated in a north-directed quadrant format.
DIP	Amount of dip, degrees from horizontal.
QUADRANGLE	The USGS 7.5-minute quadrangle in which the sample is located.
REFERENCE	Publication reference, keyed to the reference list in this report.
STRIKE_AZI	Strike direction of the inclined plane, as determined by employing the right-hand-rule (American convention).
DIP_AZI	Azimuthal direction of dip.
DIP_AMOUNT	Amount of dip, degrees from horizontal.
UTMN_NAD27	Meters north in NAD 27 UTM projection, zone 10
UTME_NAD27	Meters east in NAD 27 UTM projection, zone 10
LAT_NAD27	Latitude in NAD 27 geographic coordinates
LONG_NAD27	Longitude in NAD 27 geographic coordinates
UTMN_NAD83	Meters north in NAD 83 UTM projection, zone 10
UTME_NAD83	Meters east in NAD 83 UTM projection, zone 10
LAT_NAD83	Latitude in NAD 83 geographic coordinates
LONG_NAD83	Longitude in NAD 83 geographic coordinates
N_83HARN	Feet north in Oregon Lambert NAD 83, HARN, international feet
E_83HARN	Feet east in Oregon Lambert NAD 83, HARN, international feet

Water well logs

The well log database is derived from written drillers' logs provided by Oregon Department of Water Resources (OWRD). Well logs vary greatly in completeness and accuracy, therefore locally limiting the utility of subsurface interpretations based upon these data. Water well-logs, compiled and used for interpretation during the course of this study were not field located. The approximate locations were estimated using tax lot maps, street addresses (coordinates obtained from Google Earth™), and aerial photographs to plot locations on the map. The accuracy of the locations ranges widely, from errors of one-half mile possible for wells located only by section and plotted at the section centroid to a few tens of feet for wells located by address or tax lot number on a city lot with bearing and distance from a corner. At each mapped location the number of the well log is indicated. This number can be combined with the first four letters of the county name (e.g., CURR 5473), to retrieve an image of the well log from the OWRD web site.

The measured point data are included in the geodatabase and are also provided as a Microsoft Excel® spreadsheet named SC2014_WaterWells.xls. A readme file explaining fields listed in the spreadsheet can be found below. The locations of water well point data are given in six coordinate systems: UTM Zone 10 (datum = WGS 84, NAD 27, NAD 83, units = meters), Geographic (datum = NAD 27, NAD 83, units = decimal degrees), and Oregon Lambert (datum = NAD 83, HARN, units = international feet).

Well intervals listed in the well log database sometimes alternate between consolidated and unconsolidated lithologies and may be listed as alternating between bedrock and surficial geologic units. This may occur where bedrock units are soft (lower Pleistocene and Miocene units), where paleosols or weak zones (mélange) lie within bedrock, and, most commonly, where cemented or partly cemented zones alternate with unconsolidated zones in surficial deposits.

Readme file for southwestern Oregon coast well log database

Lithologic abbreviations used (alphabetical by group)

UNCONSOLIDATED SURFICIAL UNITS	
a	ash
bd	boulders
c	clay
ch	clay, hard (often logged as claystone but probably not bedrock)
g	gravel
gc	cemented gravel
gra	granitic alluvium
gs	gravel and sand (also sandy gravel)
m	mud
s	sand
sg	sand and gravel (also gravelly sand, or sand with gravel)
sl	soil
st	silt
ROCK, sedimentary	
a	argillite
bc	breccia
cg	conglomerate
cht	chert
cs	claystone
ls	limestone
mds	mudstone
pbs	pebbly sandstone
sh	shale
sts	siltstone
ss	sandstone
su	sedimentary, undivided
ROCK, igneous	
an	andesite
b	basalt
ba	basaltic andesite
cd	cinders
dc	dacite
d	diorite
dg	decomposed granite
gb	gabbro
gr	granite
l	lava
pl	pillow lava

r	rhyolite
sc	scoria
t	tuff
v	volcanic, undivided
vb	volcanic breccia
Rock, metamorphic	
mv	meta-volcanic rocks, undivided
ms	meta-sedimentary rocks, undivided
grn	greenstone
gn	gneiss
p	peridotite
ph	phyllite
sch	schist
slt	slate
sp	serpentine
OTHER	
af	artificial fill
cl	coal (lignite)
dg	decomposed granite
o	other (driller's unit listed in Notes column of spreadsheet)
qtz	quartz
rk	rock
sl	soil
u	unknown (typically used where a well has been deepened)

Water well log spreadsheet columns

Field	Example	Description
TRS	-10931	One digit for township, two digits for range and for section; negative if township is south of Willamette baseline
COUNTY	CURR	Curry County.
	COOS	Coos County.
GRID	53779	Well log number for wells. Wells in Curry County preceded by acronym Curr (e.g., CURR 53799). Wells in Coos County preceded by acronym Coos (e.g., COOS 53799).
WELL_EL_FT	1938	Wellhead elevation in feet as given by Google Earth™ at corresponding WGS 84 location.
LOCATED_BY	Google	Google Earth™ elevation for cursor location at a given address.
	House	Google Earth™ elevation at house in vicinity of given address.
<i>(continued in next column)</i>		

(Water well log spreadsheet columns continued)

Field	Example	Description
	Pad	Pad identifying approximate well location, visible in air photo.
	Taxlot	Approximate tax lot centroid or other best guess for well location using a combination of tax lot maps and aerial photographs.
	Owner	Owner name
	OWRD	Wells located by Oregon Water Resources Department (OWRD) using handheld GPS.
	GPS	GPS coordinates of wellhead included with well log.
	qq	Approximate Quarter-Quarter section centroid.
	q	Approximate Quarter section centroid.
	map	Approximate fit to sketch map included with well log.
LITHOLOGY	g	Best interpretation of driller's log using abbreviations above.
BASE_FT	17	Recorded base of driller's interval or, if lithology abbreviation would not change, similar intervals, in feet below wellhead.
TOP_FT	14	Calculated top of driller's interval or similar intervals, in feet below wellhead.
TOP_EL_FT	1924	Calculated elevation at top of driller's interval, or similar intervals, in feet above sea level.
BASE_EL_FT	1921	Calculated elevation at base of driller's interval, or similar intervals, in feet above sea level.
BEDRK_LITH	gr	Lists bedrock lithologies, when encountered, abbreviations listed above.
BEDRK_ELEV	1924	Calculated elevation at which bedrock or soil over bedrock was first encountered, in feet above sea level.
TAX_LOT	800	Tax lot number. Where it is determined that a tax lot number is used more than once in the section then the appropriate subdivision of the section is indicated in the Notes field.
NOTES		Notes
<i>(continued in next column)</i>		

<i>(Water well log spreadsheet columns continued)</i>		
Field	Example	Description
MAP_UNIT	Tb	Geologic unit interpreted in subsurface on the basis of drillers log and designated by map unit label used in accompanying geodatabase. Intervals labeled "suna" (surface unit not applicable) are those where the lithology as interpreted by the original drillers' log do not correspond; also denotes intervals in the subsurface where a precise unit label cannot be applied.
<i>Well location given in six coordinate systems calculated by reprojecting original WGS 84 UTM, zone 10 locations:</i>		
N_WGS84_M		Meters north in WGS84 UTM projection, zone 10
E_WGS84_M		Meters east in WGS84 UTM projection, zone 10
UTMN_NAD27_ZN10		Meters north in NAD 27 UTM projection, zone 10
UTME_NAD27_ZN10		Meters east in NAD 27 UTM projection, zone 10
LATITUDE_NAD27		Latitude in NAD 27 geographic coordinates
LONGITUDE_NAD27		Longitude in NAD 27 geographic coordinates
UTMN_NAD83_ZN10		Meters north in NAD 83 UTM projection, zone 10
UTME_NAD83_ZN10		Meters east in NAD 83 UTM projection, zone 10
LATITUDE_NAD83		Latitude in NAD 83 geographic coordinates
LONGITUDE_NAD83		Longitude in NAD 83 geographic coordinates
N_NAD83_HARN_FT		Feet north in Oregon Lambert NAD 83, HARN, international feet
E_NAD83_HARN_FT		Feet east in Oregon Lambert NAD 83, HARN, international feet